Institute of Veterinary Pathology

Department of Veterinary Medicine

Freie Universität Berlin

Establishment of Infection Models and Insights into the Pathogenesis of Invasive Aspergillosis Mediated by *Aspergillus terreus*

Thesis submitted for the fulfillment of

a doctoral degree in Veterinary Medicine

(Dr. med. vet.)

at the

Freie Universität Berlin

Submitted by

Silvia Slesiona

Veterinarian from Neuss

Berlin 2011

Journal-No.: 3544

Printed with permission of the Department of Veterinary Medicine of the Freie Universität Berlin

Dean:	Univ.-Prof. Dr. Leo Brunnberg
First reviewer:	Univ.-Prof. Dr. Achim D. Gruber, Ph.D.(Cornell Univ.)
Second reviewer:	Univ.-Prof. Dr. Bernhard Hube
Third reviewer:	PD Dr. Kerstin Borchers

Descriptors (according to CAB-Thesaurus):
mice, Aspergillus, aspergillosis, infection, respiratory diseases, virulence, pathogenesis, phagocytosis, cell wall components

Day of Doctorate: March 27th 2012

This thesis was performed at the Leibniz-Institute for Natural Product Research and Infection Biology e.V. – Hans Knöll Institute in the Department of Microbial Pathogenicity Mechanisms and the Junior Research Group Microbial Biochemistry and Physiology under the supervision of Dr. Ilse D. Jacobsen and Dr. habil. Matthias Brock.

The work was partially financed by the Deutsche Forschungsgemeinschaft DFG project BR-2216/4-1 and the Netzwerk Grundlagenforschung HKI.

Bibliografische Information der Deutschen Nationalbibliothek
Die Deutsche Nationalbibliothek verzeichnet diese Publikation in der Deutschen Nationalbibliografie; detaillierte bibliografische Daten sind im Internet über <http://dnb.ddb.de> abrufbar.

ISBN: 978-3-86387-140-6
Zugl.: Berlin, Freie Univ., Diss., 2011
Dissertation, Freie Universität Berlin
D 188

Choriner Str. 85 - 10119 Berlin
verlag@menschundbuch.de – www.menschundbuch.de

A journey of a thousand miles

must begin with a single step!

Lao-Tzu

Table of contents

List of abbreviations

ABPA	allergic bronchopulmonary aspergillosis
A.	*Aspergillus*
ALT	alanine aminotransferase
AM	alveolar macrophage
AMM	*Aspergillus* minimal medium
ANOVA	analysis of variance
AST	aspartate aminotransferase
BALF	bronchoalveolar lavage fluid
BMDM	bone marrow-derived macrophage
BSA	bovine serum albumin
C. albicans	*Candida albicans*
CFU	colony-forming unit
DAPI	4,6-diamidin-2-phenylindol
DC	dendritic cell
DHN-melanin	dihydroxynaphthalene melanin
DMEM	Dulbecco's modified Eagle's medium
E. coli	*Escherichia coli*
ELISA	enzyme-linked immunosorbent assay
et al.	et alii
FACS	fluorescence activated cell sorting
FBS	fetal bovine serum
Fig.	figure
FITC	fluorescein isothiocyanate
GM-CSF	granulocyte macrophage colony stimulating factor
HE	hematoxylin eosin (stain)
HR-ESI MS	high resolution electrospray ionisation mass spectrometry
i.p.	intraperitoneal
IBPA	invasive bronchopulmonary aspergillosis
IgG	immunoglobulin G
IgM	immunoglobulin M
IL	interleukin
INF	interferon
LDH	lactate dehydrogenase

LPS	lipopolysaccharide
M-CSF	macrophage colony stimulating factor
MDM	monocyte-derived macrophage
MOI	magnitude of infection
NETs	neutrophil extracellular traps
NRPS	non-ribosomal peptidase
PAMP	pathogen-associated molecular pattern
PAS	periodic acid Schiff (reaction)
PBS	phosphate buffered saline
PBMC	peripheral blood mononuclear cell
PFA	paraformaldehyde
p.i.	post infection
PKS	polyketide synthase
PRR	pathogen recognition receptor
RPMI	Roswell Park Memorial Institute
RT	room temperature
SD	standard deviation
s.c.	subcutaneous
spp.	species (plural)
TEM	transmission electron microcopy
TLR	toll-like receptor
TNF	tumor necrosis factor
U	unit
UV	ultraviolet
wt	wild type

1 Introduction

Aspergilli are saprobiotic fungi belonging to the ascomycetes. They occur ubiquitously in soil and decaying organic matter. In susceptible hosts, *Aspergillus* can cause several kinds of disease including allergy, mycotoxicosis, aspergilloma formation in body cavities, and invasive or disseminated aspergillosis. The most severe form of disease is invasive aspergillosis, characterised by invasive growth in single organs or as systemic disease. Invasive aspergillosis mainly occurs in human patients, but is also regularly found in dogs, horses and avian species.

This work focuses on invasive bronchopulmonary aspergillosis (IBPA), a life-threatening disease in immunocompromised hosts. Although *Aspergillus* (*A.*) *fumigatus* is the predominant cause of IBPA, *A. terreus* infections are emerging. Worldwide, between 3% and 12.5% of IBPA cases are caused by *A. terreus* (Khoo and Denning 1994; Perfect et al. 2001; Steinbach et al. 2004a; Lass-Flörl et al. 2005). IBPA mediated by *A. terreus* has often a fatal outcome, and epidemiological studies reveal mortality rates of up to 90% (Denning et al.; Lin et al. 2001). This can be attributed to still insufficient diagnostic tools resulting in delayed therapy as well as the intrinsic resistance of *A. terreus* to amphotericin B, an antimycotic drug frequently used in the initial therapy of invasive aspergillosis.

The pathogenesis of IBPA caused by *A. fumigatus* has been studied extensively and it has been assumed that the pathogenicity strategy of *A. fumigatus* is representative for all pathogenic aspergilli. However, the pathogenesis of *A. terreus* infections has not been thoroughly investigated yet and, importantly, it is unclear whether similar pathogenicity strategies are indeed employed by different aspergilli. Therefore, the aim of this study was to establish and characterise infection models for *A. terreus* to (i) analyse pathogenesis, especially in comparison to *A. fumigatus*, and (ii) as tools for future research, e.g. identification of fungal virulence determinants or therapeutic approaches.

First, an alternative infection model using chicken embryos was developed. This model allows high throughput virulence screens and has already been successfully applied for *A. fumigatus*. This model was used to compare the virulence potential of different *A. terreus* isolates to select strains for further experiments. Second, based on established models for *A. fumigatus* IBPA, two distinct murine models representing two major risk groups of IBPA were developed. Mice were either rendered leucopenic, resembling the immune status of bone marrow transplant recipients, or treated with corticosteroids, modelling immuno-suppression in solid organ transplant recipients. Intranasal infection was chosen to mimic the natural route of infection *via* inhalation of fungal spores.

The obtained results indicated differences between *A. terreus* and *A. fumigatus* in the interaction with the host's immune system. Alveolar macrophages are the first phagocytesencountering conidia in the lung. In addition to eliminating pathogens as the first line of defence, alveolar macrophages aid in orchestrating secondary immune responses. Thus, the aim of the second part of the project was to (i) elucidate the interaction of *A. terreus* with macrophages and (ii) to identify fungal factors influencing this interaction. Therefore, the cellular interaction was dissected into phagocytosis, killing and the phagolysosomal maturation. Moreover the role of the *A. fumigatus* specific pigment DHN-melanin in these interactions and *in vivo* was investigated in detail.

2 Literature Review

2.1 *Aspergillus terreus*

2.1.1 Taxonomy and morphology

Aspergillus terreus (*Emericella terreus*) is a common saprophytic soil inhabitant and may be isolated ubiquitously. For example, it has been recovered from desert soil, grass lands, compost heaps and as a contaminant on stored corn, barley or peanuts (Balajee 2009).
A. terreus belongs to the kingdom of fungi, there in the phylum of *Ascomycota* and the class of *Eurotiomycetes* (Thom 1945). To further classify *A. terreus* it was integrated into the order *Eurotiales* and in the genus *Aspergillus*. This genus is further divided into seven subgenera (Pitt 1994). Using morphological methods Raper and Fennell grouped *A. terreus* into the subgenus *Nidulantes* and there within the section *Terrei* (Raper and Fenell 1965). Additionally, two varieties (var. *africanus* and var. *terreus*) are distinguished which show morphological differences: variatio *africanus* forms bright orange spores and produces sclerotium bodies which is not described for *A. terreus* var. *terreus*.
Sporulated *A. terreus* colonies typically show a brown up to cinnamon coloured appearance. However, the morphological appearance of different strains varies from poorly sporulating, fluffy phenotypes over intermediates to heavily sporulating *A. terreus*. The growth on solid media such as Czapek agar, malt extract agar or *Aspergillus* minimal media (Fig. 1) is generally fast.

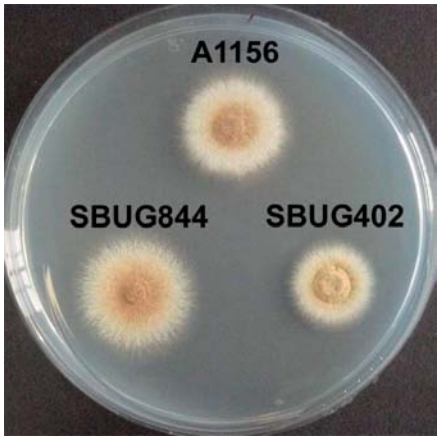

Fig. 1: Growth of various *A. terreus* wild type strains

A. terreus growth on *Aspergillus* minimal media supplemented with 50 mM glucose, 72 h at 37℃; A1156: reference strain; SBUG844/SBUG 402: environmental isolates.

Besides the normal phialidic conidia formation, *A. terreus* additionally forms globose, heavy walled hyaline cells as lateral excrescences on the hyphae. These cells are called accessory conidia or are referred to as aleurioconidia (Balajee 2009). Recently it was shown that these cells are rich in β-1,3-glucan and lead to a higher inflammatory response in intranasally infected immunocompetent mice (Deak et al. 2009; Deak et al. 2011). Since *A. terreus* is the only member of the genus *Aspergillus* that produces these form of conidia, the production of accessory conidia either *in vitro* or *in vivo* provides a diagnostic marker to differentiate *A. terreus* from other aspergilli as well as *Fusarium*, *Paecilomyces* and *Acremonium* species (Liu et al. 1998). These conidia have also been hypothesised to be responsible for the high dissemination rates in patients suffering from invasive bronchopulmonary aspergillosis (IBPA) (Raper and Fenell 1965).

2.1.2 Secondary metabolite profile

The primary metabolism is generally necessary for growth and reproduction of microorganisms. In contrast, secondary metabolism represents all functions and products not directly related to energy metabolism, it is not as essential and often dispensable for fungi. There are four classes of secondary metabolites in fungi: (i) polyketides, (ii) non-ribosomal peptides, (iii) terpenes and (iv) alkaloids (Collemare et al. 2008).

A. terreus produces a wide range of secondary metabolites. The production of these secondary metabolites in *A. terreus* depends on three different enzyme classes: (i) polyketide synthases (PKS), (ii) non-ribosomal peptidases (NRPS) and (iii) PKS/NRPS hybrids (Sanchez et al. 2008).

Secondary metabolites that are produced by *A. terreus* include asterric acid, asterriquinone, butyrolactone I, citrinin, emodin and lovastatin. Lovastatin, an anti-hypercholesterimic drug, is also known as monacolin K or mevinolin (Alberts et al. 1980). It has proven one of the most useful drugs in slowing artherosclerosis by limiting cholesterol biosynthesis (Waters et al. 1994). Therefore *A. terreus* is of industrial importance.

However, although some secondary metabolites are used therapeutically, most of the isolated secondary metabolites from *A. terreus* were identified as mycotoxins or products with toxic potential. The hepatotoxic potential of these secondary metabolites has been demonstrated in animal models (Gupta et al. 1981; Sharma et al. 1983) but their production during infection has not been shown to date. Secondary metabolites may play an important role in the pathogenesis of invasive aspergillosis mediated by *A. terreus*.

2.1.3 Resistance against amphotericin B

Amphotericin B is one of the first-line drugs used in the treatment of invasive aspergillosis (Maschmeyer et al. 2007), representing the standard therapy. Most ascomycetes such as *Aspergillus fumigatus* and *Candida albicans* are susceptible to amphotericin B. However, *A. terreus* possesses an inherent resistance to amphotericin B (Balajee 2009). This complicates treatment of invasive aspergillosis since species identification is required to initiate the appropriate treatment. The exact action of amphotericin B is still unclear and several mechanisms are proposed: First, amphotericin B can bind to ergosterol in the fungal cell membrane and induces aqueous pores in the phospholipid membrane. This disrupts the proton gradient in the fungal cell resulting in ion leaks (Vanden Bossche et al. 1994) as described for nystatin. Another mechanism proposed is the inactivation of fungal cells and finally cell death by oxidative damage (Sokol-Anderson et al. 1986). The resistance mechanism of *A. terreus* remains still unclear. Blum et al. demonstrated that neither the ergosterol content nor the cell wall composition or the lipid peroxidation level in *A. terreus* had an influence on the intrinsic amphotericin B resistance. They proposed that the strikingly high catalase activity in *A. terreus* might contribute to the increased resistance of *A. terreus* to amphotericin B (Blum et al. 2008). Hsp-90, a small heatshock protein, is also suspected to be involved in *A. terreus* amphotericin B resistance, since it promotes resistance to echinocandins and azoles in other moulds (Cowen et al. 2009).

2.2 Diseases mediated by *Aspergillus* spp.

Aspergilli are capable of inducing a wide spectrum of disease, ranging from mycotoxicosis and allergic reactions to restricted and invasive infections (Pfaller and Diekema 2010). *Aspergillus* species occur in a wide range of host species. Besides the human immunosuppressed host, *Aspergillus* infections are often found in dogs as systemic infections or sino-nasal aspergillosis. Interestingly, German Shepherds and Dalmatians appear more susceptible than other breeds (Kabay et al. 1985; Butterworth et al. 1995; Schultz et al. 2008; Day 2009). Furthermore, horses frequently develop aspergillosis in the guttural pouch (Lepage et al. 2004), resulting in life-threatening complications due to the invasive growth of the fungus. A link between exposure to *Aspergillus* spp. and chronic obstructive pulmonary disease (COPD) was also suggested (Marinkovic et al. 2007). A*spergillus* infections can be economically relevant in poultry (Beernaert et al. 2010; Arné et al. 2011), but are also a major problem in companion birds (Beernaert et al. 2010) or free-living avian species (Olias et al. 2010).

2.2.1 Mycotoxicosis

Mycotoxicoses usually occur in livestock and are associated with contaminated forage. However, mycotoxicosis does not represent a classical infectious disease, since the disease is caused by secondary metabolites of aspergilli growing saprophytically on the forage. Intoxications show a diverse clinical appearance (Pier et al. 1980). Several mycotoxins are known to induce toxicosis, such as aflatoxins, ochratoxins or zearalenon (Khlangwiset and Wu 2010). Ochratoxin, for example, is produced by *Aspergillus niger* (Frisvad et al. 2011). The mycotoxic potential of *A. terreus* is yet not fully discovered (Gressler et al. 2011). Because mycotoxicosis can represent an economic problem (Robens and Richard 1992), efforts are taken pre-harvest and during processing of the forage to reduce or prevent contaminations (Lozbin 1977).

2.2.2 Aspergilloma and rhinosinal infections

Aspergilloma are defined as fungal balls in preformed body cavities. These fungal masses can be frequently found in the lung of patients suffering from tuberculosis (Riscili and Wood 2009), but are also seen in the guttural pouch of horses (Lepage et al. 2004) or in the sinal cavities.

The guttural pouch represents a unique anatomic feature of equids. This mucosal cavity is associated to the respiratory tract and therefore well ventilated but not equipped with a ciliary epithelium as the trachea is. *A. fumigatus* is most frequently isolated from the guttural pouch. Since this anatomic structure is surrounded by arteries supplying the brain, it is suggested to be involved in cooling. The reasons for invasive growth of *A. fumigatus* in the guttural pouch are still unclear. Invasive growth in this area commonly results in severe blood losses and death of the animal due to angioinvasion. Early surgical debridement can prevent this life-threatening complication (Lepage et al. 2004).

Dogs and humans can develop rhinal sinusitis (Claeys et al. 2006) resulting in aspergilloma formation (Chakrabarti et al. 2009). Typical clinical appearance of this disease is initially similar to bacterial sinusitis but results in masses behaving like malignant neoplasms, eroding the bones and spreading into adjacent tissue in later stages of infection (Hora 1965). Therapy relies on topic and systemic treatment with antimycotics as well as surgical removal of fungal masses (Wood and Douglas 2010).

2.2.3 Allergic bronchopulmonary aspergillosis

Allergic bronchopulmonary aspergillosis (ABPA) is predominantly found in asthma patients or patients with cystic fibrosis and represents an immediate hypersensitivity reaction to aspergilli (Antunes et al. 2010). It is not associated with invasive growth of the fungus. *A. fumigatus* represents the most prevalent cause of ABPA, though other species also emerge. Allergic asthma as a form of hypersensitivity is characterised by a dominant Th2 response (Knutsen et al. 1990), while a Th1 response dominates in hypersensitivity pneumonitis (Antunes et al. 2010). The clinically relevant characteristics are impaired mucociliary clearance, mucoid impactions, wheezing, pulmonary infiltrates, bronchiectasis and fibrosis (Brown et al. 1995).

Recurrent airway obstruction (RAO, formerly chronic obstructive bronchitis: COB) represents one of the major allergic diseases with respiratory distress in horses. Especially thermophillic moulds, including aspergilli, are associated with this disease (Robinson et al. 1996). The infection is characterised by diffuse neutrophil infiltrates into the bronchioles, increased IgE levels in bronchoalveolar lavage fluid as well as increased thromboxane serum levels (Robinson et al. 1996).

2.2.4 Invasive bronchopulmonary aspergillosis

Healthy individuals inhale several thousand *Aspergillus* spores every day (Aimanianda et al. 2009). These spores usually remain resting and are either expelled by coughing or eradicated by the immune system. However, in immunocompromised patients or patients with an underlying disease, uncontrolled growth of aspergilli can lead to severe life-threatening infections.

Invasive bronchopulmonary aspergillosis (IBPA) can develop in immunocompromised patients after inhalation of conidia. It represents one of the major life-threatening complications in high risk groups, such as solid organ transplant recipients and patients with hematologic malignancies (Wald et al. 1997; Patterson et al. 2000). The main cause is *A. fumigatus* (Marr et al. 2002). However, several other *Aspergillus* species, including *A. terreus*, have been identified as causative agents (Malani et al. 2007). Approximately 3 – 12.5% of IBPA cases are caused by *A. terreus* (Khoo and Denning 1994; Perfect et al. 2001; Steinbach et al. 2004a; Lass-Flörl et al. 2005) with dramatic mortality rates of up to 98% (Denning et al. 1998; Lin et al. 2001). In the immunocompromised patient IBPA, independent of the causative fungal species, is characterised by the development of a severe bronchopneumonia. In neutropenic patients this is due to unrestricted, extensive fungal

growth and angioinvasion, while during corticosteroid treatment the immune system tries to restrain the fungus by pyogranuloma formation which blocks bronchi and brochioles (Latgé 1999; Latgé 2001). Patients with IBPA show severe dyspnoea which is often refractory to therapeutic treatment.

Therapy of IBPA caused by *A. terreus* is further complicated by its intrinsic resistance to amphotericin B (Lass-Flörl et al. 1998; Lass-Flörl 2010). Prophylactic amphotericin B monotherapy in high risk patients results in an increased likelihood to acquire IBPA caused by *A. terreus* (Auberger et al. 2008). In addition, invasive aspergillosis due to *A. terreus* is accompanied by a high rate of dissemination to secondary organs further complicating the treatment of affected patients (Baddley et al. 2001; Lass-Flörl et al. 2005).

2.3 Virulence determinants of *Aspergillus* spp.

Aspergilli are capable of inducing devastating systemic mycoses. As *A. fumigatus* and *A. terreus* are commonly found in the environment and only cause disease in predisposed hosts, they are considered as facultative pathogens. Unlike primary pathogens, which possess virulence factors that evolved in close association to the specific host, virulence determinants of aspergilli have likely evolved to resist hostile environments in decaying vegetation. These factors enhance the organism's survival in its environmental niche, and also promote growth in patients (Askew 2008).

2.3.1 Thermotolerance and secretion of secondary metabolites

A prerequisite for a pathogen to establish and maintain an infection in the mammalian or avian host is the ability to grow at body temperature. Since the original habitat of aspergilli is the compost that represents a highly dynamic environment with enormous fluctuations in temperature, it is not surprising that aspergilli are thermotolerant (Beffa et al. 1998; Bhabhra and Askew 2005). Thus, *A. fumigatus* appears to be better adapted to growth at higher temperatures than *A. terreus* (Fig. 2). This might contribute to the higher incidence of *A. fumigatus* infections in patients.

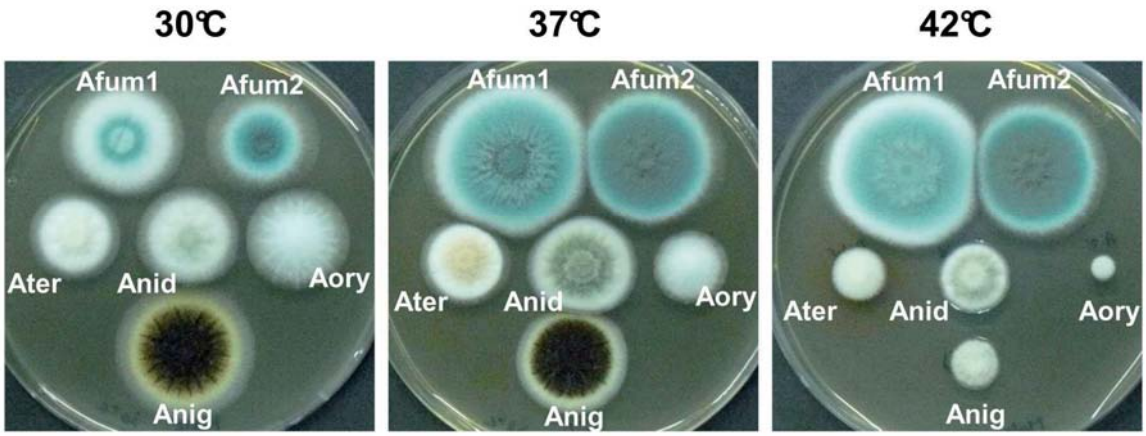

Fig. 2: Growth of *Aspergillus* spp. at different temperatures

The different species were grown on malt extract agar at the indicated temperature for 44 h (Afum= *A. fumigatus*; Ater= *A. terreus*; Anid: *Aspergillus nidulans*; Aory: *Aspergillus oryzae*; Anig: *Aspergillus niger*; picture kindly provided by Dr. Matthias Brock).

In addition to thermotolerance, aspergilli possess several other properties to interfere with hostile environments. *A. fumigatus* and *A. terreus* have the capacity to produce several secondary components with toxic potential (see 2.1.2). These metabolites can be secreted and then interact with microbial competitors in the environment. For example, *A. fumigatus* produces gliotoxin, which was shown to have immunosuppressive activity in the murine host (Sugui et al. 2007; Spikes et al. 2008).

Another important feature of aspergilli is the rigid cell wall and pigments which protect the fungus against several environmental stresses and are involved in virulence. The fungal cell wall and pigments are described below in more detail.

2.3.2 The fungal cell wall

Besides providing structural integrity, the cell wall represents the major contact interface of the fungus with the environment (Askew 2008).

The cell wall of aspergilli is a network of several polysaccharides (Fig. 3). The central core is composed of a branched β-1,3-glucan back bone cross-linked to chitin (Latgé 2007). This glucan-chitin complex is further linked to other polysaccharides, e.g. galactomannan and β-1,3-1,4-glucan (Fontaine et al. 2000). It is important to note that the cell wall of aspergilli is a highly dynamic structure which continuously changes composition in response to

environmental and nutritional conditions as well as the cell cycle (Latgé 2007). Furthermore, the cell wall of conidia is fundamentally different from that of hyphae. In *A. fumigatus* conidia hydrophobins mask the immunogenic structures on the cell wall such as glucans or mannans (Aimanianda et al. 2009). This so called rodlet layer is composed of the hydrophobin RodA and removed when conidia are activated and swell before germination. Subsequently, structures like β-1,3-glucan are exposed on the surface, enabling detection by immune cells (Aimanianda et al. 2009).

Thus, the cell wall provides the most important armour of aspergilli against the immune system. The inertness and rigidity of the conidial cell wall aids fungi in resisting attacks by the immune system (Latgé 2007). Furthermore, pigments incorporated in the conidial cell wall mediate resistance against environmental stressors, such as ultraviolet light, thus enhancing survival in the environment. The role of these pigments will be discussed in more detail below (2.3.4).

The fungal cell membrane and cell wall are targets for several antimycotic agents, such as amphotericin B, azoles or echinocandins which are frequently used against *Aspergillus* infections as mono- or combinatory therapy. Amphotericin B formulations were and in some cases are considered as the “gold” standard in antifungal treatment, though showing dose-limiting nephrotoxicity (Gallis et al. 1990). Amphotericin B and azoles interfere with the ergosterol biosynthesis of the fungal cell membrane (Kontoyiannis et al. 2003), while echinocandins are cell wall-active compounds, inhibiting non-competitively the (1,3)-β-D-glucan synthetase. The inhibition depletes cell wall glucans in growing cells and leads to osmotic instability and subsequently to cell lysis (Debono and Gordee 1994; Onishi et al. 2000; Georgopapadakou 2001).

However, the cell wall is of essential interest in the investigation of the pathogenesis of fungal infections, since it represents the interface between the fungus and the immune system and therefore provides a major target for therapeutic approaches.

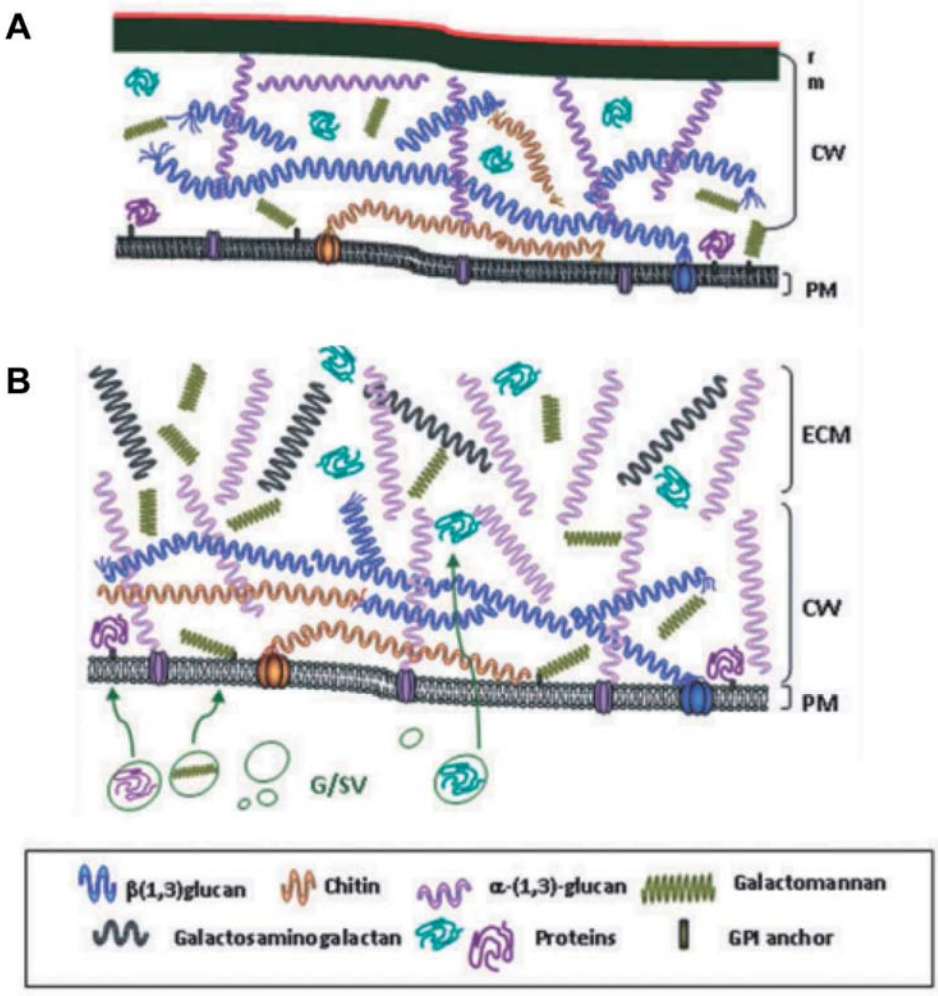

Fig. 3: The fungal cell wall composition

(A) Cell wall of an *A. fumigatus* conidium. The melanin rich electron dense layer is marked in black and the hydrophobin layer in red. (B) Structural organisation of the hyphal cell wall of *A. fumigatus*. Figure adopted from (Latgé 2010) (CW= cell wall, PM= phospholipid membrane, ECM= extracellular matrix).

2.3.3 Nutritional requirements

In order to compete in the environment, aspergilli must be able to adjust the metabolism and nutrient acquisition to fluctuant nutrient availability. Therefore the primary metabolism is highly dynamic in carbohydrate, protein and lipid acquisition (Askew 2008).

Several studies have shown the importance of amino acids like lysine or uridine/uracil in virulence, suggesting that amino acid availability is limited at the site of infection (Sandhu et

al. 1976; D'Enfert et al. 1996; Brown et al. 2000; Liebmann et al. 2004; Schöbel et al. 2010). Moreover, as aspergilli continuously extract nutrients from the environment, it is extremely important for the fungus to maintain metabolic homeostasis. An adverse consequence of amino acid metabolism is the toxic accumulation of propionyl-CoA in the methylcitrate cycle, a cell toxic compound. In the methylcitrate cycle, the methylcitrate synthase detoxifies propionyl-CoA to methylcitrate. Deletion of the *mcsA* gene encoding the methylcitrate synthase was shown to be essential for growth and virulence of *A. fumigatus* (Maerker et al. 2005; Ibrahim-Granet et al. 2008).

Iron and zinc are essential trace elements which are limited within the host. Thus, acquisition of iron and zinc is essential for virulence (Moreno et al. 2007). *A. fumigatus* uses siderophores for iron acquisition and storage, disruption of the correlating genes results in the inability to maintain an infection (Hissen et al. 2005; Schrettl et al. 2007; Schrettl et al. 2010).

2.3.4 Pigments and stress tolerance

Aspergillus conidia are usually distributed by air and water in the environment. During the distribution conidia are exposed to several environmental stresses which led to the evolution of protective factors in aspergilli. A very important protective factor is the production of pigments which allow resistance against UV radiation or oxidative stress (Grosse et al. 2008; Jorgensen et al. 2011).

The most important protective pigment is melanin. Fungal melanins are macromolecules formed either by oxidative polymerisation of tyrosine and phenylallanine (pyomelanine) or by polyketide synthases. The derived pigments are brown or black (Brakhage and Liebmann 2005) and have hydrophobic properties. In fungi several types of melanin have been described. 1,8-dihydroxynaphthalene melanin (DHN-melanin; precursor: 1,8-dihydroxy-naphthalene) and DOPA-melanin (precursor: L-3,4-dihydroxyphenylalanine) are the most important ones and show a contribution to pathogenesis in fungi (Jacobson 2000; Hamilton and Gomez 2002; Langfelder et al. 2003). The grey-greenish spore colouration of *A. fumigatus* derives from DHN-melanin as reviewed by Brakhage and Liebmann (Brakhage and Liebmann 2005). Deletion of the polyketide synthase PksP essential for the production of DHN-melanin in *A. fumigatus*, results in a strain producing pigmentless, white conidia (Jahn et al. 1997). This strain shows increased susceptibility to hydrogen peroxide, sodium hypoclorite and damage by macrophages as well as reduced virulence in a murine infection model (Jahn et al. 1997; Jahn et al. 2000).

The biosynthesis of DHN-melanin in *A. fumigatus* involves several enzymes. The polyketide synthases PksP (Alb1) and Ayg1 condense acetyl-CoA and malonyl-CoA units and form a heptaketide as the first detectable intermediate of the pathway (1,3,6,8-tetrahydroxynaphthalene: T4HN) (Fig. 4). The polyketide synthase PksP of *A. fumigatus* shows high homology to the polyketide synthase wA of *A. nidulans* (Langfelder et al. 2003), but only low homologies to polyketide synthases in the genome of *A. terreus* (see Fig. 40 this work).

For *A. terreus*, pigment synthesis has not yet been studied and it is unclear from which origin *A. terreus* pigments derive.

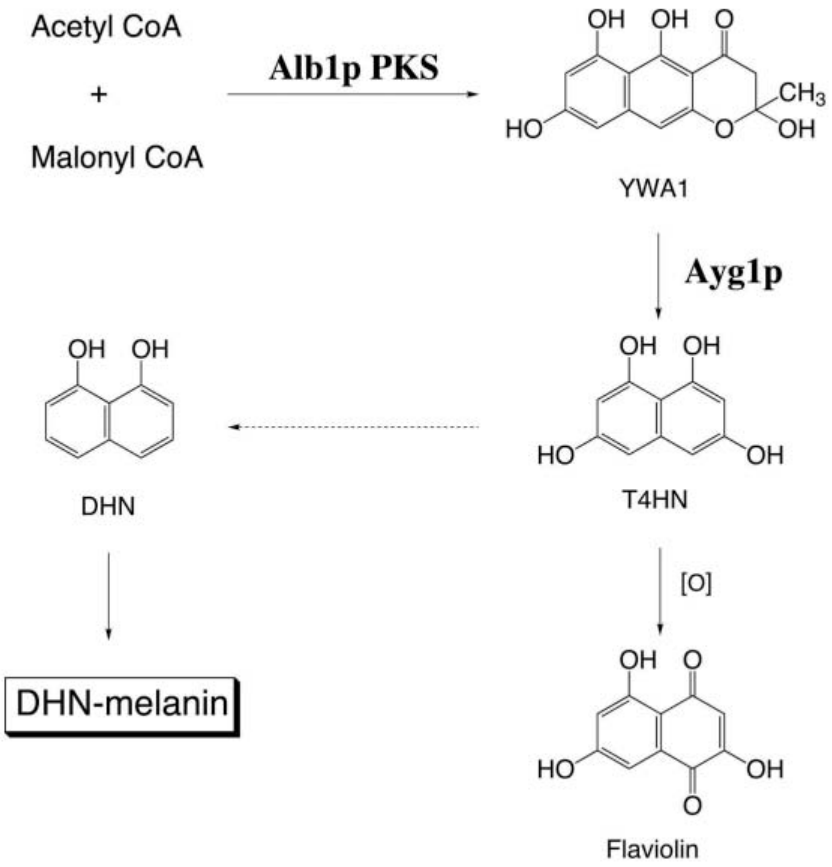

Fig. 4: Scheme of the biosynthesis of dihydroxynaphthalene melanin of *A. fumigatus*

Melanin biosynthesis in *Aspergillus* needs the enzymes Alb1 and Ayg1p; adopted from (Fujii et al. 2004).

2.4 Interactions of *Aspergillus* spp. with components of the immune system

2.4.1 Defence mechanisms of the host

Aspergillus conidia are ubiquitous and, due to their small size, reach the lower airways upon inhalation. In the immunocompetent host, these spores are cleared by phagocytic immune cells (Aimanianda et al. 2009). If the phagocytic immune defence is impaired, e.g. by prolonged corticosteroid therapy or chemotherapy, conidia are able to germinate and form hyphae that invade the lung tissue and establish an infection (Ben-Ami et al. 2010b; Ibrahim-Granet et al. 2010).

Alveolar macrophages (AM) are the first professional phagocytic cells encountering pathogens in the lung. In addition to eliminating pathogens by phagocytosis, AM participate in orchestrating the immune response (Segal 2007). Therefore, the initial step of successful infection depends on the pathogen's ability to prevent or survive recognition and phagocytosis by macrophages. Consequently, pathogens have developed diverse escape and survival strategies (Weidenmaier et al. 2003; Klenerman and Hill 2005; Brakhage et al. 2010; Seider et al. 2010). The interaction of *A. fumigatus* with macrophages has been well studied: In immunocompetent mice, AM phagocytose *A. fumigatus* conidia and control fungal burden unless overwhelmed by a large number of conidia (Chignard et al. 2007; Bhatia et al. 2011), demonstrating the relevance of *A. fumigatus*–macrophage interaction for the clearance of inhaled *A. fumigatus* conidia. Survival of *A. fumigatus* upon phagocytosis depends on its ability to inhibit phagolysosome acidification, which allows a rapid germination and escape from the phagocyte (Ibrahim-Granet et al. 2003). Blocking of phagolysosome acidification depends on the presence of DHN-melanin on the surface of *A. fumigatus* conidia (Jahn et al. 2002; Ibrahim-Granet et al. 2003).

In addition to macrophages, other components of the immune system such as neutrophils, natural killer cells and the complement system interact with *Aspergillus* spp. during infection. In invasive aspergillosis neutrophils are recruited in large numbers to the site of infection. These granulocytes have proven to efficiently inactivate hyphae but not conidia (Ibrahim-Granet et al. 2010). Furthermore, neutrophils produce extracellular traps (NETs) which immobilise conidia *in vitro* and *in vivo* (Bruns et al. 2010). Natural killer cells also inactivate hyphal elements of *A. fumigatus* (Schmidt et al. 2011). Interestingly, platelets display antifungal activity against *Aspergillus* conidia and further enhance the activity of antifungals *in vitro* (Perkhofer et al. 2011).

Humoral components such as the complement system have been shown to bind to the surface of *A. fumigatus*. Conidia of *A. fumigatus* specifically bind laminin and human

fibrinogen as well as factor H which likely contributes to immune evasion of the fungus (Larcher et al. 1992; Tronchin et al. 1993; Coulot et al. 1994; Behnsen et al. 2008).

Although the cellular innate immunity appears to play a critical role in invasive aspergillosis, the adaptive immunity contributes to host defence by reacting to signals elicited by the innate immune system (McCormick et al. 2010). The therapeutic administration of β-1,3-glucan specific antibodies showed protective effects in murine infection models of IBPA (Torosantucci et al. 2009). In human patiens suffering from IBPA *Aspergillus*-specific antibodies have been detected, though their functional importance is unclear (Thornton 2010).

In invasive aspergillosis circulating dendritic cells (DCs) infiltrate infected regions, phagocytose fungal elements and process specific antigens in order to then migrate to a regional lymph node (McCormick et al. 2010). Furthermore, DCs direct the immune system either towards a balanced Th1 response which is beneficial for the host or towards an excessive Th17 response being detrimental as shown in animal experiments (Zelante et al. 2009). What kind of DCs mediate the Th1 or the Th17 response is still unclear but this might depend on specific DC subsets.

During invasive aspergillosis T-cells are activated by antigen presenting DCs in pulmonary lymph nodes and subsequently move to the site of infection. There, T-cells subsequently activate phagocytes by cytokine signalling (Zelante et al. 2009). Furthermore regulatory T-cells have been shown to limit the inflammatory response in aspergillosis and act antagonistically to the Th17 response (Zelante et al. 2007).

2.4.2 Pathogen recognition

Critical for the defence against pathogens is the capacity of the immune system to recognise the pathogen. Recognition involves several receptors present on immune effector cells that interact with specific ligands on the fungal cell wall.

The direct interaction of pathogens and immune cells is mediated by the recognition of pathogen-associated molecular patterns (PAMPs) by pathogen recognition receptors (PRRs) on immune cells. This step is an essential prerequisite for phagocytosis and cytokine production which results in immune cell recruitment. The PRRs dectin-1, TLR-2 and TLR-4 (Hohl et al. 2005; Chignard et al. 2007; Luther et al. 2007; Segal 2007) are involved in this interaction recognising β-1,3-glucan and yet unidentified PAMPs, respectively.

Dectin-1 was identified to bind β-glucans (Brown and Gordon 2001; Brown et al. 2003). It possesses an ITAM-like motif and can associate with molecules like CD63, a tetraspanin, or

Pentraxin-3 (Diniz et al. 2004; Mantegazza et al. 2004). It was demonstrated that recognition of *A. fumigatus* by dectin-1 is limited to specific fungal growth forms (Hohl et al. 2005). On the conidial cell wall of *A. fumigatus* β-1,3-glucans are masked by the rodlet layer as described above (2.3.2) and cannot be detected by dectin-1. During conidial swelling and germination the rodlet layer is removed and β-1,3-glucans are exposed. β-1,3-glucans accumulate on the hyphal tip of *A. fumigatus* germlings and are then recognised by dectin-1 (Hohl et al. 2005; Luther et al. 2007). Dectin-1 signalling subsequently activates the phagocyte and leads to internalisation of the fungus. After the initial phagocytosis process dectin-1 is internalised, recruited to the phagosomes and processed in *Aspergillus*-containing phagolysosomes (Herre et al. 2004). This suggests an additional role of dectin-1 in intracellular glucan processing.

The mannose receptor is a type-I transmembrane protein and was first described on macrophages in mammalian tissue (Kruskal et al. 1992). The receptor recognises mannose, fucose or N-acetylglucosamine sugar residues on microorganisms (Largent et al. 1984) and is a putative receptor for galactomannan (Segal 2007; Balloy and Chignard 2009). The contribution of the mannose receptor to phagocytosis of *Aspergillus* is still not fully elucidated.

Toll-like receptors have diverse functions in phagocytosis and signalling. During *A. fumigatus* infections TLR2 has been demonstrated to be involved in phagocytosis of *A. fumigatus* conidia (Luther et al. 2007). In contrast, a contribution of TLR4 to phagocytosis has not yet been described but TLR4 is important during the activation of immune cells (Braedel et al. 2004). The ligands recognised by TLR2 and 4 are still under investigation. Recently it has been shown that TLR9 contributes to signalling and recognition of *A. fumigatus* conidia in the mature phagosome, but the corresponding ligand is also unknown (Kasperkovitz et al. 2010).

2.5 Infection models

Infection models are essential to study a variety of aspects in the pathogenesis of infectious diseases, innate and adaptive immune responses, transmission routes as well as therapeutic approaches. To ensure a valuable outcome using infection models several factors should be considered prior to experimentation. (i) Does the chosen model reflect the clinical situation in patients and is the selected host species suitable for the experiment? (ii) Is the model reproducible and are the protocols easy to standardise? (iii) Is the desired model economical?

2.5.1 Classical animal models

The different species used in aspergillosis research range from avian over murine to rabbit models. For the investigation of avian aspergillosis, hatchlings or adult birds were either infected via a pulmonary or an intravenous route (Chaudhary and Singh 1983; Richard and Thurston 1983; Kunkle and Rimler 1996). It was demonstrated that chicken are less susceptible than for example turkeys or Japanese quails (Ghori and Edgar 1973; Ghori and Edgar 1979; Chaudhary and Singh 1983). Investigations of vaccination strategies using germling fractions of *A. fumigatus* were successful in these models (Richard et al. 1982; Richard et al. 1984; Richard et al. 1991; Schmidt 2002).
Mammalian models employ guinea pigs, rats or rabbits for experimental *Aspergillus* research besides mice. These models were used to generally investigate therapeutic approaches, such as systemic antimycotic treatments (Olenchock et al. 1983; Kirkpatrick et al. 2000; Kirkpatrick et al. 2002a; Kirkpatrick et al. 2002b; Walsh et al. 2003). Disadvantageous of these models are elevated costs compared to mice and the need for further specialised handling in comparison to murine models.

In general, mice are frequently used as host species for pathogenesis studies because they are relatively easy to handle, low in costs, and additionally allow genetic manipulation on the host side. They are the most commonly used host species for studies of invasive aspergillosis and are considered as the “gold” standard for pathogenesis research. For *A. fumigatus*, several murine pulmonary and disseminated infection models have been developed (Dixon et al. 1989; Nawada et al. 1996; Sarfati et al. 2002; Sheppard et al. 2004; Steinbach et al. 2004b; Stephens-Romero et al. 2005) which address differences in the immune status of the host, such as leucopenia or long-term corticosteroid application. These models mimic the immune status of two major risk groups for aspergillosis, bone marrow transplant recipients in case of leucopenia and solid organ recipients often treated with corticosteroids (Denning et al. 1998; Latgé 1999; Marr et al. 2002).
These two models are substantially different and allow the detailed investigation of fungal factors either in the interaction with the immune system or in the pulmonary environment with limited immune cell interaction. In leucopenic models the fungus grows extensively in the lung tissue. The interaction with cellular compounds of the immune system is limited to resident alveolar macrophages while circulating immune cells are almost absent due to the immunosuppressive treatment. This model allows the detailed investigation of general fungal metabolic properties, but is not suitable to investigate factors involved in the interaction with immune cells (Berenguer et al. 1995).

Solid organ transplant recipients are also at risk to acquire invasive aspergillosis as mentioned above. Mimicking this patient group's immune status corticosteroid-based models were developed. These models are characterised by an impaired but not depleted immune system allowing the investigation of fungal factors involved in immune cell interaction (Berenguer et al. 1995). It is noteworthy that the host immune status significantly influences pathogenesis, since certain fungal factors might only be required under specific conditions.
Gliotoxin, for example, has been shown to have immunosuppressive properties on immune cells *in vitro* (Kamei and Watanabe 2005). The gliotoxin deficient mutant of *A. fumigatus* Δ*gliP* displays similar virulence compared to the wild type in an intranasal leucopenic infection model (Cramer et al. 2006; Kupfahl et al. 2006). In contrast, in the corticosteroid-based infection model where immune cells interact with the fungus, the gliotoxin deficient strain displayed reduced virulence (Sugui et al. 2007; Kwon-Chung and Sugui 2009). This example illustrates the importance of choosing the appropriate infection model in the investigation of virulence attributes.
Further refinement of the applied murine infection models can be achieved by using *in vivo* imaging methods, such as luminescence or fluorescence detection using bioluminescent or fluorescent fungal reporter strains. The successful use of bioluminescence imaging to monitor progression of invasive aspergillosis was first reported by Brock et al. (Brock et al. 2008). The method also allows to distinguish disease patterns according to the immunological status of the host (Ibrahim-Granet et al. 2010).
In contrast to *A. fumigatus*, investigations on *A. terreus* mainly focused on disseminated infections in intravenously infected leucopenic animals with the aim to test therapeutic approaches (Johnson et al. 2000). Bronchopulmonary infections have only been described for leucopenic rabbits (Walsh et al. 2003), where IBPA caused by either *A. terreus* or *A. fumigatus* progressed at similar rates (Walsh et al. 2003). Importantly, pulmonary infections with *A. terreus* using mice have not yet been described. It is unclear whether mice are susceptible to *A. terreus* IBPA and whether intranasal infection is a suitable route for the induction of IBPA mediated by *A. terreus*.

2.5.2 Alternative infection models

Although mammalian models represent a valuable tool in aspergillosis research, ethical as well as economical aspects limit their applicability, e.g. if large-scale screenings of fungal strains need to be performed. To reduce the number of mammals used in infection studies, several alternative models were developed, mainly using insect hosts.

The most commonly used alternative model hosts are the fruit fly *Drosophila melanogaster*, larvae of the greater wax moth *Galleria mellonella* and the nematode *Caenorhabditis elegans* (Reeves et al. 2004; Tournu et al. 2005; Ben-Ami et al. 2010a). The advantages of these models are the relatively low costs, the comparatively easy handling, the possibility of large scale testing and the reduced ethical concerns. However, these hosts are generally infected with conidia by injection into the haemolymph or by ingestion of conidia (Lionakis et al. 2005). Thus, these infection routes do not resemble the lung infection characteristic for IBPA. Furthermore, although basic aspects of immunology are conserved across the taxa, the invertebrate immune system is less complex than the avian and mammalian. This likely explains why differences in pathogenicity such as hypervirulence compared to corresponding wild types occur (Jackson et al. 2009) and clearly demonstrates the limitations of insect models.

Chicken embryos have been traditionally used in infection research before standardised mouse strains became available. Similar to invertebrate hosts, the costs are relatively low, the model is comparatively easy to handle and large scale testing is feasible. The developing avian immune system is more complex than in invertebrates and likely reflects the mammalian situation more accurately (Chute 1975; Lehmann 1985; Martinez-Quesada et al. 1993). Chicken embryos can be used to determine the virulence of *A. fumigatus* strains and the results closely resemble those obtained in murine models (Jacobsen et al. 2010).

2.5.3 Models using cell culture or primary cells

To dissect the interaction of pathogens with specific cell types, cell-based interaction assays can be used (Clemons et al. 2000a; Wasylnka and Moore 2002; Wasylnka and Moore 2003). Cell lines are easy to handle and are advantageous for large scale screens, while the availability of primary cells is usually limited (Clemons et al. 2000a). However, primary cells might reflect *in vivo* properties more accurately than cell lines do. For *A. fumigatus* interaction assays, macrophage cell lines or primary macrophages were primarily used, showing that conidia are phagocytosed and eliminated over time (Ibrahim-Granet et al. 2003; Philippe et al. 2003). Investigations using human neutrophils revealed that conidia induce the formation of NETs *in vitro,* and that neutrophils are able to eliminate hyphae but not conidia efficiently (Bruns et al. 2010). Studies using the lung epithelial cell line A549 demonstrated that *A. fumigatus* is also endocytosed by epithelial cells *in vitro* and furthermore resides in acidified phagosomes in A549 cells (Wasylnka and Moore 2003; Wasylnka et al. 2005).

The interaction of *A. terreus* with host immune cells has only been addressed in a single comparative study: Perkhofer et al. investigated phagocytosis and inactivation of conidia from several *Aspergillus* spp. by human monocyte-derived macrophages (Perkhofer et al. 2007). This study revealed no difference between *A. fumigatus* and *A. terreus* in the observation period used.

2.6 Hypothesis and strategy of the thesis

Although *Aspergillus terreus* is frequently found in the environment (Vesper et al. 2007), IBPA caused by this fungus is less common than infections caused by *A. fumigatus*. This might suggest that *A. terreus* is overall less virulent than *A. fumigatus*. However, established *A. terreus* infections are often as fatal as *A. fumigatus* infections (Lass-Flörl et al. 2005; Malani and Kauffman 2007). This led to the hypothesis that *A. terreus* may be less effective in establishing infections and that the initiation of disease might differ from *A. fumigatus*.

To investigate the pathogenesis of *A. terreus* in comparison to *A. fumigatus*, suitable infection models needed to be established. Therefore, the first part of this work aimed to establish and characterise alternative and murine infection models to investigate bronchopulmonary infections mediated by *A. terreus*.

During the analysis of these models differences between both fungi were discovered in regard to the required inoculum dose, onset of clinical symptoms of disease and host response. This partially confirmed the hypothesis of differences in disease establishment and led to the investigation of the interaction of *A. terreus* with macrophages.

Alveolar macrophages represent the first professional phagocytes facing inhaled conidia. Therefore, the ability to avoid clearance by these immune cells likely affects the pathogen's ability to establish clinical infections. Thus, the interaction of alveolar macrophages with *A. terreus* conidia in comparison to *A. fumigatus* conidia was investigated. The analysed aspects included: (i) Phagocytosis of conidia, (ii) fungal viability after phagocytosis, (iii) phagolysosome maturation as well as (iv) escape from macrophages and phagolysosomes. To obtain further mechanistic insides, the accessibility of conidial PAMPs and the impact of a fungal melanin precursor on intracellular growth *in vitro* and *in vivo* was studied.

3 Material and Methods

3.1 Chemicals, reagents and equipment

Chemicals and reagents used in this study were purchased from Sigma Aldrich (Munich, Germany), Applichem (Darmstadt, Germany) or Roth (Karlsruhe, Germany) unless stated otherwise. Cell culture media, fetal bovine serum, phosphate buffered saline and supplementary antibiotics were purchased from PAA Laboratories (Coelbe, Germany) unless indicated in the text. Fungal growth media were purchased from Applichem. Equipment and specific antibodies as well as test systems used are indicated in the text.

3.2 Fungal cultures

3.2.1 Strains and culture conditions

3.2.1.1 Maintenance of strains and harvesting of conidia

All strains used in this study are listed in Table 1. Strains were maintained as cryostocks (cryobank, Mast Diagnostica, Reinfeld, Germany), at -80°C. To obtain conidia, strains were grown on malt extract agar slants for seven days at room temperature. Conidia were harvested in 5 ml sterile phosphate buffered saline (PBS) and filtered twice through 40 µm cell-strainers (BD, Heidelberg, Germany). Conidia were counted with a Neubauer counting chamber and diluted with the appropriate buffer to the desired concentration.

Media:	**Malt extract agar:**	Malt extract	3%
		Peptone	0.5%
		Agar agar	2%

Strain	Function	Reference and Source
A. fumigatus CBS 144.89	wild type	Centraalbureau voor Schimmelcultures (CBS), Utrecht, Netherlands, clinical isolate
A. fumigatus Af 293	wild type	American Type culture condition (ATCC), Manassas, USA, clinical isolate
A. fumigatus ATCC 46645	wild type	American Type Culture Collection (ATCC), Manassas, USA, clinical isolate
A. terreus SBUG 844	wild type	HKI strain collection, Jena, Germany, environmental isolate
A. terreus A1156	wild type	NIH 2624, Fungal genetics stock center, Kansas, USA, clinical isolate
A. terreus SBUG 402	wild type	HKI strain collection, Jena, Germany, environmental isolate
A. terreus T9	wild type	Cornelia Lass-Flörl, Medizinische Universität Innsbruck, Innsbruck, Austria, clinical isolate
A. terreus luc opt 2/7/15	luminescent reporter	provided by Dr. Matthias Brock; HKI, Jena, Germany
A. terreus wA	pigment production	provided by Markus Gressler; HKI,Jena, Germany

Table 1: Fungal strains used in this study

3.2.1.1 Pre-swelling of conidia

For cell culture experiments, pre-swollen conidia were obtained by placing freshly harvested conidia for 7 h (*A. terreus*) or 3.5 h (*A. fumigatus*) into sterile Roswell Park Memorial Institute (RPMI) 1640 medium supplemented with 10% heat-inactivated fetal bovine serum (FBS) at 37℃ and gentle shaking (Philippe et al. 2003). Hea t inactivation was facilitated by exposing the FBS 20 min to 56℃. After incubation cells were centrifuged, washed three times with sterile PBS and diluted to the desired concentrations. Absence of clumping was confirmed in all conidial preparations by microscopy immediately prior to use.

3.2.1.2 Labelling of conidia

For phagocytosis and killing assays conidia were pre-labelled with fluorescein isothiocyanate (FITC) after swelling as described before (Sturtevant and Latgé 1992). In brief, conidia were incubated in 100 mM $NaCO_3$ buffer containing 1 mg/10 ml FITC for 1 h at 37°C and gentle shaking. After incubation cells were centrifuged, washed two times with PBS containing 0.01% Tween 20 and then three additional times with PBS. Conidia were subsequently counted with a Neubauer counting chamber and diluted in sterile PBS.

3.3 Virulence studies

3.3.1 Chicken embryo model

The model was performed as described previously (Härtl et al. 1995; Jacobsen et al. 2010). In brief, on developmental day ten, the shell of the egg was disinfected with Braunoderm® (Braun, Melsungen, Germany) prior to perforation on the blunt end as well as on the longitudinal side with a dentist drill. The shell membrane was subsequently perforated with a sterile dentist hook. An artificial air chamber was then generated by applying under pressure with a peleusball on the blunt side of the egg, resulting in an air chamber at the perforation on the longitudinal side. Infection of the egg was facilitated by applying 0.1 ml of inoculum directly onto the chorio-allantoic membrane (CAM) at the artificial air chamber. After infection the holes were sealed with liquid paraffin and eggs were incubated at 37.6°C for up to seven days. Embryonic viability was checked daily by candling.

For histological analysis, embryos were killed humanely by chilling on ice for 1 h. The egg surface was disinfected with 70% ethanol and the egg was split in half by longitudinal dissection. The CAM was cut into pieces that were directly fixed in 4% paraformaldehyde dissolved in H_2O (PFA). Samples were embedded in paraffin, cut into 5 µm sections, and stained with periodic acid Schiff (PAS) reaction using standard protocols. Sections were examined by bright-field microscopy.

3.3.2 Murine infection models

Female mice 6 - 8 weeks old (18 to 20 g, Charles River, Germany or Centre d'Elevage R. Janvier, Le Genest Saint-Isle, France) were used in all studies. Animals were housed in individually ventilated cages and cared for in accordance to the principles outlined in the *European Convention for the Protection of Vertebrate Animals Used for Experimental and Other Scientific Purposes* (http://conventions.coe.int/Treaty/en/Treaties/Html/123.htm). All

animal experiments were approved by the responsible Federal State authority (Thüringer Landesamt für Verbraucherschutz) and ethics committee (permit no. 03-002/09; 03-012/10) and were in accordance with the German animal welfare act.

After infection, animals were monitored at least twice daily and humanely sacrificed if moribund (defined by severe lethargy, severe dyspnoea or hypothermia) by an overdose of ketamin (Inresa Arzneimittel, Freiburg, Germany). All survival experiments were terminated on day 14 after infection. Additionally, groups of five mice were sacrificed at defined time points (as indicated in the results section) to analyse kinetics of infection. Organ samples for subsequent analyses were collected during post mortem analysis and processed immediately.

Confirmation of immunosuppression was performed by differential blood cell counts before immunosuppression, on the day of infection and on post mortem analyses. In brief, 5 µl murine blood were elapsed on a microscope slide, stained according to Giemsa using standard protocols and subsequently analysed using light microscopy. 200 immune cells per animal were differentiated.

3.3.2.1 Intranasal infection

To obtain the infection inoculum, conidia were harvested as described above (3.2.1.1) and diluted to the desired concentration in sterile PBS. Intranasal infection of mice was performed under general anaesthesia using a mixture of Medetomidin (0.5 mg/kg, Fort Dodge Veterinär GmbH, Würselen, Germany), Midazolam (5 mg/kg, Roche, Mannheim, Germany) and Fentanyl (0.05 mg/kg, Janssen-Cilag, Neuss, Germany) injected intraperitoneally (i.p.). Mice were placed on a heating pad in dorsal position with the head lifted. 20 µl of the inoculum were applied dropwise onto the nostrils to be inhaled. General anaesthesia was then antagonised with Antipamezol (2.5 mg/kg, Pfizer GmbH, Berlin, Germany), Flumazenil (0.5 mg/kg, Roche, Mannheim, Germany) and Naloxon (1.2 mg/kg, Hameln Pharma Plus GmbH, Hameln, Germany). The day of infection was designated as day 0.

3.3.2.2 Leucopenic mouse model

To induce leucopenia, Balb/C mice were immunosuppressed by i.p. injection of cyclophosphamide (140 mg/kg) on days -4, -1, 2, 5, 8, 11 and an additional subcutaneous (s.c.) dose of cortisone acetate (200 mg/kg) on day -1. Immunosuppression was confirmed by differential blood cell counts as described above (3.3.2.)

Mice were challenged intranasally with conidia on day 0 with 5×10^6 for cohort studies and with 5×10^5, 1×10^6 and 1×10^7 conidia/mouse for luminescence monitoring as described above (3.3.2.1) to evaluate the infectious dose for cohort studies.

3.3.2.3 Corticosteroid mouse model

For the corticosteroid model, Balb/C (bioluminescence imaging) or CD-1 (survival studies) mice received cortisone acetate (25 mg / mouse) i.p. on days -3 and 0. Immunosuppression was confirmed by differential blood cell counts as described above (3.3.2.). Time course experiments in this model were performed as described above, though additionally a 24 h time point was investigated.
Mice were challenged intranasally on day 0 with 1×10^7 conidia in 20 µl PBS in cohort studies and with 1×10^6, 5×10^6 and 1×10^7 under general anaesthesia for luminescence monitoring as described above (3.3.2.1) to evaluate the infectious dose for cohort studies.

3.3.2.4 Immunocompetent mice

To investigate infections in immunocompetent mice, untreated female specific pathogen-free CD-1 mice were challenged intranasally with 1×10^7 conidia in 20 µl PBS, as described above (3.3.2.1).

3.3.3 *In vivo* bioluminescence imaging

Images were acquired using an IVIS 100 system (Caliper life science, Hopkinton, USA) as described before (Ibrahim-Granet et al. 2010). In brief, 100 µl PBS containing 3.33 mg D-luciferin (Synchem, Felsberg/Altenburg, Germany) were injected i.p. 10 min prior to imaging. Mice were anaesthetized with 2.5% isoflurane (Delta Select GmbH, Dreieich, Germany) in medical oxygen using a XGI-8 anaesthesia system (Caliper life science). Imaging was performed using the Living Image software version 3.1 (Caliper life science), by photon acquisition for 5 min with small filter and a binning of 4.

3.3.4 Clinical scoring

Weight and surface body temperature were recorded once daily in the morning, while clinical examinations were performed and recorded twice daily. The clinical score was defined by the sum of three individual parameters: Fur (normal: 0, ruffled: 1), dyspnoea (absent: 0, mild: 1, moderate: 2, severe: 3) and percent loss of body weight (> 10%: 1, > 25%: 2). Thus, healthy animals scored 0, the maximal possible score was 6.

3.3.5 Quantification of serum marker enzymes

Alanine aminotransferase (ALT), aspartate aminotransferase (AST), alkaline phosphatase (AP) and pancreatic amylase were determined from serum samples using the EuroLyser CCA 180 Vet system (QinLAB Diagnostik, Martinsried, Germany) according to standard methods recommended by the International Federation of Clinical Chemistry. Sterile blood samples were taken from mice on the day of sacrifice under general anaesthesia by heart puncture.

3.3.6 Pathology and histology

Gross pathological changes were recorded during post mortem analysis. For histological analysis, representative parts of lung, liver, kidney and spleen were fixed in 4% PFA dissolved in H_2O, embedded in paraffin and 5 µm sections were stained with hematoxylin-eosin (HE) or PAS reaction according to standard protocols.

3.3.7 Quantification of myeloperoxidase and cytokines from tissue homogenates

Organs were homogenised in ice cold tissue lysis buffer and centrifuged twice (1500 × g, 10 min, 4°C). The supernatants were aliquoted and stored at -80°C until use. Myeloperoxidase (MPO) and cytokine levels of TNFα, IL-1β, GM-CSF, INFγ, IL-6, IL-10, IL-17 and IL-22 were determined using commercially available murine enzyme-linked immunosorbent assays (ELISA) (MPO, Hycult Biotechnology, Uden, Netherlands; cytokine ELISA, eBioscience, Hatfield, UK) according to the manufacturer's recommendations. Measurements were performed with an Infinite M200 pro ELISA reader (Tecan, Männedorf, Switzerland). Standard curves, routinely performed for every ELISA, were used to quantify the cytokine amount in the samples tested.

Semiquantitative cytokine analysis was performed using the mouse inflammation antibody array G series (RayBiotech, Norcross, USA, ELISA-array), allowing the measurement of 40 inflammation relevant cytokines using one sample. For each sample tested in the array, 200 µg protein from the lung homogenate diluted in 50 µl tissue lysis buffer were applied to the array and further processed to the manufacturer's recommendations. Scanning was performed using the GenePix 4000B Microarray Scanner (Axon Instruments, Sunnyvale, USA). Data analysis was performed using the Gene Spring GX10 software (Agilent Technologies, Santa Clara, USA). Relative expression was calculated to the internal array control.

Buffer: Tissue lysis buffer:
200 mM NaCl
5 mM EDTA
10 mM Tris
10% glycerol
1 mM phenylmethylsulfonyl fluorid (PMSF)
1 µg/ml leupeptide
28 µg/ml aprotinin

3.4 Cell culture

Cell lines and primary cells used in this study are listed in Table 2.

3.4.1 Macrophage cell lines

The alveolar macrophage cell line MH-S, originally derived from the lung of a Balb/C mouse and immortalised by simian virus SV40 transfection (ATCC, Mannassas, USA), was routinely kept in RPMI 1640 supplemented with 10% heat-inactivated FBS. These alveolar macrophages display the morphologic features and functions of normal, mature alveolar macrophages derived from bronchoalveolar lavages (Mbawuike and Herscowitz 1989). The peritoneal macrophage-like cell line J774.A1 (Deutsche Sammlung von Mikroorganismen und Zellkulturen (DSMZ), Braunschweig, Germany) derived from an ascites of a Balb/C mouse and was kept in Dulbecco's modified Eagle medium (DMEM) with 10% heat-inactivated FBS. These cells show the morphological, cytotoxic and adherence properties of primary peritoneal macrophages (Ralph et al. 1975). Both cell lines were maintained and propagated at 37°C and 5% CO_2 atmosphere.
For interaction experiments macrophages were used between passages 10 and 20 and seeded at a concentration of 2×10^5 per well in 8 well chamber slides (Nunc, Roskilde, Denmark) 24 h prior to the experiment, resulting in a confluent monolayer at the time of experimentation.

3.4.2 Primary macrophages

3.4.2.1 Human monocyte-derived macrophages

The use of human primary cells in this study was conducted according to the principles expressed in the Declaration of Helsinki. All protocols used in this study were approved by the local ethics committee of the University of Jena under the permit no. 2207-01/08. Written informed consent was provided by all study participants. Human peripheral blood mononuclear cells (PBMCs) were isolated with Histopaque-1077 by density centrifugation

from buffy coats donated by healthy human volunteers. To differentiate PBMCs into monocyte-derived macrophages (MDMs), 2×10^7 PBMCs were plated in RPMI 1640 media containing 10% heat-inactivated FBS (Gibco, Invitrogen, Karlsruhe, Germany) in cell culture dishes. Ten ng/ml human M-CSF (ImmunoTools, Friesoythe, Germany) were added to the cultures to induce the differentiation of macrophages. After 5 days at 5% CO_2 and 37°C, non-adherent cells were removed and purity of MDMs was determined by staining with an anti-CD14 antibody using flow cytometry. The percentage of CD14-positive cells was ≥ 80%. All experiments were performed with cells isolated from at least three different donors.
For infection experiments, adherent MDMs were detached with 50 mM EDTA and plated in flat-bottom 96 or 24 well plates (Nunc, Rosskilde, Denmark) containing RPMI 1640 with 10% heat-inactivated FBS (Gibco, Invitrogen) to give a final concentration of approximately 5×10^4 cells/well or 2×10^5 cells/well respectively. For microscopic analyses 2×10^5 cells/well were allowed to adhere over night to 8 well chamber slides prior to infection.

3.4.2.2 Murine alveolar macrophages

Murine alveolar macrophages were isolated from lungs of healthy, specific pathogen-free eight to ten weeks old CD-1 mice. In brief, mice were euthanised, and the trachea was prepared *in situ*. 1 ml of sterile PBS was instilled *via* the trachea into the lung and the procedure was repeated twice. The bronchoalveolar lavage fluid (BALF) of ten mice was pooled and centrifuged for 10 min at $300 \times$ g. The pellet was resuspended in RPMI 1640 supplemented with 10% heat-inactivated FBS and 1% Penicillin/Streptomycin. Cells were plated in 8 well chamber slides at a density of 2×10^5 cells/well and used one day after inoculation.

3.4.2.3 Murine bone marrow-derived macrophages

To obtain murine bone marrow-derived macrophages, the femurs of healthy, specific pathogen-free eight to ten weeks old CD-1 mice were opened aseptically and the bone marrow was removed by washing with 2 ml of sterile, ice-cold PBS. After washing, the cell suspension was vortexed vigorously. The cells were pelleted by centrifugation for 10 min at 4°C and 300 $\times$ g, resuspended in RPMI 1640 supplemented with 10% heat-inactivated FBS and filtered through a 40 µm cell strainer. Cells were seeded at 1×10^6 cells/well in 6 well polystyrene plates containing RPMI 1640 supplemented with 10% heat-inactivated FBS, 1% Penicillin/Streptomycin and 10 ng/ml murine M-CSF (ImmunoTools). After five days of incubation at 37°C and 5% CO_2, non-adherent cells were removed by washing three times

with sterile PBS. Fresh RPMI 1640 supplemented with 10% heat-inactivated FBS was added prior to challenge with conidia.

Name	Cell type	Donor and Source	Culture medium
MH-S	alveolar macrophage	mouse; cell line	RPMI 1640 + FBS
J774.A1	peritoneal macrophage-like	mouse; cell line	DMEM + FBS
MDM	monocyte-derived macrophage	human; primary	RPMI 1640 + FBS
AM	alveolar macrophage	mouse, primary	RPMI 1640 + FBS
BMDM	bone marrow-derived macrophage	mouse; primary	RPMI 1640 + FBS

Table 2: Cell lines and primary cells used in this study

3.5 Cell-based interaction assays

3.5.1 Phagocytosis assay

Phagocytosis assays were performed as described previously (Ibrahim-Granet et al. 2003) with some modifications. Macrophage cell lines were plated in 8 well chamber slides in RPMI or DMEM, depending on the cell line, supplemented with 10% heat-inactivated FBS. Cells were infected with FITC-labelled conidia at a magnitude of infection (MOI) of 0.1 (1 conidium per 10 macrophages). After brief centrifugation, slides were incubated for the periods indicated in the results section. At the end of each incubation period the assay medium was removed and cells were fixed directly with 4% PFA for 10 min at room temperature (RT). After washing with 0.05 M NH_4Cl (dissolved in PBS) cells were incubated for 10 min in 0.05 M NH_4Cl.

Prior to addition of antibodies, cells were blocked for 30 min at RT with blocking buffer (1% bovine serum albumin (BSA) dissolved in sterile PBS). After blocking, slides were incubated for 30 min at RT with a specific rabbit anti-conidia antiserum (kindly provided by Frank Ebel) at a dilution of 1:50 in blocking buffer. For fluorescence detection, slides were

incubated with a specific anti-rabbit Texas Red conjugated antibody (Invitrogen, Groeningen, Germany) diluted 1:1000 in blocking buffer for 30 min at room temperature in the dark.
Slides were then washed three times with PBS and analysed by microscopy. Phagocytosed conidia showed a bright green fluorescence (derived from the FITC-labelling) signal only whereas extracellular conidia additionally showed a red signal (derived from the Texas Red antibody). Phagocytosis rate in percent was determined per well as the number of intracellular conidia per 1,000 conidia counted. Three individual wells were evaluated per slide, strain and time point and experiments were performed in biological triplicates.

3.5.2 Receptor blocking assay

In general, blocking of pathogen recognition receptors was performed by incubating macrophages prior to infection with blocking agents in culture medium containing 10% heat-inactivated FBS. For dectin-1 blocking, macrophages were incubated with 2 mg/ml laminarin (from *Laminaria digitata*) for 10 min on ice. The mannose receptor was blocked by addition of 2 mg/ml mannan from *Saccharomyces cerevisiae* for 15 min at RT (Schulert and Allen 2006). Blocking of TLR2 and TLR4 was performed overnight at 37°C using 15 µg/ml of specific antibodies (eBioscience, Frankfurt, Germany) (Graveline et al. 2007). Prior to infection medium containing blocking reagents was removed, the cells were washed three times with sterile PBS and then infected with conidia in medium containing 10% heat-inactivated FBS. After infection, the standard phagocytosis assay was performed as described above (3.5.1).

3.5.3 Killing assays

3.5.3.1 Single-cell killing assay

Co-incubations of macrophages and pre-swollen conidia were stained with the FUN-1 dye (Invitrogen, Darmstadt, Germany) (Marr et al. 2001) according to the manufacturer's guidelines. The FUN-1 dye indicates metabolic activity by distinct fluorescence patterns. Living conidia showed green to yellowish cytoplasm with a bright red vacuole, while dead conidia showed a yellow cytoplasm. Fluorescence was observed using the Axio Imager M1 microscope equipped with the Filter Set 01; BP 365/12, FT 395, LP 397, (Zeiss, Jena, Germany). Viability of the conidia without co-incubation was assessed additionally in each experiment. Both *Aspergillus* species were analysed in parallel. The killing rate was determined from the number of metabolically inactive/dead conidia per number of conidia investigated. In each experiment 1,000 conidia per strain and well were evaluated. The experiments were performed in three biological replications each containing three technical replicates.

3.5.3.2 Determination of colony-forming units

Additionally, killing was quantified as colony-forming units (CFU). Here, either primary murine BMDMs or the alveolar macrophage cell line MH-S were plated at a density of 1×10^6 cells/well in 6 well polystyrene plates (Nunc, Rosskilde, Denmark) one night prior to infection. Conidia of the indicated strains were added at an MOI of 0.1 and incubated for 3 h and 10 h. After incubation, macrophages were lysed with ice-cold sterile deionised water for 15 min. Then cells were scraped from the bottom of the well with a rubber policeman. Serial dilutions were plated on malt extract agar plates and incubated for at least 36 h at 37℃. The percentage of survival was calculated with reference to control conidia incubated in the absence of macrophages.

3.5.4 Macrophage damage assay

Damage to macrophages after co-incubation with pre-swollen conidia was determined as the release of lactate dehydrogenase (LDH) into the medium using the Cytotoxicity Kit-LDH (Roche, Mannheim, Germany). The assays were performed according to the manufacturer's instructions. Three biological replicates in technical triplicates were evaluated. To measure cell damage, the following calculation was used: 100 × LDH release (infected macrophages – uninfected macrophages – conidia only) / (100% lysed macrophages – uninfected macrophages) = relative cytotoxicity (%). Uninfected macrophages, conidia only and 100% macrophage lysis (achieved by adding 0.2% Triton X-100) served as controls and were determined individually for each treatment and incubation period.

3.5.5 Inhibition of macrophage v-ATPase

To inhibit phagolysosome acidification, bafilomycin A1 was added to macrophage monolayers at a final concentration of 25 nM 10 min prior to infection. Cells treated with bafilomycin in the absence of conidia served as controls.

3.6 Microscopic analysis of macrophage fungal interaction

3.6.1 Analysis of phagolysosome maturation

All antibodies and dyes used for analysis are indicated with the respective dilutions in Table 3.

Phagolysosome maturation was determined from co-incubations with pre-swollen conidia in 8 well chamber slides as described in (3.2.1.2) using specific antibodies and fluorescence

microscopy. For immunofluorescence analysis, cells were fixed with 4% PFA in H_2O after 3 h and 8 h of co-incubation, permeabilised for 15 min with 0.1% Triton X-100 dissolved in PBS and blocked for 30 min with Image IT FX signal enhancer (Invitrogen). Samples were then washed with PBS and either incubated for 1 h at RT with primary antibodies against Lamp-1 (anti-mouse Lamp-1 Alexa Fluor 647; Santa Cruz Biotechnology, Heidelberg, Germany; diluted in blocking solution (1% BSA in PBS, pH 7.4); or Cathepsin D (rabbit anti-mouse Cathepsin D antibody; Epitomics Inc., Burlingame, United States, diluted in blocking solution). For fluorescence detection of Cathepsin D antibodies, samples were then incubated for 1 h at RT with a anti-rabbit Dylight 549 conjugated antibody (Rockland Immunochemicals, Gilbertsville, USA; diluted in blocking solution).

To investigate acidification of phagolysosomes, macrophages were incubated with Lysotracker DND99 (Invitrogen; diluted in RPMI supplemented with 10% heat-inactivated FBS) for 2 h at 37℃ prior to infection.

For general visualisation of nuclei, cells were stained with DAPI (Pro Long Gold antifade reagent with DAPI, Invitrogen).

Fluorescence microscopy was performed on a Zeiss LSM 710 microscope (Carl Zeiss, Jena, Germany).

Antibody or Staining	Specificity	Colour	Dilution
anti Lamp-1 Alexa Fluor 647	murine LAMP-1	red	1:100
anti Cathepsin D	murine Cathepsin D	non-fluorescent	1:1000
goat-anti rabbit Dylight 549	rabbit	red	1:5000
Lysotracker DND99	acidic cell compartments	red	1:5000
FITC	general cell wall label	green	1:10000
DAPI	nucleic acids	blue	

Table 3: Antibodies and dyes used for fluorescence microscopy

3.6.2 Transmission electron microscopy

For transmission electron microscopy (TEM), alveolar macrophages were grown in 24 well plates with a polystyrene bottom at a concentration of 2×10^5 cells per well, reaching confluency at the time of experimentation. *A. terreus* was added at a MOI of 1. Eight and 24 h post infection, samples were washed 3 times with PBS to remove non-adherent cells. Samples were directly fixed with Karnovsky fixative (3% paraformaldehyde, 3.6% glutaraldehyde, pH 7.2) for 24 h.
Further processing and processing of images was kindly performed by B. Fehrenbacher and Prof. M. Schaller (Eberhard Karls University, Tübingen, Germany).

3.7 Analysis of conidial cell wall components and resistance to pH

3.7.1 Flow cytometric analysis of β-1,3-glucan and galactomannan exposure on conidia

Flow cytometry was used to quantify the β-1,3-glucan and galactomannan exposure of *A. terreus* and *A. fumigatus* on resting and pre-swollen conidia by using specific antibodies as indicated in Table 4. Mouse IgG2b or IgM (eBioscience) were used as isotype controls. Resting and pre-swollen conidia were investigated in parallel. Resting and pre-swollen conidia were incubated for 1 h in 4% PFA dissolved in H_2O at RT, then for 1 h in NH_4Cl (0.05 M dissolved in PBS) and finally washed three times with PBS. To inhibit unspecific binding of primary antibodies, conidia were incubated in blocking solution (1% BSA in PBS) for 1 h at RT. After washing with PBS, conidia were incubated at 4℃ overnight on a vertical rotator with 10 µg/ml primary antibodies diluted in blocking solution. Following three times washing with PBS 10 µg/ml of a FITC-labelled goat anti mouse IgG/IgM antibody (Invitrogen) were applied, and conidia were incubated for 3 h at RT in the dark. After additional five washings with PBS, measurement was performed in flow cytometry buffer (BD) on a Becton Dickinson LSRII (BD). 20000 events were counted. Data were further analysed with the FlowJo software (Tree Star, Ashland, USA). At least three biological replicates were analysed.

Antibody	Isotype	Donor	Reference
anti β-1,3-glucan	IgG2b	mouse	Torosantucci et al. 2009
anti galactomannan	IgM	mouse	Heesemann et al. 2011
goat anti mouse IgG	IgG2b	goat	Invitrogen
goat anti mouse IgM	IgM	goat	Invitrogen

Table 4: Antibodies used for flow cytometry analysis

3.7.2 pH resistance of conidia

1×10^6 pre-swollen conidia were incubated for up to seven days at 37°C and shaking in 1 ml 0.1 M sodium phosphate buffer supplemented with 0.3 M potassium chloride and adjusted to the desired pH. At the indicated time points (4.2.7), suspensions were analysed microscopically for clumping and germination and serial dilutions were plated in triplicates on malt extract agar plates. CFU were counted after 24 h at 37°C. Additionally, the pH of the buffer was measured to confirm that the suspension maintained the desired pH. Experiments were performed in biological triplicates. Survival at pH 7 was set to 100%, and the relative survival compared to pH 7 is shown.

3.7.3 Microscopical analysis of germination speed

Analysis of the germination speed at different pH values was performed by fluorescence microscopy. Therefore FITC-labelled resting conidia were incubated for 8 h at 37°C and 5% CO_2 in Aspergillus minimal medium (Prasad and Sandhu 1975) with the pH adjusted to the desired value. Germination was analysed using an Axio Imager M1 (Zeiss, Jena, Germany).

3.8 Statistical analyses

Data were plotted and analysed statistically using GraphPad Prism 5.0 (GraphPad software Inc., La Jolla, USA).

In vivo infection experiments were evaluated for survival by Kaplan Meyer curves and log rank test. Cytokines, myeloperoxidase, and blood enzyme data were analysed using 1-way

ANOVA followed by Tukey-Kramer test. *p*-values < 0.05 were considered as significant (*) or < 0.01 or < 0.001 as highly significant, abbreviated as (**) or (***/#), respectively.

In vitro experiments were evaluated either by Student's t-test or 1-way ANOVA as indicated in the respective results section and corresponding figure. *P*-values < 0.05 were considered as significant (*) or < 0.01 or < 0.001 as highly significant, abbreviated by (**) and (***), respectively.

4 Results

4.1 Establishment and characterisation of infection models for the investigation of *A. terreus* mediated invasive bronchopulmonary aspergillosis

For the investigation of *A. fumigatus* mediated IBPA several infection models had previously been developed. To compare *A. terreus* directly *in vivo* to *A. fumigatus*, an alternative infection model using embryonated chicken eggs, and two distinct murine infection models were developed using analogous protocols to already existing *A. fumigatus* infection models.

4.1.1 Strain selection by virulence studies in embryonated eggs

Embryonated chicken eggs had previously been shown to provide a suitable screening model for virulence of *A. fumigatus* wild type and mutant strains (Jacobsen et al. 2010; Olias et al. 2011). Thus, to select a strain and estimate the infectious dose for murine virulence studies, the virulence of *A. terreus* wild-type strains A1156, SBUG402 and SBUG844 were investigated in embryonated eggs. Dose-dependent killing was observed with 1×10^4 to 1×10^7 conidia per egg (Fig. 5A). For comparable mortality rates, a 1,000 times higher dose of *A. terreus* conidia was needed compared to the *A. fumigatus* wild type CBS144.89 (Fig. 5B and C). *A. terreus* SBUG844, which showed very homogenous growth phenotypes, displayed the highest reproducibility and virulence in these experiments (Fig. 5B and C) and was thus selected for subsequent studies. Furthermore, as shown for *A. fumigatus* (Jacobsen et al. 2010), the embryonated egg infection model revealed excellent reproducibility for *A. terreus* (data not shown).

Histologically, conidia were detected inside or closely attached to the upper epithelial layer of the chorio-allantoic membrane (CAM) 8 h and 24 h after infection (Fig. 6B). 48 h after infection hyphae already penetrated the underlying tissue (Fig. 6C). These hyphae induced recruitment of immune cells (Fig. 6D). Embryos which succumbed to infection showed massive destruction of the CAM by fungal mycelia. In contrast, surviving embryos displayed typical granuloma formation which likely restricted and demarked tissue invasion (Fig. 6E). Demonstrating invasive growth of *A. terreus*, these experiments also implied, compared to *A. fumigatus*, that a significantly higher infectious dose might be required in murine infection models to induce bronchopulmonary aspergillosis by *A. terreus*.

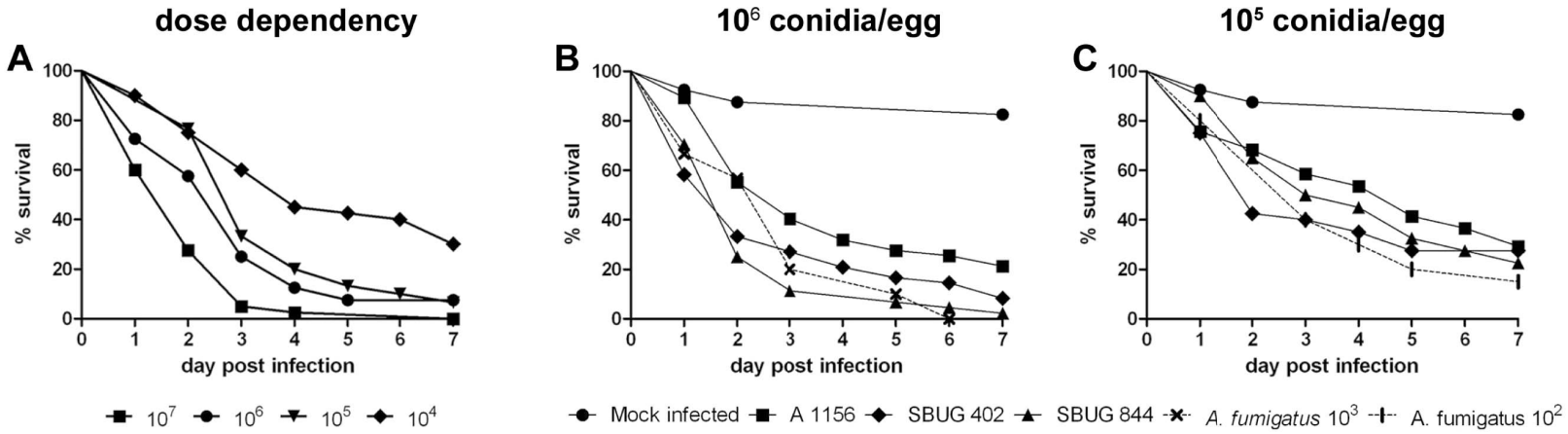

Fig. 5: Analysis of dose dependency and strain specificity in the embryonated egg model

A: Dose-dependent survival of embryonated eggs after infection with *A. terreus* strain SBUG844 (n= 3 × 20). B and C: Strain-dependent survival after infection with 1×10^6 (B) and 1×10^5 (C) conidia, PBS mock infected eggs served as controls (n= 3 × 20). For comparison, survival after infection with *A. fumigatus* wild-type strain CBS144.89 is shown by dotted lines (B: 1×10^3 conidia/egg; C: 1×10^2 conidia/egg).

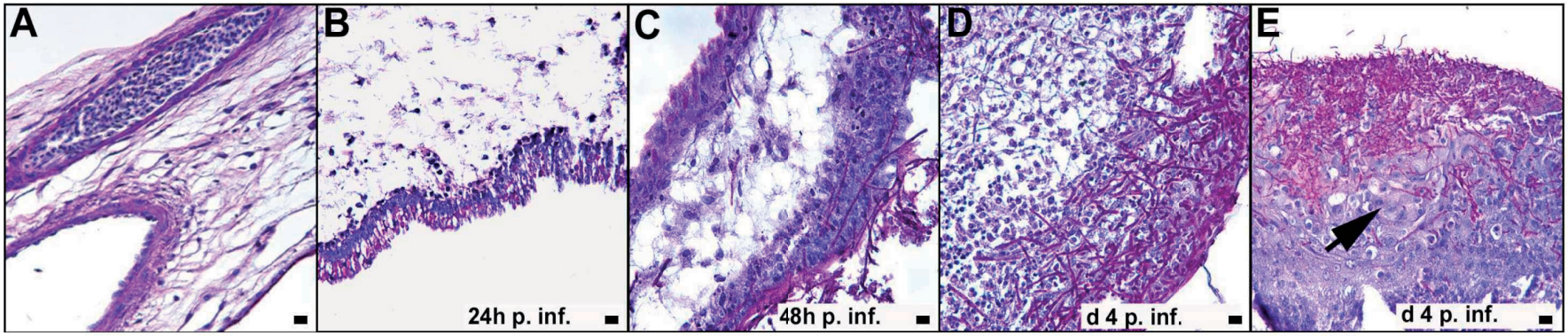

Fig. 6: Histological analysis of *A. terreus* infected embryonated eggs

A - E: Histology of the CAM, PAS reaction. A: CAM of a mock-infected egg. B - E: Infection with 1×10^6 conidia of strain SBUG844. (B) After 24 h conidia (stained in pink) are attached to the upper epithelial layer. (C) Hyphae (stained in pink) start penetrating the CAM after 48 h. (D, E) Four days post infection and at later time points, immune cell and fibroblast infiltration (visualised by an arrow in E) become visible to demark the invading mycelium; scale bars represent 10 µm (p. inf.= post infection).

4.1.2 Dose-dependent survival of leucopenic and corticosteroid-treated mice infected with *A. terreus*

A bioluminescent *A. fumigatus* strain had been shown to be useful for investigating the progression of bronchopulmonary aspergillosis in mice (Brock et al. 2008; Ibrahim-Granet et al. 2010). Therefore, a bioluminescent *A. terreus* strain was constructed (kindly constructed and provided by Dr. Matthias Brock), in which expression of a codon-optimised luciferase gene was driven by the *A. fumigatus gpdA* promoter, a very strong and mostly constitutively expressed promoter regulating the glutaraldehyde-3-phosphatase dehydrogenase gene. The strain SBUG844_2/7/15_luc$_{OPT}$ was chosen for mouse experiments because it displayed a high bioluminescent signal under various *in vitro* growth conditions, no growth defects and virulence comparable to the parental strain in the embryonated egg model (data not shown).
For bioluminescence imaging mice were either rendered leucopenic or immunosuppressed with corticosteroids prior to infection. Immunosuppressive effects were confirmed by leucocyte counts and differential blood counts (Fig. 7A and B).

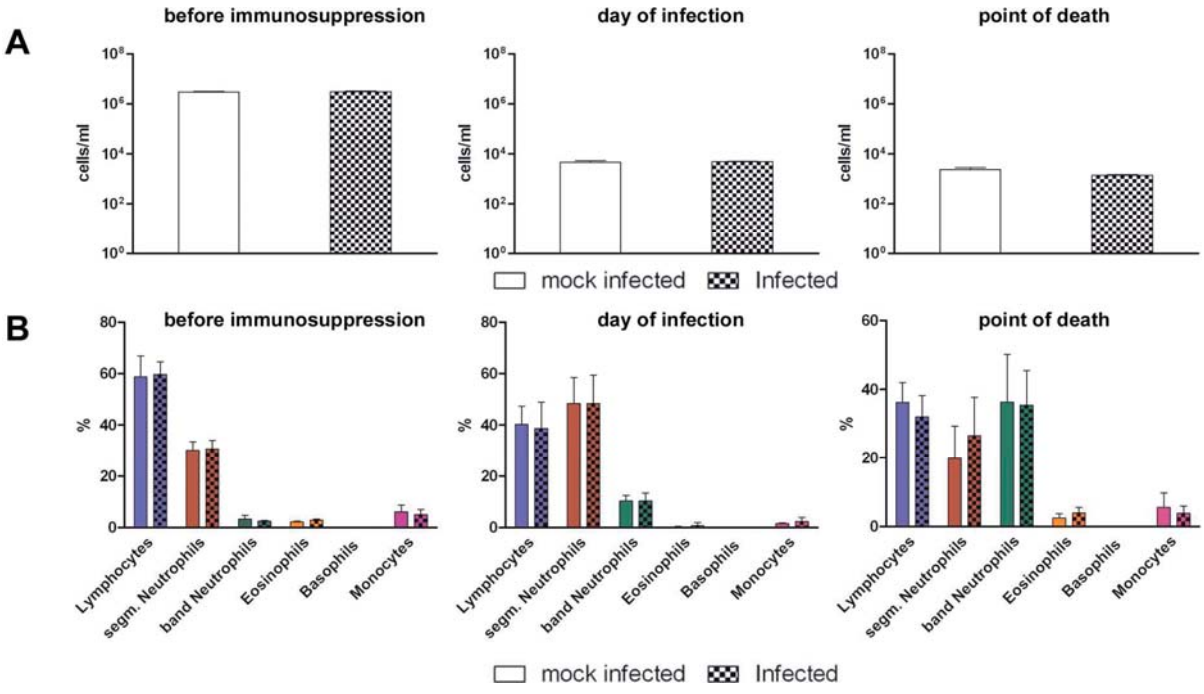

Fig. 7: **Monitoring of immunosuppressive treatment effects in mice**

A: Cyclophosphamide model. Total leucocyte counts were performed; mean + SD (n= 30). B: Corticosteroid-treated animals. Relative leucocyte populations in % were determined by cell differentiation; mean + SD (n= 30). Total white blood cell counts remained unaltered, whereas the proportion of neutrophils increased.

To induce lethal *A. fumigatus* infections in mice 5×10^4 conidia per mouse are sufficient in a leucopenic model (Liebmann et al. 2004), while 1×10^5 conidia are routinely used in the corticosteroid-based model (Schöbel et al. 2010). Since a 1,000 times higher infectious dose was needed for *A. terreus* infections in the egg model, at least 100 times higher infectious doses were estimated to be needed for lethal murine infections. To detect the minimal lethal dose and prove dose dependency groups of five leucopenic animals were infected with 5×10^5, 1×10^6 or 1×10^7 conidia. Analogous groups of corticosteroid-treated mice were infected intranasally with 1×10^6, 5×10^6 or 1×10^7 conidia per animal. Additionally to monitoring survival of the animals, fungal development was monitored daily by bioluminescence imaging. Leucopenic mice developed luminescence signals mainly four to six days after infection when challenged with 1×10^6 or 1×10^7 conidia (data not shown). Signal intensity steadily increased until mice succumbed to infection (Fig. 8A). This result was similar to that obtained for *A. fumigatus* infections (Ibrahim-Granet et al. 2010), but significantly higher conidia concentrations were needed with *A. terreus* and resulted in 3 - 4 days retarded luminescence (Ibrahim-Granet et al. 2010).

Corticosteroid-treated mice only developed lethal disease if infected with 1×10^7 conidia which is 100fold higher than for *A. fumigatus* (Schöbel et al. 2010). These animals displayed weak luminescence within the first 48 h. The signal then increased significantly and remained at high levels up to day 4 (Fig. 8B upper panel, graph mouse 1). In surviving animals, the signal intensity declined strongly after day 4 and reached basal levels from day seven onwards (Fig. 8B lower panel, graph mouse 2). These animals recovered and showed no clinical symptoms at the end of the experiment on day 10. In contrast, a severe decline of bioluminescence signals in *A. fumigatus* infected corticosteroid-treated mice correlated regularly with strong inflammation, tissue necrosis accompanied by severe respiratory distress and loss of body weight (Brock et al. 2008). These symptoms then finally accounted for the death of the animal.

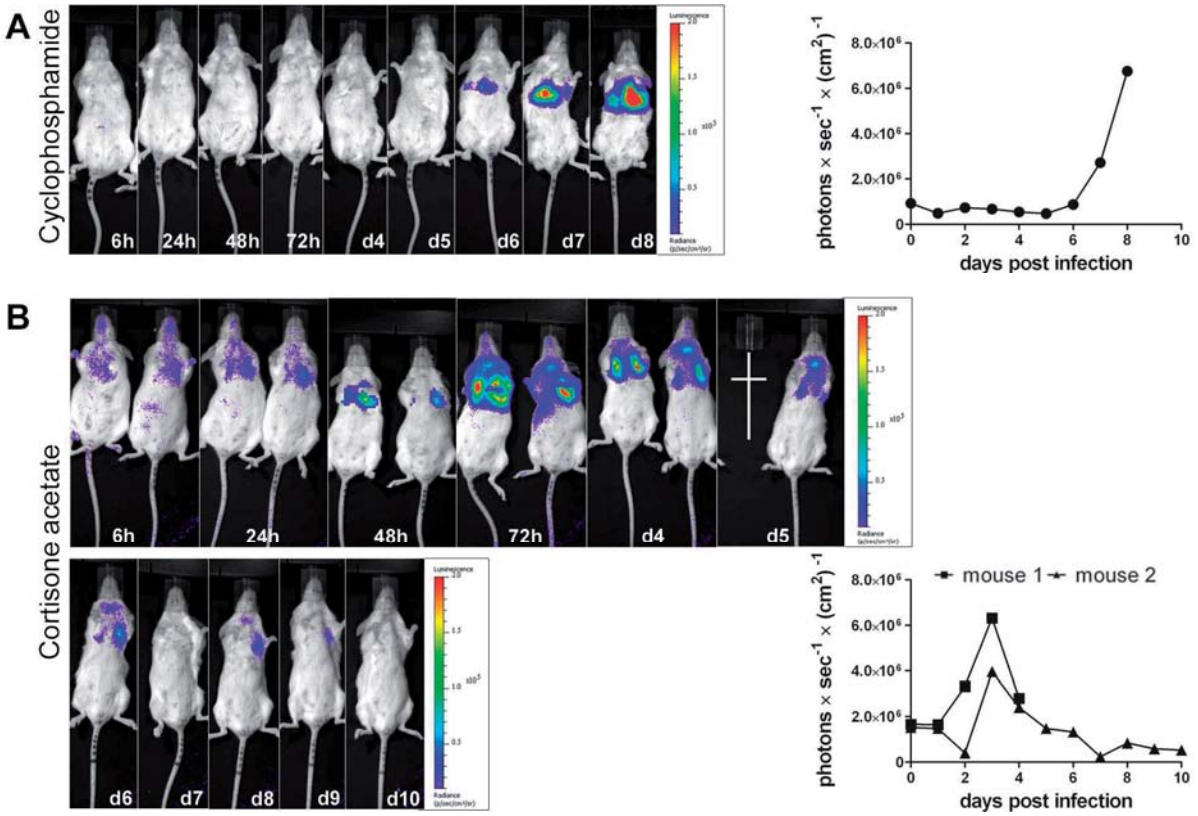

Fig. 8: Fungal distribution and development in the lung of leucopenic and corticosteroid-treated mice infected with *A. terreus* SBUG844 monitored by bioluminescence imaging

A: Representative time course of a leucopenic mouse infected with 1×10^7 conidia. The graph on the right shows quantification of light emission. B: Representative time course of corticosteroid-treated mice infected with 1×10^7 conidia. The mouse on the left hand side succumbed on day 5. The graphs on the right show quantification of light emission (n= 2×5 for each immunosuppression regimen).

To further confirm the challenge doses required for lethal infections in the bioluminescence studies and to ensure that the use of a bioluminescent *A. terreus* strain did not influence the results in any perspective, three additional independent experiments per immunosuppression regimen were performed using the corresponding wild type strain SBUG844. Within each experiment, ten mice were infected with *A. terreus* and five animals received PBS, serving as mock infected control. Leucopenic mice were infected with 5×10^6 conidia leading to 100% mortality within fourteen days (Fig. 9A – D left panel). Nearly all infected corticosteroid-treated mice (1×10^7 conidia per mouse) showed clinical symptoms of disease (ruffled fur, weight loss, dyspnoea). However, only 50% succumbed to infection (Fig. 9A – D right panel).

Moreover, survival curves were higly reproducible between experiments (Fig. 9B – D panels according to the regimen). The clinical status of the surviving 50% improved from day 6 onwards and mice fully recovered towards the end of the experiment at day 14, as shown by the clinical score (Fig. 10).

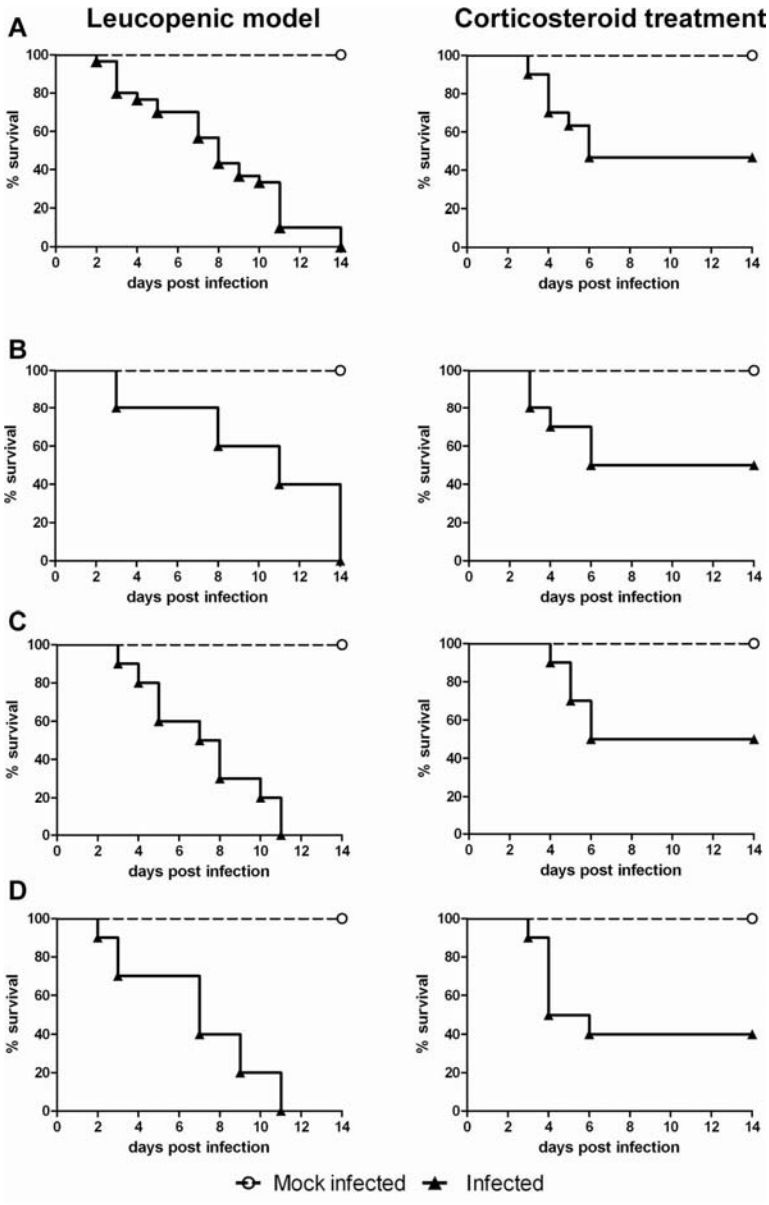

Fig. 9: Survival and reproducibility of leucopenic and corticosteroid-treated mice infected with *A. terreus*

A: Combined data from three independent experiments (B – D) (infected mice: n = 3 × 10; PBS mock infected: n= 3 × 5 for each immunosuppression regimen). Survival of leucopenic mice infected with 5×10^6 conidia (left panel) and survival of corticosteroid-treated animals infected with 1×10^7 conidia (right panel).

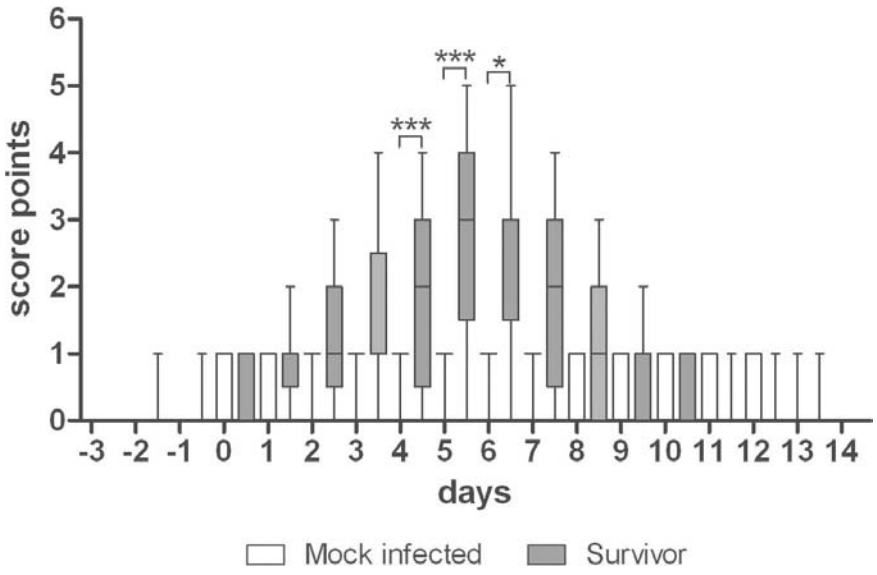

Fig. 10: Clinical course of disease in corticosteroid-treated surviving animals

Clinical symptoms occurred between day three and seven in infected mice. * $p < 0.05$; *** $p < 0.001$ compared to mock infected animals, analysed by 1-way-ANOVA.

To further characterise *A. terreus* IBPA in both murine models, histological analysis and quantification of cytokine response and neutrophil influx of moribund animals from survival experiments was performed. To analyse the kinetics of histological alterations and the immune response, five mice were sacrificed for analysis 48 h, 72 h or 5 days after infection for both immunosuppression regimens or PBS mock infection.

4.1.3 Characterisation of infection in leucopenic mice

All results raised for the characterisation of the leucopenic model were compared to leucopenic PBS mock infected control animals, designated as mock infected or control. Mock infected animals showed no macroscopic or histologic alterations compared to immunocompetent PBS mock infected controls.

4.1.3.1 Characterisation of the pulmonary infection in leucopenic mice

Up to 72 h after infection of leucopenic mice, only swollen conidia but no germlings were observed histologically within the lung. Conidia resided within macrophages and were also observed in epithelial cells (Fig. 11B and C). Germlings became visible at day five (Fig. 11D), coinciding with the late appearance of bioluminescent signals in the imaging experiments. Moribund mice displayed lung alterations characterised by invasive growth of *A. terreus*

hyphae, angio-invasion and necrosis (Fig. 10E). Additionally intact, ungerminated conidia were observed in epithelial cells in moribund animals. Consistent with leucopenia, only sparse immune cell infiltrations were observed. The absence of a strong neutrophil influx in the lungs of infected animals was confirmed by quantification of the myeloperoxidase (MPO) content, a neutrophil marker, in lung homogenates which was indistinguishable from mock infected control animals (data not shown). To investigate the inflammatory response to the fungus the levels of TNFα, GM-CSF, IL-10, IL-17A, INFγ, IL-6, and IL-22 were determined from lung homogenates by quantitative ELISA measurements and were indistinguishable between infected and mock infected control animals at all time points investigated (data not shown). Only IL-1β, quantitatively measured by ELISA, increased moderately (Fig. 11F) in moribund animals. The designated cytokines were selected as they represent pro-inflammatory markers (TNFα, GM-CSF, IL-17A, INFγ, IL-6, IL-1β, IL-22) and the most important regulatory marker in aspergillosis, IL-10.

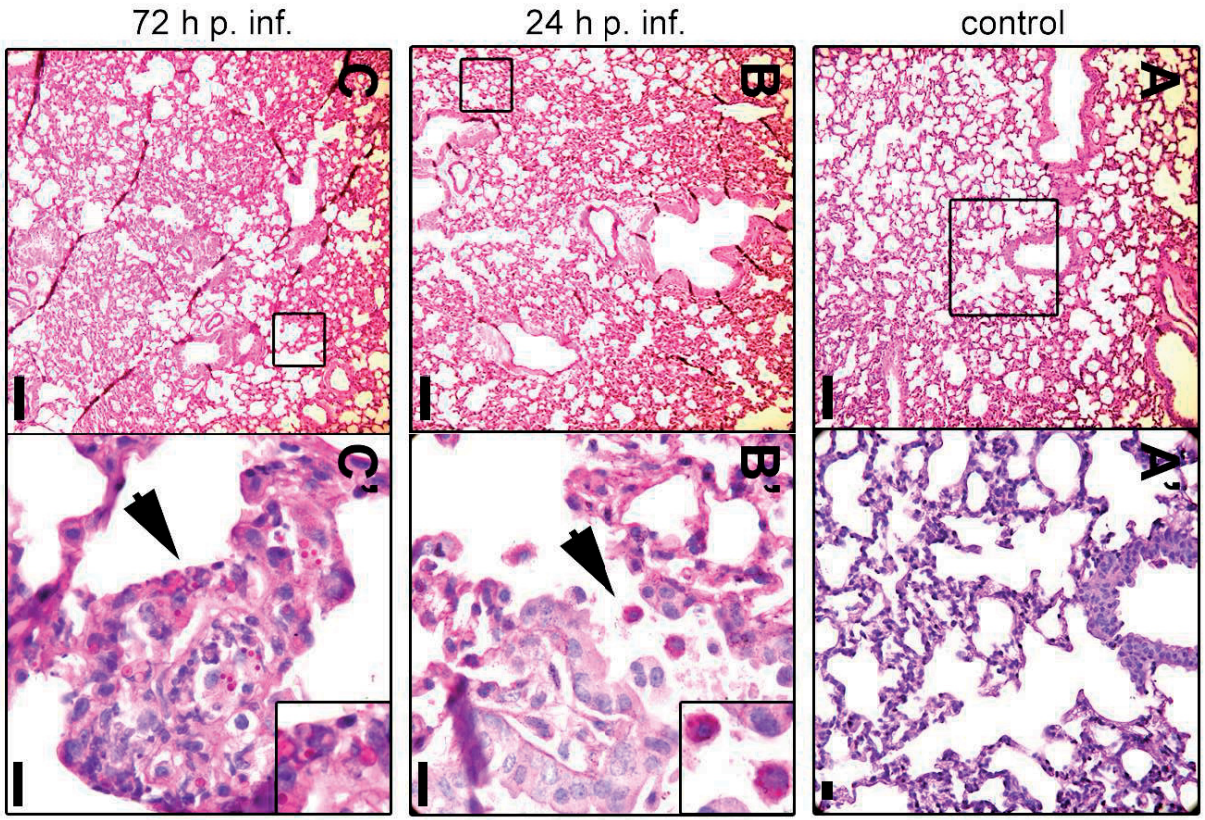

Fig 11: Histological analysis of lungs of leucopenic mice infected with *A. terreus* SBUG844

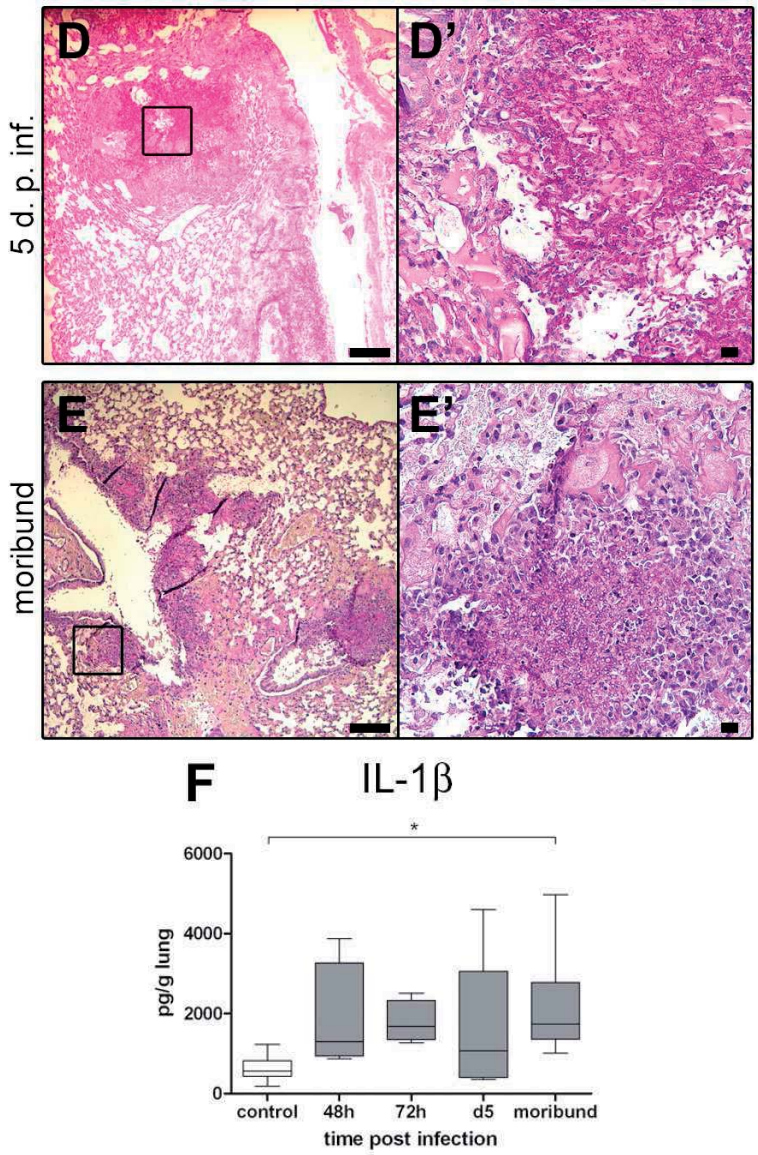

Fig. 11: Histological analysis of lungs of leucopenic mice infected with *A. terreus* SBUG844

A-E: Representative lung histology, PAS reaction. d p. inf.: day post infection. The right panel shows a magnification of the boxed area marked in the respective left panel. Inlays in the right panel (B and C) show additional digital magnifications of a selected area. A: Mock infected control; B-D: Infected lungs at different time points; B', C': Conidia within macrophages and epithelial cells (arrows). D, E: Invasive hyphal growth. Scale bars in the left panel represent 100 µm and 10 µm in the right panel. F: IL-1β levels in lung homogenates, ELISA measurement, mean ± SD; control = mock infected; moribund = sacrificed in moribund conditions. * $p < 0.05$ compared to mock infected animals (1-way- ANOVA).

4.1.3.2 Abdominal organs affected during infection of leucopenic mice

All organs in the abdomen were macroscopically unaltered except the liver. Spleen and kidneys were chosen for histological examination but appeared unaltered at the investigated time points. In contrast, 48 h after infection and onwards, livers of infected mice appeared pale at the periphery of the lobes. Histological analysis revealed small vacuolar, fatty alterations of hepatocytes (Fig. 12A and B) at the lobules' periphery. However, neither conidia nor mycelium were detected histologically and by reisolation in the liver. Furthermore, no signs of inflammation were observed histologically and MPO levels were comparable to controls (data not shown). The serum levels of the liver marker enzymes ALT and AST were not significantly elevated and the liver weight was similar in the compared groups (data not shown).

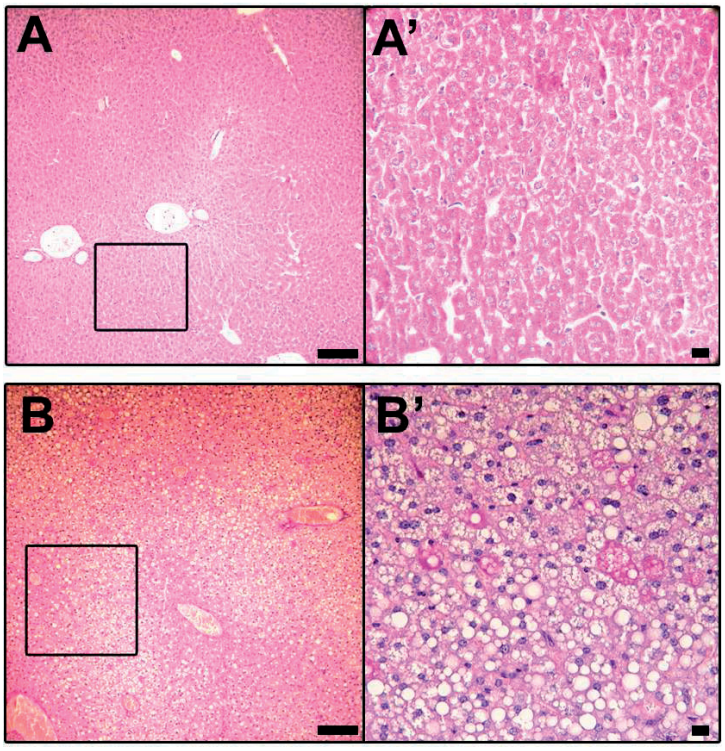

Fig. 12: Liver histology in the leucopenic mouse model

A and B: Representative liver sections, PAS reaction. Fatty, vacuolar liver alterations were observed in infected but not in mock infected control mice. Right panels show magnifications of the area boxed in the respective left panel. A: Mock infected leucopenic mouse. B: Leucopenic mouse infected with *A. terreus* 10 days p. inf.; scale bars represent 100 µm (left panel) and 10 µm (right panel).

4.1.4 Characterisation of infection in corticosteroid-treated mice

All results raised for the characterisation of the corticosteroid treatment model were compared to corticosteroid-treated PBS mock infected control animals, designated as mock infected or control. Mock infected animals showed no macroscopic or histologic alterations compared to immunocompetent PBS mock infected controls.

4.1.4.1 Characterisation of the pulmonary infection in corticosteroid-treated mice

Similar to the leucopenic model, within the first 48 h conidia residing within host cells were observed in corticosteroid mice (Fig. 13B and C). Swelling of conidia started on day three (Fig. 13D) and hyphae were visible on day 5 (Fig. 13E). Infiltration of neutrophils and monocytes accumulating at the site of infection was observed earliest 48 h after infection and increased over time (Fig. 13C-F). In moribund animals, accumulations of hyphae and surrounding immune cells blocked the main air passages likely leading to the observed severe respiratory distress. This also corresponded with severe lung hepatisation observed at necropsy (data not shown), showing the typical pattern of an acute severe bronchopneumonia. Additionally intact but ungerminated conidia were observed in macrophages and epithelial cells in lung areas without pyogranuloma formation. Surviving animals showed only sparse immune cell infiltrates on day 14 after infection, but resting conidia were observed in macrophages and epithelial cells (Fig. 13G).

The recruitment of neutrophils to the lung of infected animals was further reflected by increased MPO levels, which peaked in moribund animals (Fig. 14).

To initially characterise the host response in corticosteroid-treated animals, an inflammation-specific semiquantitative cytokine ELISA-array was performed (see 3.3.7). Based on the array results (Fig. 15), and on the importance in *A. fumigatus* IBPA, the cytokines TNFα, IL-1β, GM-CSF, INFγ, IL-6, IL-10, IL-17 and IL-22 were chosen for quantification by specific ELISAs. TNFα, IL-1β and IL-6 increased over time and showed maximal peaks in moribund animals (Fig. 16). Interestingly, the regulatory cytokine IL-10 was significantly reduced in all animals infected with *A. terreus*. GM-CSF, INFγ, IL-17 and IL-22 levels were indistinguishable from controls (data not shown).

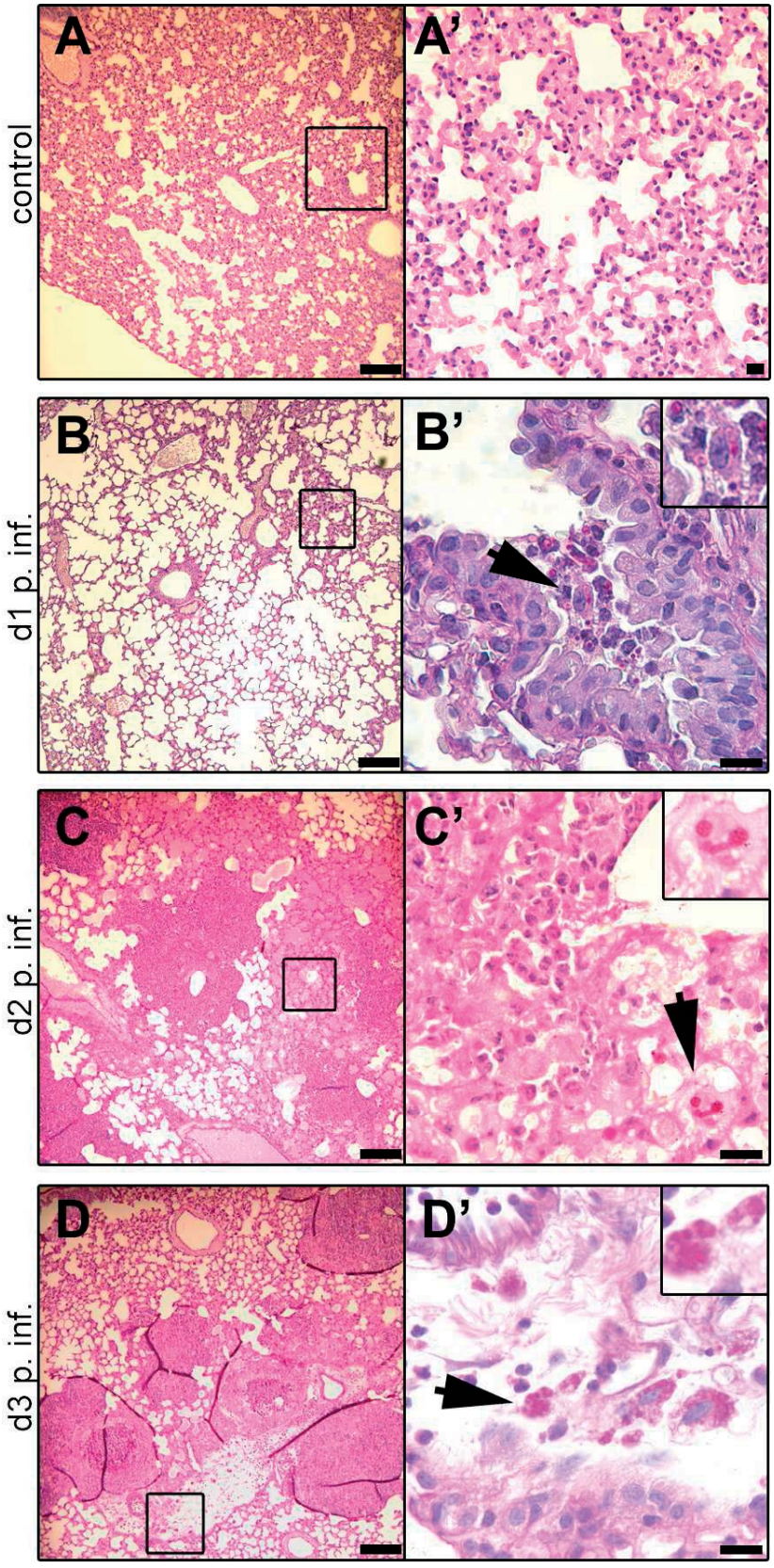

Fig.13: Histological analysis of lungs of corticosteroid-treated mice infected with *A. terreus* SBUG844

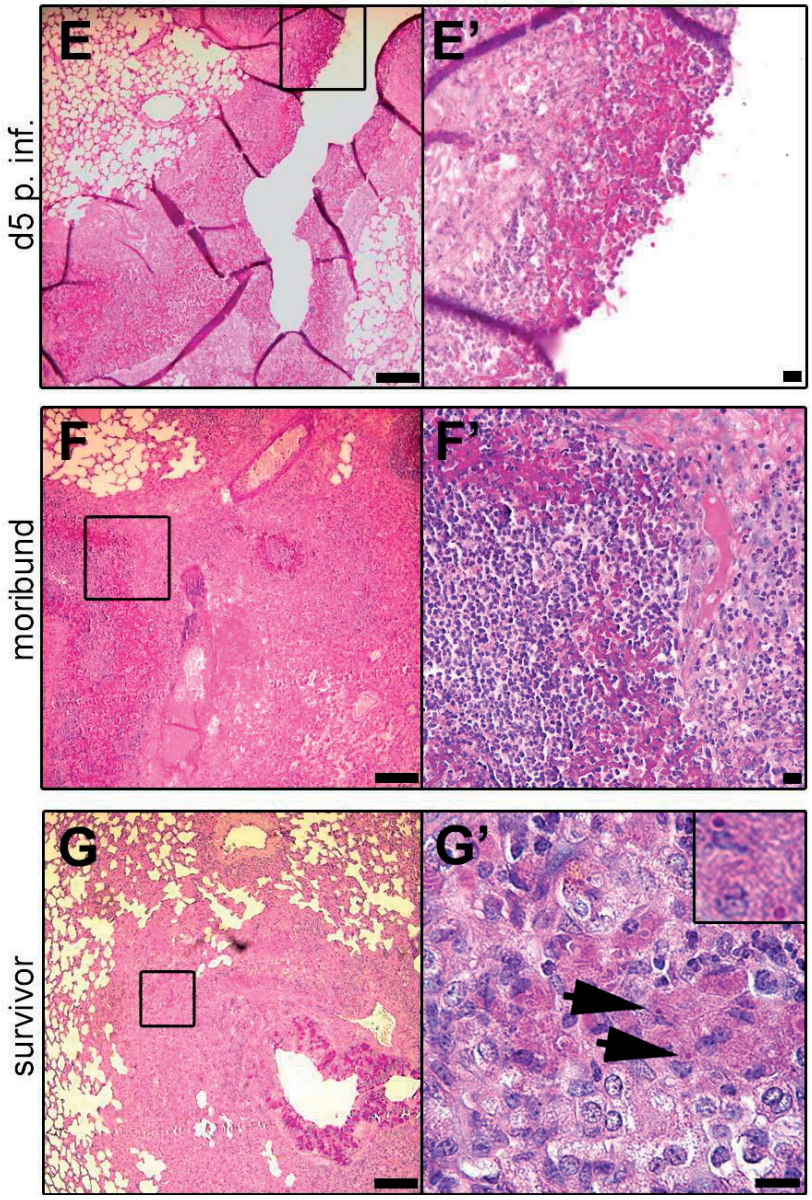

Fig. 13: Histological analysis of lungs of corticosteroid-treated mice infected with *A. terreus* SBUG844

A-G: Representative lung sections, PAS reaction. d p. inf.: day post infection. The right panel shows a magnification of the boxed area marked in the respective left panel. Inlays in the right panel (B-D, G) show additional digital magnifications of a selected area. A: Mock infected lung. B-G: Infected lungs at different time points. B'-D': Conidia within macrophages (arrows). E: Germinating conidia. F: Mycelium and immune cell recruitment. G: Surviving animals, day 14 p. inf.: Minor immune cell infiltrations, conidia residing within macrophages (arrows); scale bars represent 100 µm (left panel) and 10 µm (right panel).

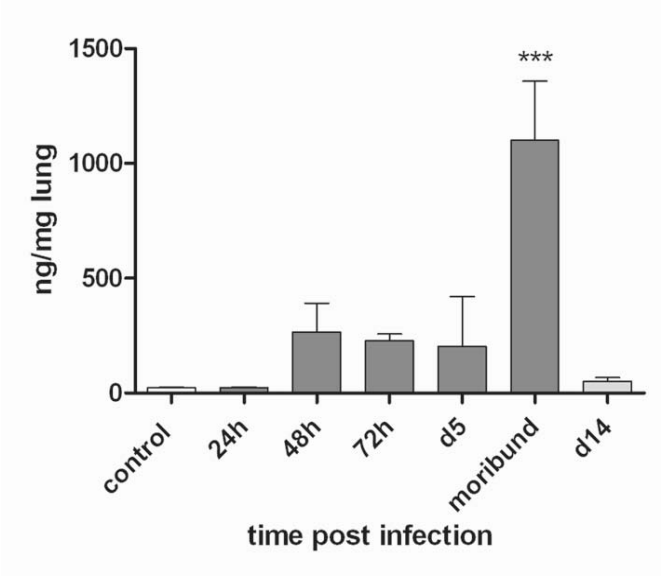

Fig. 14: Myeloperoxidase levels in *A. terreus* infected lungs

MPO levels in the lung of mice sacrificed at the indicated time points or in moribund conditions (moribund) compared to immunosuppressed mock infected mice designated as control; mean + SD; *** $p < 0.001$.

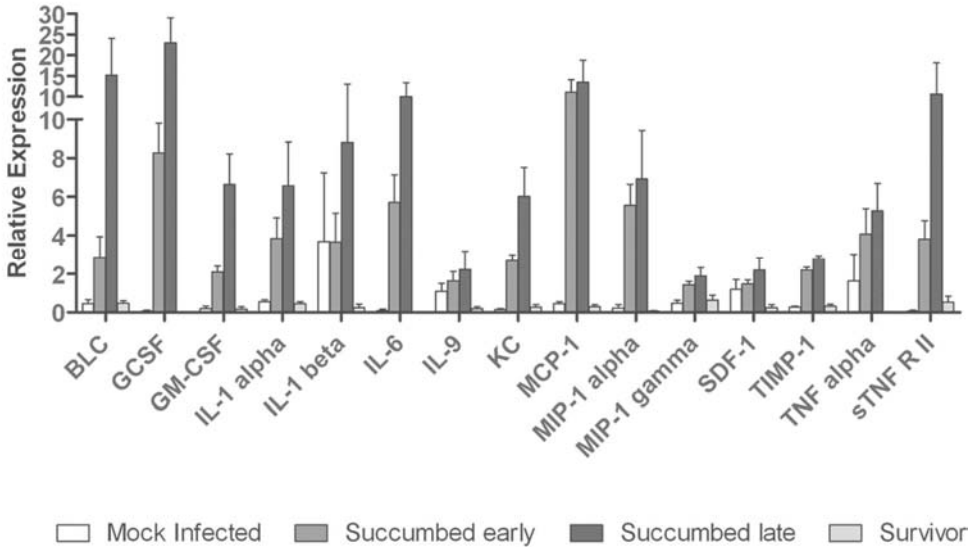

Fig.15: Semiquantitative cytokine array of corticosteroid-treated mice

Semiquantitative analysis of cytokine patterns from lungs of corticosteroid-treated mice relative to the internal array control; mean + SD. Mock infected: immunosuppressed PBS mock infected; Succumbed early: succumbed on day 2 to 4; Succumbed late: succumbed on day 5 to 7; Survivor: sacrificed on day 14.

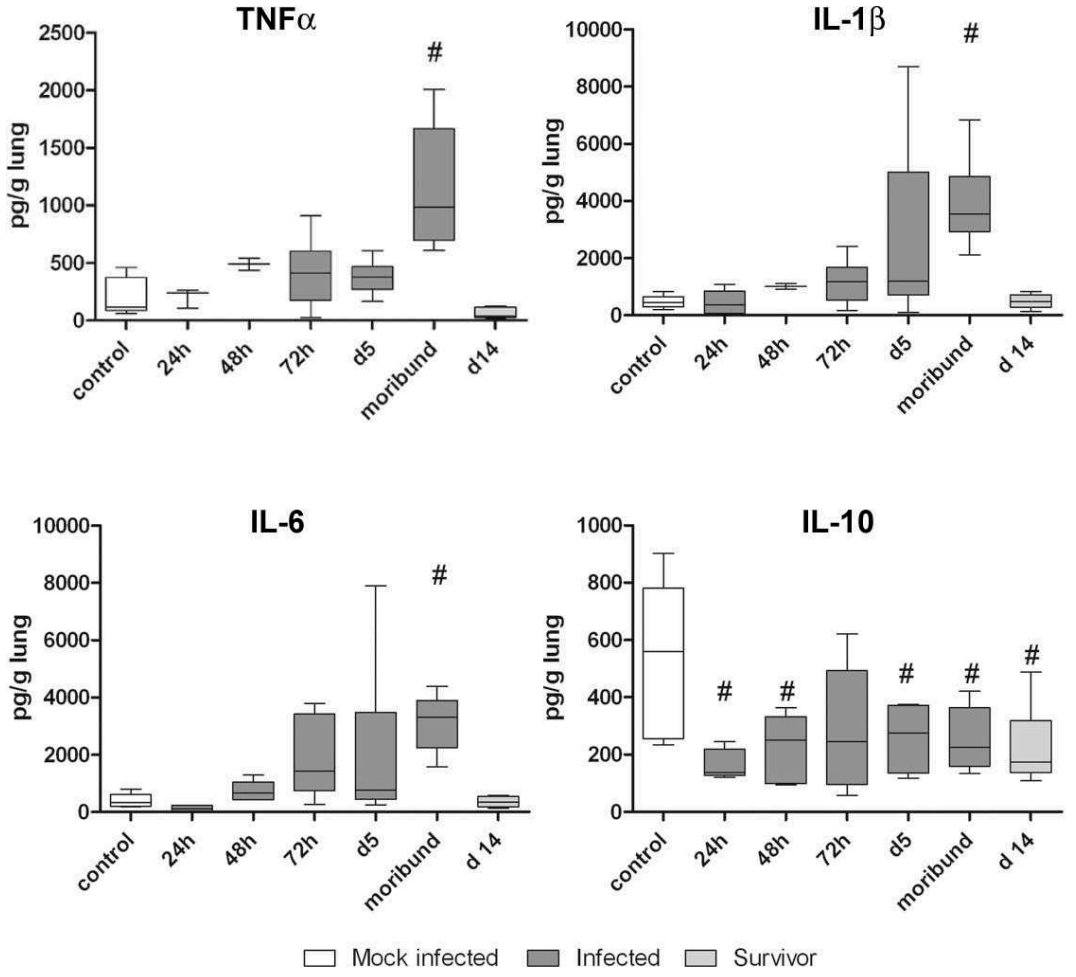

Fig. 16: Cytokine response in corticosteroid-treated *A. terreus* infected lungs

TNFα, IL-1β, IL-6 and IL-10 levels in the lungs of infected animals sacrificed at the indicated time points or in moribund conditions compared to mock infected control animals. Control: immunosuppressed PBS mock infected; mean ± SD; # $p < 0.001$. Statistics were performed using 1-way ANOVA.

To determine whether the observed ungerminated conidia in surviving animals were viable, lung homogenates were plated for isolation of the fungus. Surprisingly, *A. terreus* could be isolated in large numbers from 87% of the *A. terreus* surviving animals (Fig. 17). This suggested that viable fungal cells might persist within the lung during clinical convalescence. MPO, TNFα, IL-1β and IL-6 levels of surviving animals at the end of the experiment were similar to mock infected controls (Fig. 14 and 16).

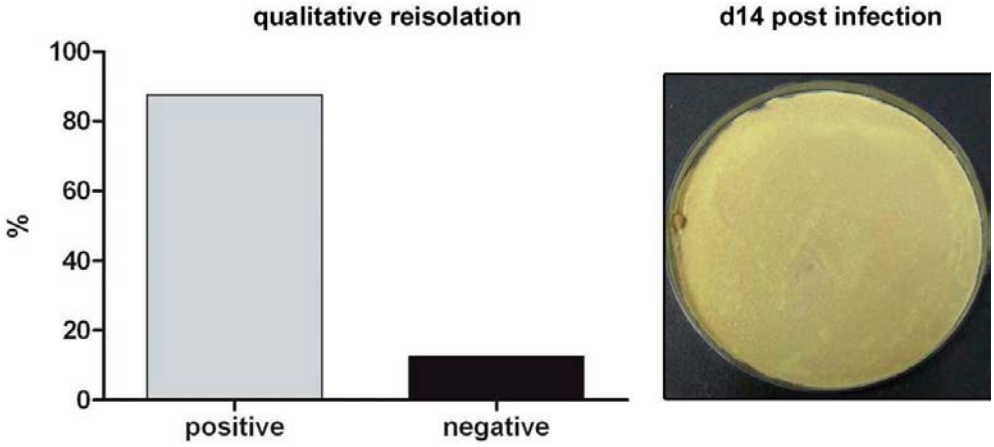

Fig. 17: Qualitative reisolation from lungs of *A. terreus* infected surviving animals

Left: Positive: % infected mice culture positive after sacrifice for *A. terreus*; Negative: % infected mice culture negative for *A. terreus* after sacrifice (n=30). Right: Representative picture of qualitative isolation of *A. terreus* from lung homogenates of corticosteroid-treated mice surviving the infection. Confluent growth on malt extract agar plates inoculated with approximately 20 mg lung homogenate and incubated for 24 h at 37℃.

4.1.4.2 Abdominal organs affected during infection of corticosteroid-treated mice

Similar to leucopenic mice, corticosteroid-treated animals infected with *A. terreus* showed small vacuolar, fatty alterations of hepatocytes in the periphery of the lobules from day 2 onwards (Fig. 18A and B). Mycelium and signs of inflammation were not detectable. MPO levels were not significantly elevated while ALT serum levels were unaltered and AST levels were moderately increased in moribund animals (Fig. 19A and B). Additionally, the liver weight was significantly reduced in moribund animals (Fig. 19B). As hepatocyte alteration was observed in infected animals independent of the immunosuppressive regimen but not in mock infected immunosuppressed control mice, these alterations appear to be infection-specific.

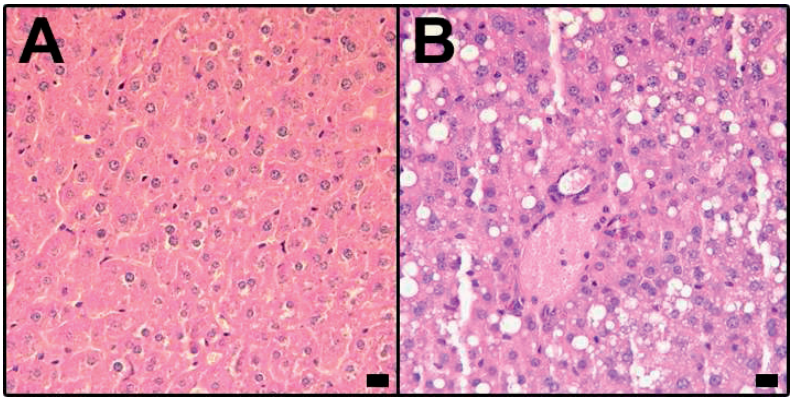

Fig. 18: Liver histology in the corticosteroid mouse model

Representative liver sections of mock infected and infected corticosteroid-treated mice. Fatty, vacuolar liver alterations were observed in infected but not in mock infected control mice. A: mock infected, B: *A. terreus* infected mouse 14 days p. inf.; PAS reaction; scale bars represent 10 µm.

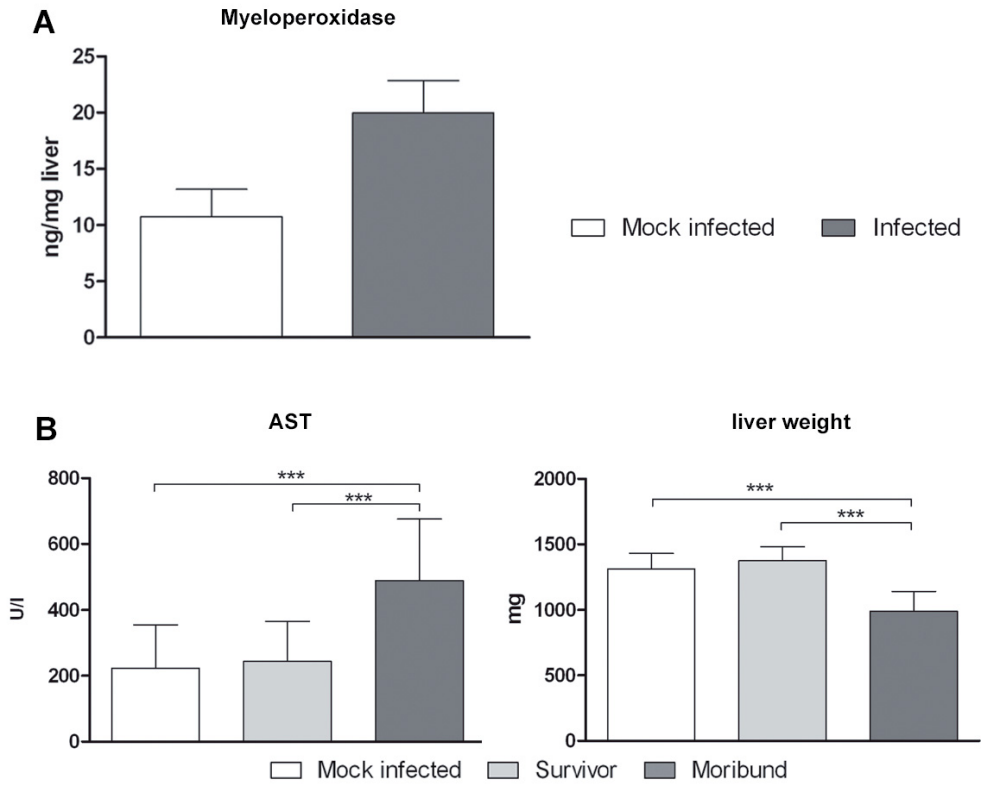

Fig. 19: Inflammatory response and liver damage in the *A. terreus* infected mouse

A: MPO levels in livers of control and infected animals; mean + SD. B: AST levels (left) and liver weight (right); mean + SD. *** $p < 0.001$, analysed by 1-way ANOVA.

4.1.5 Persistence of *A. terreus* conidia in immunocompetent mice

The *in vivo* data suggested that *A. terreus* conidia are able to survive for a prolonged time within macrophages in immunocompromised hosts. These conidia did not induce a pronounced immune response in surviving animals. To elucidate whether persistence in macrophages also occurs in immunocompetent hosts, immunocompetent mice were infected intranasally with 1×10^7 *A. terreus* conidia. Animals were monitored for up to 5 days and compared to immunocompetent PBS mock infected animals. Furthermore, the cytokine response was investigated over time to elucidate whether conidia of *A. terreus* are recognised by the intact immune system and consequently eliminated.

As shown for *A. fumigatus* (Duong et al. 1998; Brieland et al. 2001), all animals remained clinically healthy and displayed no macroscopic alterations at necropsy 24 h, 3 days or 5 days after infection. Semiquantitative isolation of *A. terreus* from the lungs of infected animals revealed persistently high fungal burdens of 5×10^5 or higher without differences between the time points. Histologically, un-swollen but intact conidia within macrophages could be observed in the lungs at all time points (Fig. 20). No germlings or hyphae were found. The lung tissue itself appeared unaltered 24 h and 3 days after infection. However, in all infected mice analysed on day 5 small, single foci of mononuclear cell infiltrates were found in the lungs (Fig. 20). In accordance with cellular infiltrations, the levels of MPO, TNFα, INFγ, GM-CSF, IL-1β and IL-6 transiently increased in lungs of infected compared to PBS mock infected animals (Fig. 21), while levels of IL-10, IL-17A and IL-22 were indistinguishable from mock infected controls. Thus, *A. terreus* conidia did persist *in vivo* for several days within macrophages in the lung despite a severe detectable immune response.

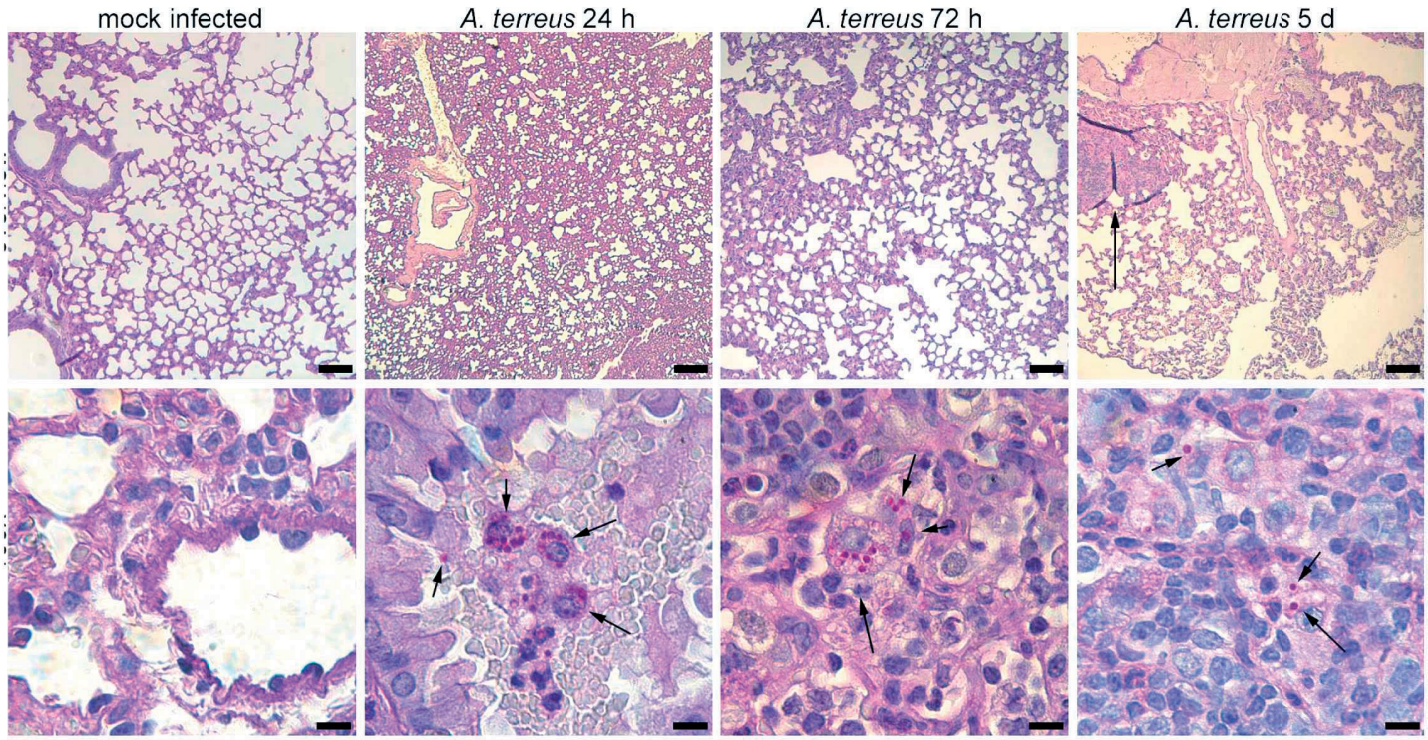

Fig. 20: Persistence of *A. terreus* conidia in the lungs of immunocompetent mice.

Infection was performed with *A. terreus* SBUG844. Histological sections, PAS reaction. 24 h, 72 h, day 5: time after infection. Upper panel: the arrow indicates immune cell infiltrates. Lower panel: arrows indicate *A. terreus* conidia stained in pink; scale bars represent 100 µm (upper panel) and 10 µm (lower panel).

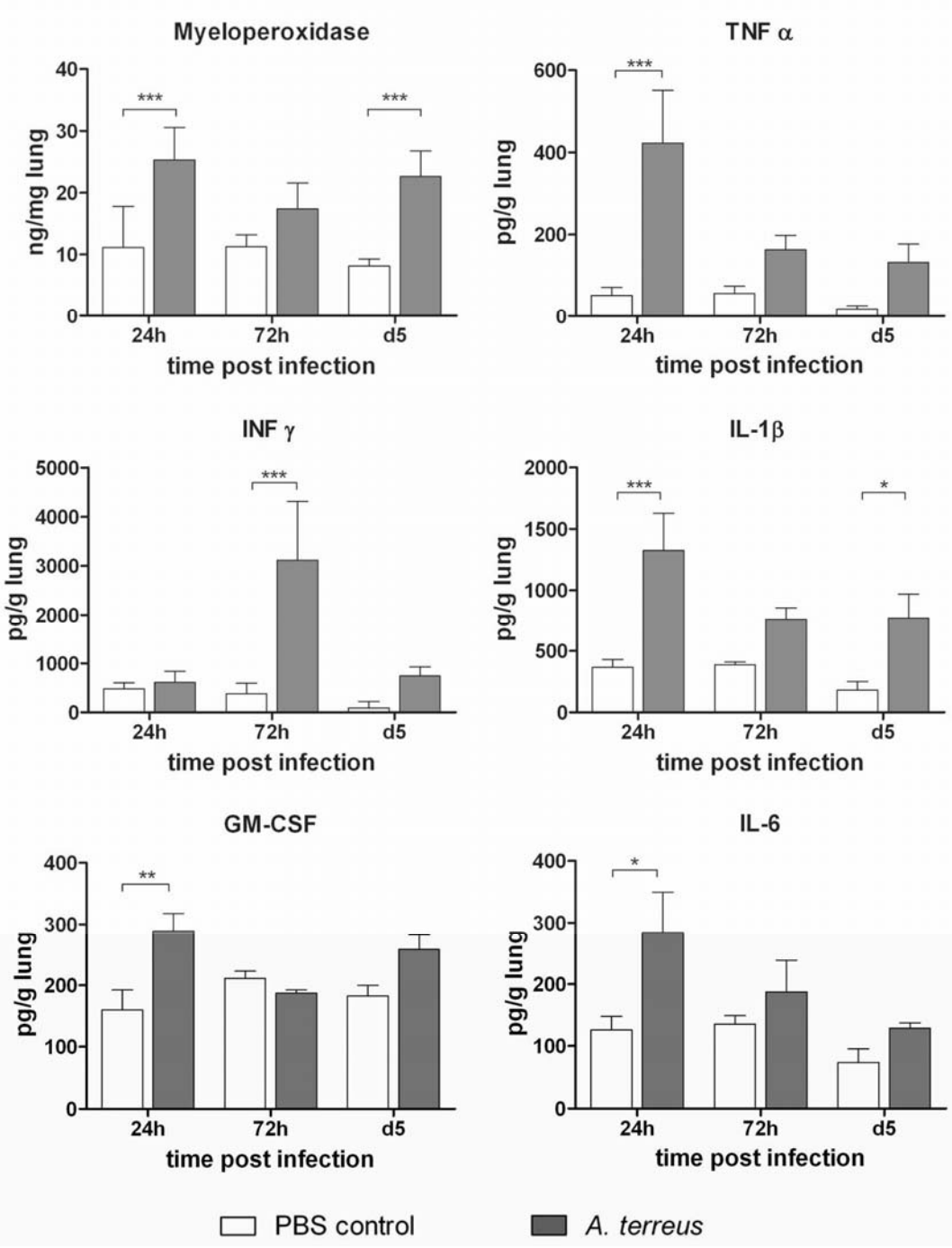

Fig. 21: Determination of myeloperoxidase and cytokine response in immuno-competent mice

Immune response in the lungs determined by myeloperoxidase and cytokine levels. White bars: PBS mock infected mice = PBS control; grey bars: *A. terreus* infected mice. Data shown as mean + SD from 5 animals per group. Statistical analysis was performed per time point by unpaired, two-tailed t-test. * $p < 0.05$; ** $p < 0.01$; *** $p < 0.001$.

4.2 Interaction of *Aspergillus fumigatus* and *Aspergillus terreus* with macrophages

Several disparities between *A. fumigatus* and *A. terreus* IBPA occurred *in vivo* in terms of (i) persistence, (ii) incomplete germination within phagocytes in reconvalescent and immunocompetent animals, as well as (iii) differences in the cytokine response to *A. terreus*. Alveolar macrophages as the first professional phagocytes encountering conidia have been demonstrated to be of importance in *A. fumigatus* mediated IBPA. Furthermore, alveolar macrophages aid in orchestrating the initial immune response and might influence elimination and the cytokine pattern during infection. While the interaction of *A. fumigatus* conidia with macrophages has been extensively studied (Lundborg and Holma 1972; Richard and Thurston 1975; Roilides et al. 1998), little is known about *A. terreus*. Therefore, in the second part of this project the interaction of *A. terreus* with macrophages was analysed in comparison to *A. fumigatus*.

4.2.1 Phagocytosis kinetics of *A. terreus* in comparison to *A. fumigatus*

Alveolar macrophages are the first professional phagocytic cells facing inhaled particles reaching the lower respiratory tract, including fungal conidia. Since phagocytosis represents a prerequisite for subsequent killing by macrophages, phagocytosis of both *Aspergillus* species by alveolar and peritoneal macrophage cell lines (MH-S and J774.A1) was compared. Resting *A. terreus* conidia were phagocytosed significantly faster than resting *A. fumigatus* conidia by the alveolar macrophage cell line MH-S (Fig. 22A). While phagocytosis of resting *A. terreus* conidia was completed after 3 h (96% phagocytosed), the ratio of phagocytosed resting *A. fumigatus* conidia continued to increase for at least 8 h (Fig. 22A). Pre-swelling led to a significant increase in the phagocytosis of *A. fumigatus* conidia. In contrast, phagocytosis of *A. terreus* conidia was not affected by pre-swelling (Fig. 22B). Using pre-swollen conidia, no difference between *A. terreus* and *A. fumigatus* was observed for initial (30 min) and late phagocytosis (8 h).

However, a small but significant difference was observed after 3 h. Therefore, phagocytosis of pre-swollen conidia was analysed on a more detailed time scale (Fig. 22B). Significant differences in the proportion of phagocytosed pre-swollen conidia were observed between 1 h and 6 h.

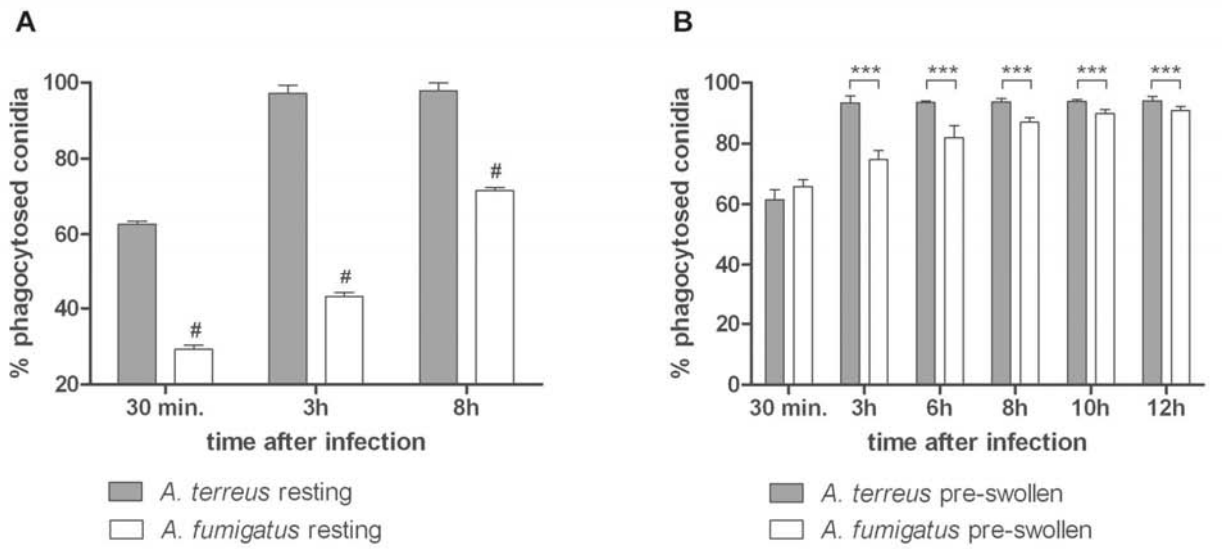

Fig. 22: Phagocytosis of resting and pre-swollen conidia

Results are shown for *A. terreus* SBUG844 and *A. fumigatus* CBS144.89. (A, B) Phagocytosis of conidia by alveolar macrophages (MH-S cell line). Phagocytosis rates are shown as mean + SD from three independent experiments. Statistical analysis was performed using 1-way ANOVA. # and *** $p < 0.001$. (A) Phagocytosis of resting conidia after 0.5, 3 and 8 h of co-incubation. (B) Phagocytosis of pre-swollen conidia up to 12 h.

Since resting *Aspergillus* conidia swell in cell culture media, leading to changes in size and accessibility of cell wall components, the phagocytosis of pre-swollen conidia was determined. Preliminary experiments revealed that *A. terreus* conidia required a prolonged time for germination and grew more slowly than *A. fumigatus*. To account for these differences, the swelling and germination speed of both fungi was evaluated in different cell culture media. Swelling was judged by microscopic and flow cytometry analysis using the (i) increase of conidial diameter, (ii) opacity of conidia and (iii) the loss of spore colouration as markers. Homogeneous populations containing > 95% swollen conidia but no germlings were obtained for *A. fumigatus* by 3.5 h pre-incubation in RPMI and 6 h pre-incubation in DMEM medium, respectively (Fig. 23). Due to slower swelling of *A. terreus* conidia, pre-incubation for 7 h in RPMI and 10 h in DMEM medium was required to obtain homogeneous populations of swollen conidia (Fig. 23).

Since phagocytosis can be influenced by particle size, the sizes of resting and pre-swollen conidia using flow cytometry were determined. The diameters of both resting and swollen *A. terreus* conidia were smaller than those of *A. fumigatus* conidia (Fig. 24).

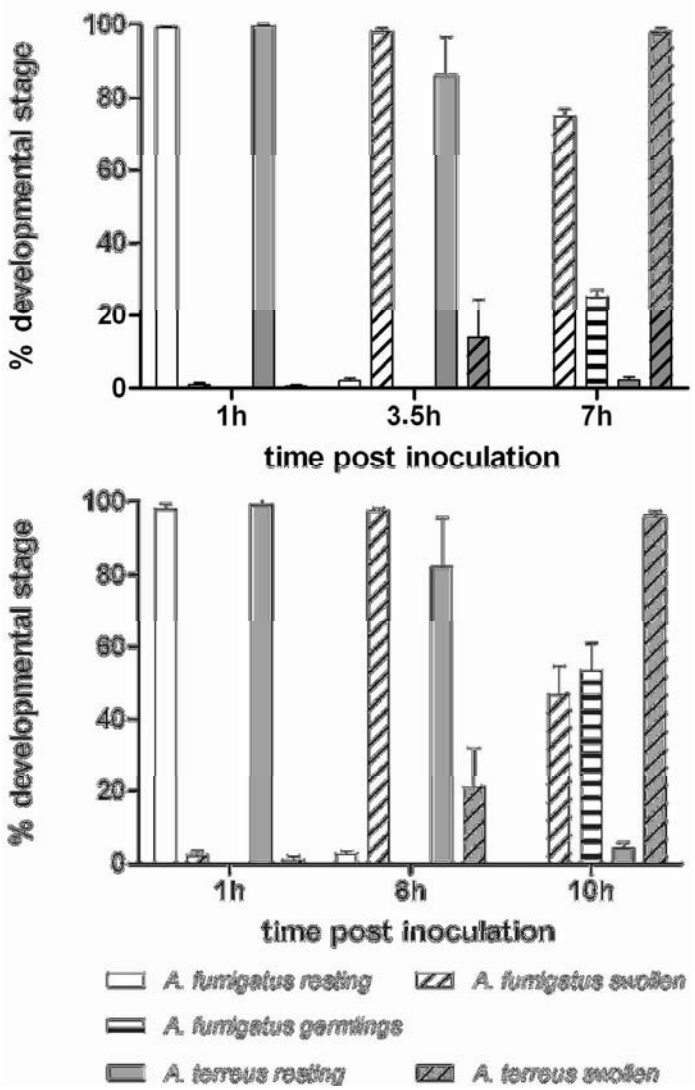

Fig. 23: Analysis of germination of *A. fumigatus* and *A. terreus* conidia in two different cell culture media

Resting conidia were used for inoculation and incubated at 37℃. At distinct time points the developmental state was analysed microscopically from at least 500 conidia. Top: RPMI, bottom: DMEM. Data represent means + SD from three independent experiments.

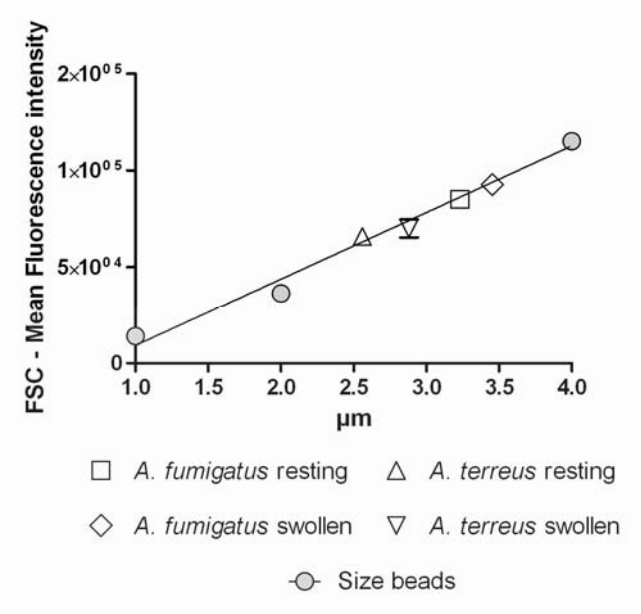

Strain	Mean Fluorescence Intensity	Standard Deviation
A. fumigatus resting	85,239	3,089.35
A. terreus resting	65,957	3,128.24
A. fumigatus swollen	92,770	2,310.83
A. terreus swollen	70,051	4,634.38

Fig. 24: Size determination of resting and swollen conidia by flow cytometry

The average sizes of *A. terreus* and *A. fumigatus* resting and swollen conidia were determined by flow cytometry using calibrated size beads as standard. Data show the average diameter of 20,000 conidia. Mean and SD are indicated in the table below.

4.2.2 Expression of β-1,3-glucan and galactomannan on the conidial surface

It has been shown that phagocytosis of *A. fumigatus* conidia depends on the exposure of pathogen-associated molecular patterns (PAMPs) such as β-1,3-glucan and galactomannan. To test whether the observed differences in phagocytosis rates could result from differences in PAMP exposure and receptor recognition, the β-1,3-glucan and galactomannan exposures on the surface of resting and swollen conidia were quantified by flow cytometry using specific antibodies (kindly provided by A. Cassone and F. Ebel). Resting conidia of *A. terreus* displayed significantly higher exposure of β-1,3-glucan, as recently shown by Deak et al.

(Deak et al. 2011), and galactomannan than resting *A. fumigatus* conidia. The pre-swelling conditions applied to both fungi did not significantly increase the exposure of β-1,3-glucan determined by mean fluorescence levels (Fig. 25), confirming that no germ tubes were formed, which have been shown to display high β-1,3-glucan levels (Hohl et al. 2005).
Swelling of conidia increased the exposure of galactomannan in both fungi as indicated by an increase in specific fluorescence (Fig. 25). However, swollen conidia of *A. terreus* showed higher exposure of both β-1,3-glucan and galactomannan than *A. fumigatus*. Furthermore the histogram suggested that β-1,3-glucan and galactomannan are exposed inhomogeneously within the *A. terreus* conidial populations.

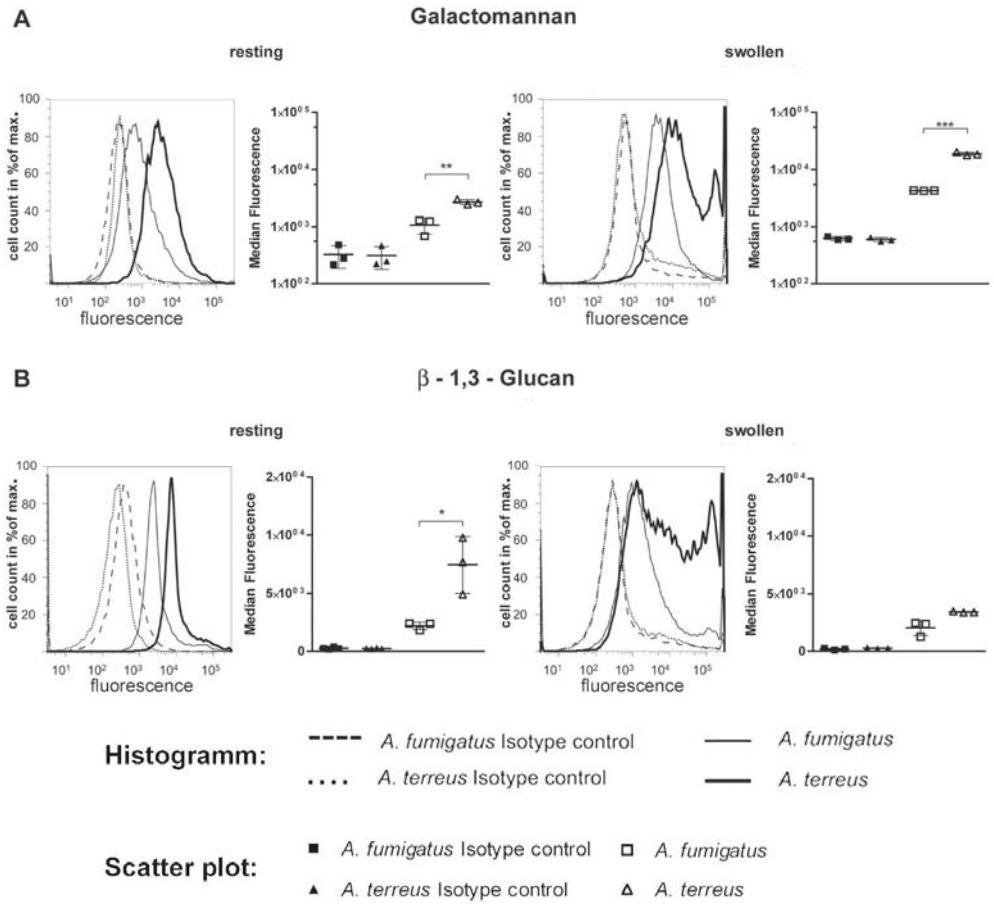

Fig. 25: FACS analysis of galactomannan and β-1,3-glucan on resting and pre-swollen conidia

FACS analysis of (A) galactomannan and (B) β-1,3-glucan exposure. Histograms (one representative result from three independent experiments) and scatter plots of median fluorescence intensity are shown (mean ± SD, three independent experiments). Statistical analysis was performed using paired t-test. * $p < 0.05$; ** $p < 0.01$; *** $p < 0.001$.

4.2.3 Contribution of different pathogen recognition receptors to phagocytosis

PAMPs are recognised by pathogen recognition receptors (PRRs) located on the surface of immune cells. Known PRRs involved in recognition of fungi include dectin-1 recognising β-1,3-glucan (Gersuk et al. 2006), the mannose receptor recognising galactomannan (Bennett et al. 1987), and the toll-like receptors TLR2 and TLR4 recognising yet unknown factors (Netea et al. 2006). To investigate the role of different PAMPs, phagocytosis of pre-swollen conidia was determined after blocking the corresponding receptors on MH-S cells by specific substrates or specific antibodies. Pre-swollen conidia were chosen for these and subsequent *in vitro* experiments since differences in phagocytosis rates between *A. fumigatus* and *A. terreus* were less pronounced for pre-swollen compared to resting conidia.

Blocking of dectin-1 by laminarin and blocking of the mannose receptor by mannan significantly decreased the phagocytosis of *A. terreus* conidia within the first three hours by 50% and 30%, respectively, and the overall phagocytosis rate of *A. terreus* did not further increase after prolonged co-incubation (Fig. 26A and B). In contrast, blocking of either dectin-1 or the mannose receptor did not influence phagocytosis of *A. fumigatus* (Fig. 26A and B). These data suggested that recognition by dectin-1 and the mannose receptor plays a major role in the early recognition of *A. terreus*, but not *A. fumigatus*. Blocking of either TLR2 or TLR4 led to a moderate but significant reduction in phagocytosis, but these differences were only observed after 8 h (Fig. 26C and D). The influence of TLR2 and TLR4 on the long-term phagocytosis of pre-swollen *A. fumigatus* conidia coincided with the occurrence of germlings (Fig. 20), suggesting that the ligands for TLR2 and TLR4 are either exposed on germlings or that the recruitment of PRRs to the phagosome and the subsequent antigen presentation affects long-term phagocytosis (Segal 2007).

It appeared possible that blocking of a single receptor can be bypassed by other receptors. Thus, simultaneous blocking of the mannose receptor and dectin-1 as well as simultaneous blocking of all four tested receptors was performed. Simultaneous blocking of the mannose receptor and dectin-1 nearly completely abolished phagocytosis of *A. terreus*, but had only a moderate effect on *A. fumigatus* (> 60% phagocytosed, Fig. 26E). Blocking of all receptors did not further reduce phagocytosis of *A. terreus* (Fig. 26F), but further decreased phagocytosis of *A. fumigatus* conidia (50% phagocytosed, Fig. 26F). These data confirm that dectin-1 and the mannose receptor are the main PRRs recognising *A. terreus* conidia, whereas different and probably yet unknown receptors are involved in phagocytosis of *A. fumigatus* conidia.

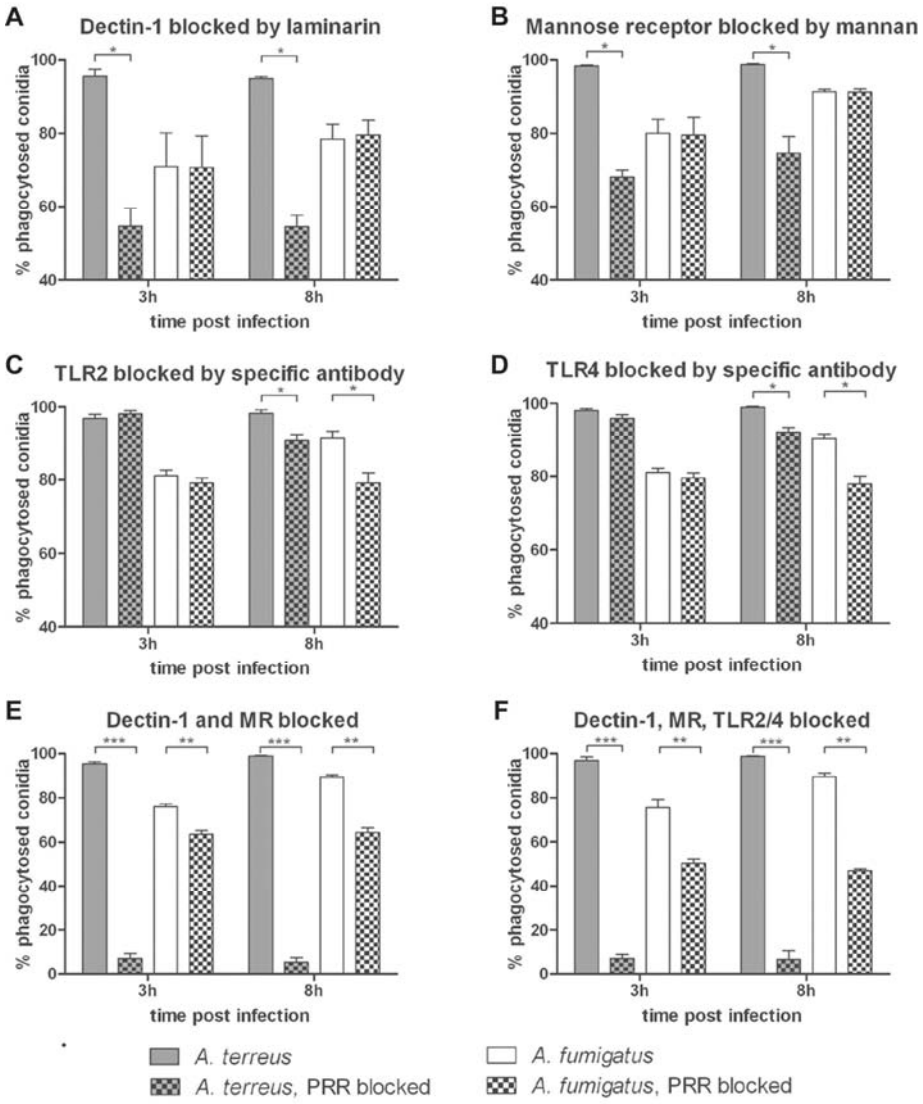

Fig. 26: Role of PRRs in phagocytosis of pre-swollen *A. terreus* and *A. fumigatus* conidia by MH-S cells

Results are shown for *A. terreus* SBUG844 and *A. fumigatus* CBS144.89. Phagocytosis rates represent mean + SD from three independent experiments. Statistical analysis was performed using 1-way ANOVA. * $p < 0.05$, ** $p < 0.01$, *** $p < 0.001$. (A) Blocking of dectin-1 by laminarin. (B) Blocking of the mannose receptor by mannan. (C) Blocking of TLR2 or (D) of TLR4 by specific antibodies. (E) Simultaneous blocking of dectin-1 and mannose receptor. (F) Simultaneous blocking of dectin-1, mannose receptor, TLR2 and TLR4.

4.2.4 Survival of conidia in alveolar macrophages after phagocytosis

Phagocytosis is one of the first steps in the inactivation of many microbial pathogens. However, some microbes are able to escape killing after phagocytosis (Sansonetti 2001; Ogawa and Sasakawa 2006; Schulert et al. 2009). Thus, the survival rates of conidia after phagocytosis were determined.

In a first set of experiments a fluorescent dye which indicates metabolic activity of cells was used to discriminate dead and viable conidia on a single-conidia level. The ratio of inactivated *A. fumigatus* conidia steadily increased over time after phagocytosis by MH-S cells (Fig. 27A). Furthermore, in addition to the metabolic inactivation indicated by colour changes of the dye, *A. fumigatus* conidia appeared deformed suggesting that conidia were not only inactivated, but also partially degraded. In striking contrast, no inactivation of *A. terreus* conidia was observed (Fig. 27A) indicating an increased resistance of *A. terreus* within macrophages. As an independent method, survival was determined as colony-forming units (CFU) 3 h and 10 h after infection. *A. fumigatus* showed the expected time-dependent inactivation, while *A. terreus* CFUs remained stable (Fig. 27B). Increased survival of *A. terreus* was likewise observed upon interaction with primary murine bone marrow-derived macrophages (Fig. 27C). To confirm that differences in survival rates were not strain but species-specific, two additional strains from each fungal species were investigated for their survival within MH-S cells. No significant differences between species-specific strains were observed, confirming that the results are not limited to a specific fungal strain (Fig. 27D).

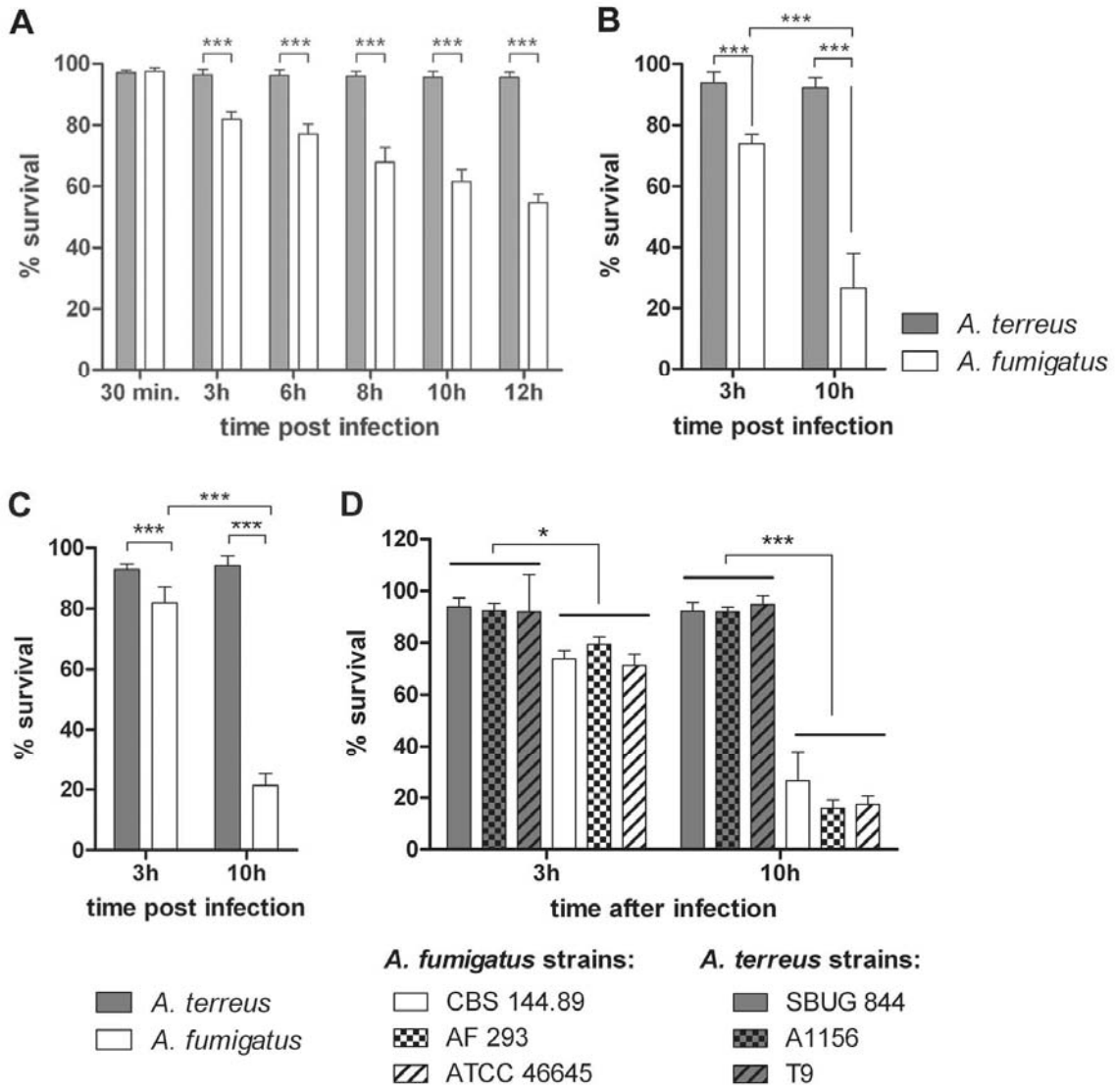

Fig. 27: *A. fumigatus* and *A. terreus* survival in co-incubation with macrophages

Results are shown for *A. terreus* SBUG844 and *A. fumigatus* CBS144.89. (A-C) Survival of *A. fumigatus* and *A. terreus* upon co-incubation with macrophages. Data are shown as mean + SD from three independent experiments; statistical analysis by 1-way ANOVA and Tukey's multiple comparison test. * $p < 0.05$; ** $p < 0.01$; *** $p < 0.001$. (A, B, D) Co-incubation with MH-S cells and (C) with bone marrow-derived murine macrophages (A) Survival of *A. terreus* and *A. fumigatus* determined by fluorescence microscopy using the metabolic dye FUN1. (B, C) Survival determined by CFU. (D) Survival of three independent *A. fumigatus* and *A. terreus* isolates after co-incubation with MH-S cells determined by CFU.

4.2.5 Macrophage damage after phagocytosis of conidia

A. fumigatus conidia, which are not inactivated after phagocytosis, tend to form germ tubes that pierce macrophages and eventually lead to lysis of phagocytic cells (Roilides et al. 1995). To investigate whether the increased persistence of *A. terreus* conidia in macrophages was likewise associated with host cell damage, the release of lactate dehydrogenase (LDH) as a marker for macrophage damage was determined. Pre-swollen conidia were used to minimise effects caused by the overall slower germination (Fig. 23) and growth of *A. terreus* compared to *A. fumigatus*, which could affect damage of macrophages by *A. terreus* in co-culture experiments (Rippon et al. 1974). Furthermore, fungal germination and growth in cell culture medium in the absence of macrophages were analysed to assess potential differences in growth rates which might affect macrophage damage. No gross differences between *A. fumigatus* and *A. terreus* were observed in these experiments (Fig. 28).

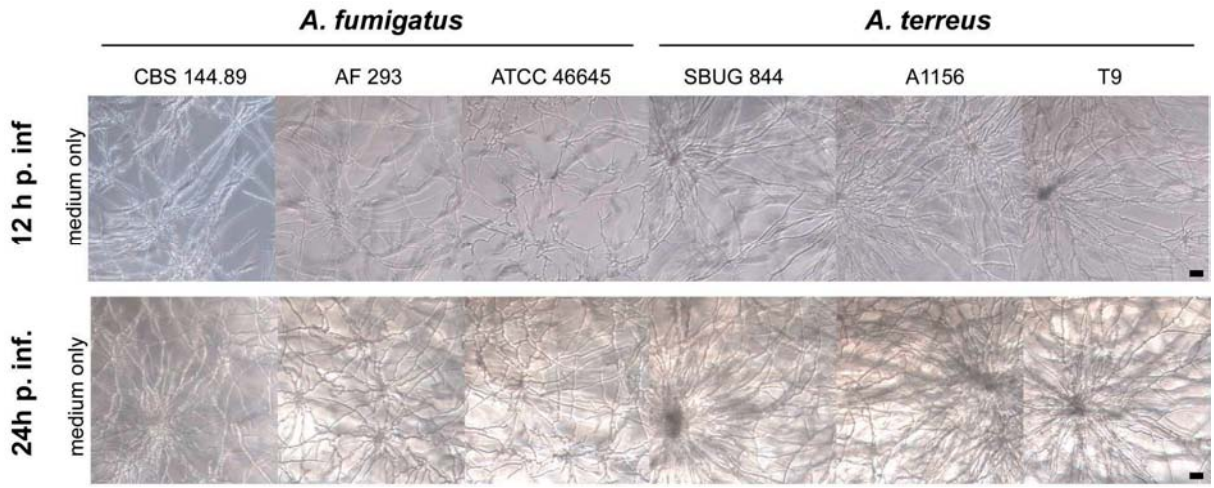

Fig. 28: Growth in cell culture media

Micrographs of fungal growth in cell culture medium without macrophages. No gross differences in growth were observed between the isolates and species; scale bars represent 10 µm.

In co-incubation with macrophages, only mild cell damage was observed with either of the two fungi within the first 12 h (Fig. 29A). However, cell damage caused by *A. fumigatus* strongly increased 24 h post infection, whereas *A. terreus* caused significantly less damage. This difference was significant after 24 h in MH-S cells (Fig. 29A), independent of the *A. terreus* and *A. fumigatus* strain used (Fig. 29 B). The difference in cytotoxicity caused by

A. terreus and *A. fumigatus* respectively, was even more pronounced in human primary macrophages (Fig. 29C).

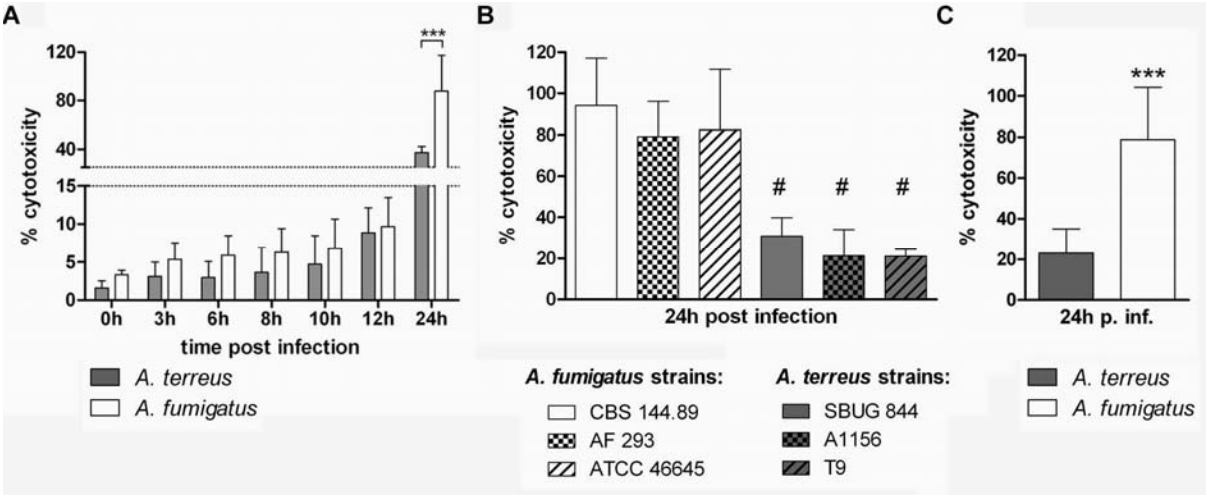

Fig. 29: Host cell damage by *A. fumigatus* and *A. terreus*

Damage of (A) MH-S cells, (B) MH-S cells co-incubated with several *A. fumigatus* and *A. terreus* strains and (C) human monocyte-derived macrophages determined by release of lactate dehydrogenase (LDH). Mean values + SD from three independent experiments; statistical analysis was performed per time point by unpaired, two-tailed t-test. * $p < 0.05$; ** $p < 0.01$; # and *** $p < 0.001$.

Microscopy revealed that phagocytosed *A. fumigatus* conidia developed hyphae, which pierced macrophages within the first 12 h (Fig. 30). In contrast, germination of phagocytosed *A. terreus* conidia was not observed after 12 h and rarely after 24 h (Fig. 30). Non-phagocytosed conidia (approximately 5% of both *A. fumigatus* and *A. terreus* total conidia) of both species formed filaments to the same extent (data not shown). Thus, despite the high survival rate of *A. terreus* conidia, the slow germination of phagocytosed *A. terreus* conidia compared to *A. fumigatus* likely led to low macrophage damage.

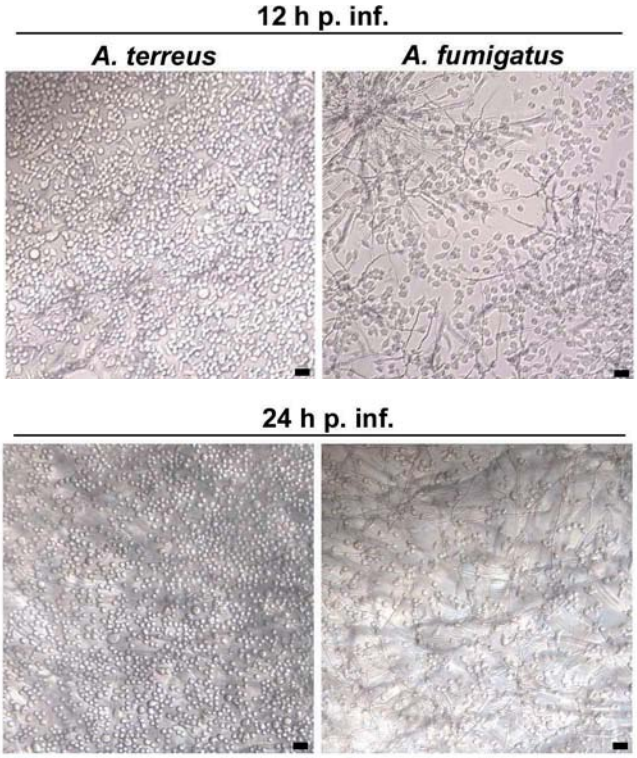

Fig.30: Growth of conidia in co-incubation with alveolar macrophages

Brightfield microscopic images showing germination and filamentous growth of *A. fumigatus* and *A. terreus* 12 h (upper row) and 24 h (lower row) after infection; scale bars represent 40 µm.

4.2.6 Maturation of *A. terreus* or *A. fumigatus* containing phagolysosomes

Upon phagocytosis phagosomes maturate *via* a series of fusion events to mature, acidified phagolysosomes. The fusion events are characterised by the recruitment of several marker proteins including LAMP-1 (lysosome-associated membrane protein) and Cathepsin D (lysosomal aspartyl protease) (Haas 2007; Lambeth et al. 2007). In fully mature phagolysosomes the lysosome-specific v-ATPase integrates into the phagolysosomal membrane builds up a proton gradient which results in a decrease in pH. The low pH provides an optimal environment for phagolysosomal enzymes and is essential for successful killing of most pathogens (Steinberg et al. 2007) including *A. fumigatus* (Jahn et al. 2002; Ibrahim-Granet et al. 2003). Viable *A. fumigatus* conidia inhibit this acidification (Jahn et al. 2002; Ibrahim-Granet et al. 2003) allowing the fungus to germinate within the phagolysosome and to escape by piercing through the macrophage membrane as shown previously (Wasylnka et al. 2005) and in the experiments described above (4.2.5). To determine whether the observed differences in fungal inactivation of *A. terreus* and *A.*

fumigatus by macrophages and the observed macrophage damage might be related to differences in phagosome maturation, analysis of phagosome maturation using fluorescence microscopy was performed.

Phagosomes of MH-S cells containing pre-swollen conidia of either *A. fumigatus* or *A. terreus* successfully underwent fusion with lysosomes 3 h (Fig. 31) and 8 h (data not shown) after infection as indicated by the presence of LAMP-1 and Cathepsin D, characterising a mature phagolysosome (Haas 1998). However, as determined by using the acidic probe Lysotracker DND99, only phagolysosomes containing *A. terreus* conidia were invariably (> 99%) acidified at both time points, whereas few *A. fumigatus* conidia were found in acidified phagolysosomes (10-15% after 3 h; 25-30% after 8 h) (Fig. 31).

All *A. fumigatus* conidia in acidified phagolysosomes looked deformed. Similar results were obtained using primary murine alveolar macrophages and primary human monocyte-derived macrophages (Fig. 32).

Inhibition of acidification by *A. fumigatus* and acidification of phagolysosomes containing *A. terreus* was likewise observed with two additional strains of each *A. fumigatus* and *A. terreus* (Fig. 33). Thus, in combination with the observation that phagocytosed *A. terreus* conidia remain viable, these findings suggest that *A. terreus* cannot block acidification but survives in acidified phagolysosomes. The persistence of intact *A. terreus* conidia within phagolysosomes was additionally confirmed by transmission electron microscopy 8 h and 24 h after infection (Fig. 34, images kindly provided by Prof. Martin Schaller, Tübingen). Microscopy showed that intact *A. terreus* conidia are enveloped in a double membrane at both time points investigated.

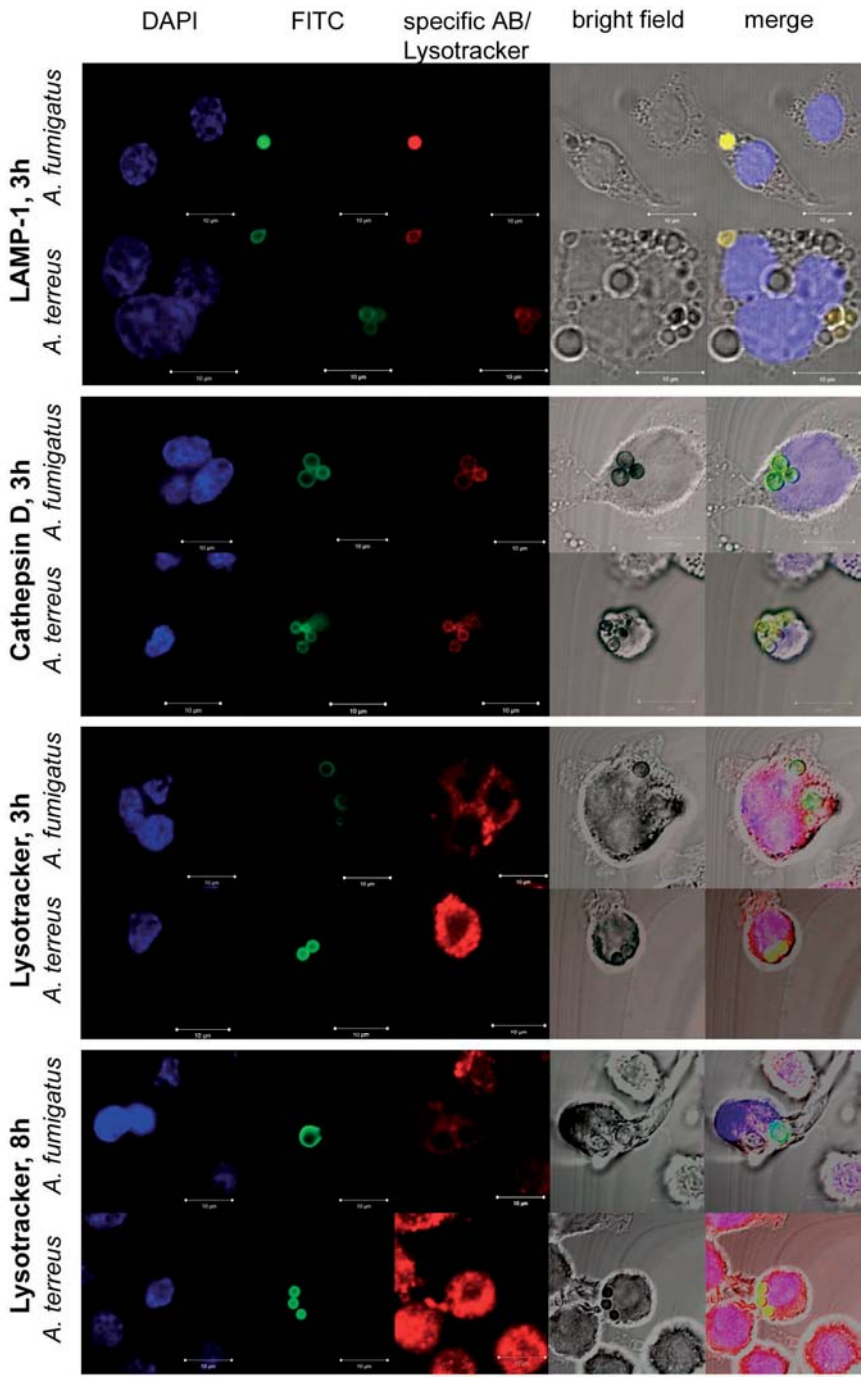

Fig.31: Maturation of phagolysosomes containing *A. fumigatus* or *A. terreus* conidia

Results are shown for *A. terreus* SBUG844 and *A. fumigatus* CBS144.89 with MH-S cells. FITC-labelled conidia were used. Yellow signal in the merged images indicate co-localization of conidia with the specific phagolysosome stain. All lanes show representative fluorescence microscopy images. Blue: DAPI (nucleus); green: FITC-labelled conidia; red: specific antibody for the phagolysosomal marker indicated on the left. Bars represent a size of 10 µm.

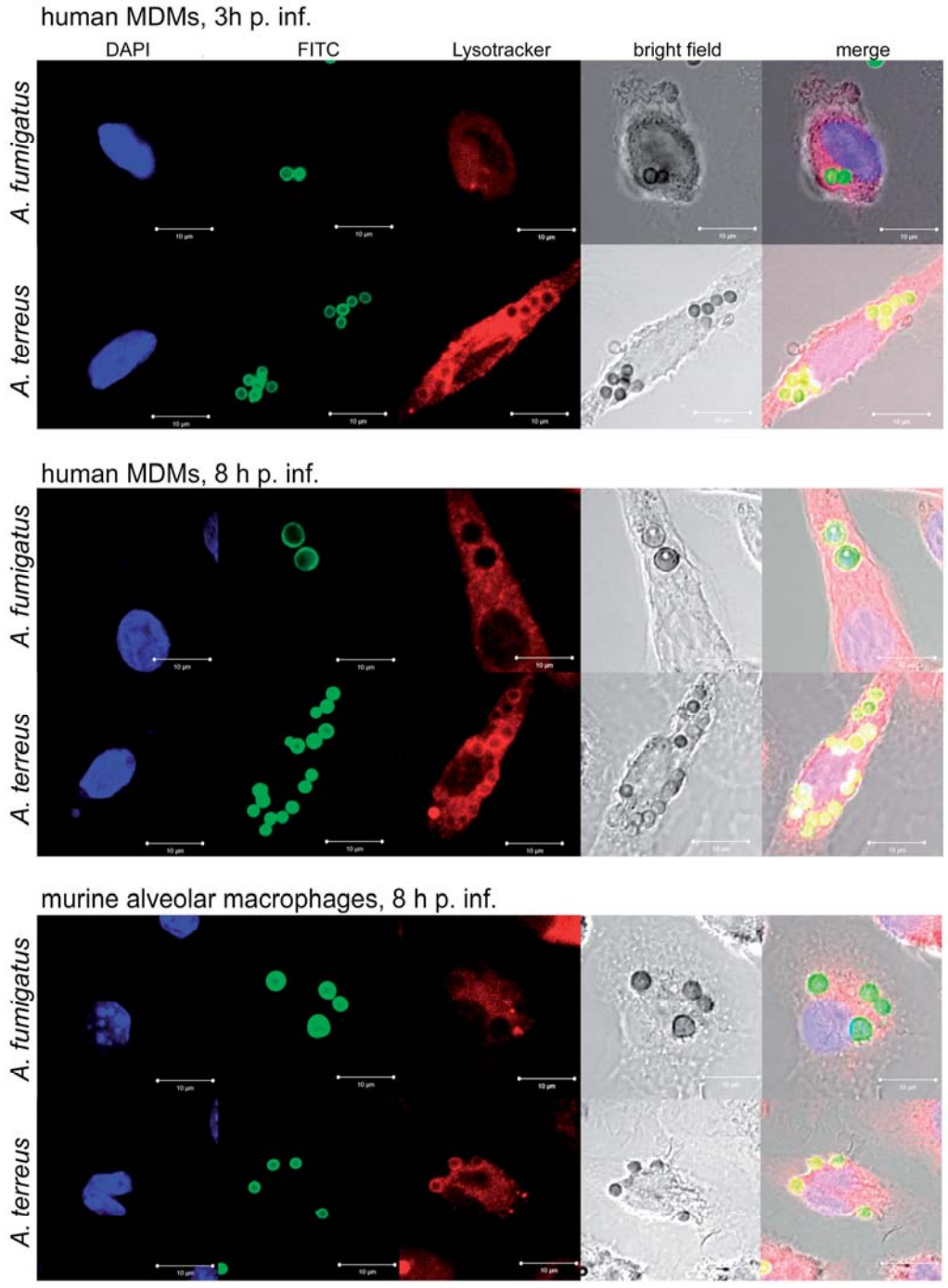

Fig.32: Phagolysosome acidification in primary macrophages after phagocytosis of *A. fumigatus* and *A. terreus*

FITC-labelled conidia were used. Yellow signal in the merged images indicate co-localization of conidia with the lysotracker stain. All lanes show representative fluorescence microscopy images. Blue: DAPI (nucleus); green: FITC-labelled conidia; red: Lysotracker. Bars represent a size of 10 µm. The strains are indicated on the left side of the lanes.

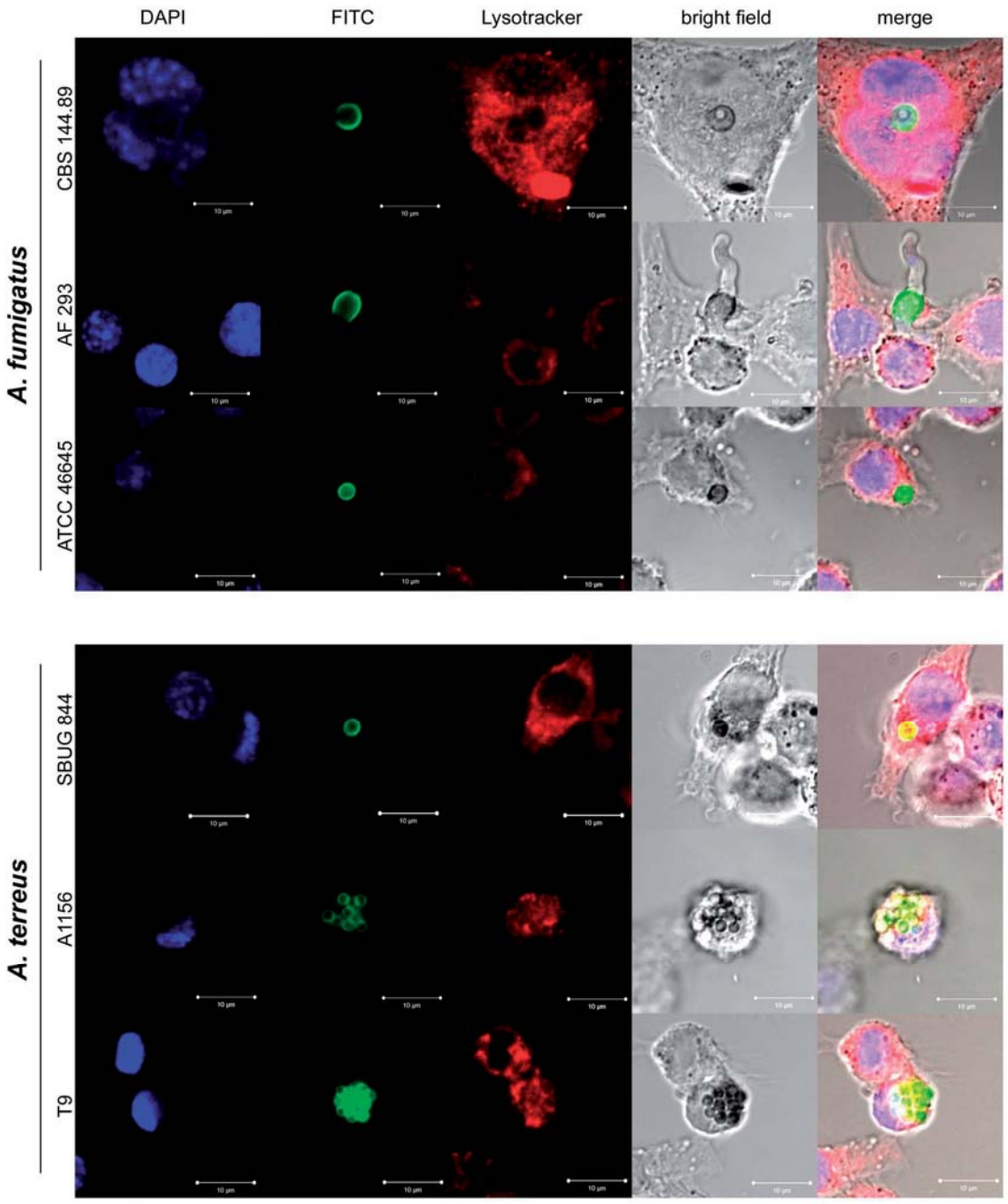

Fig. 33: Phagolysosome acidification in MH-S cells after phagocytosis of different *A. fumigatus* and *A. terreus* strains

FITC-labelled conidia were used. Yellow signal in the merged images indicate co-localization of conidia with the lysotracker stain. All lanes show representative fluorescence microscopy images. Blue: DAPI (nucleus); green: FITC-labelled conidia; red: Lysotracker. Bars represent a size of 10 µm. The strains are indicated on the left side of the lanes.

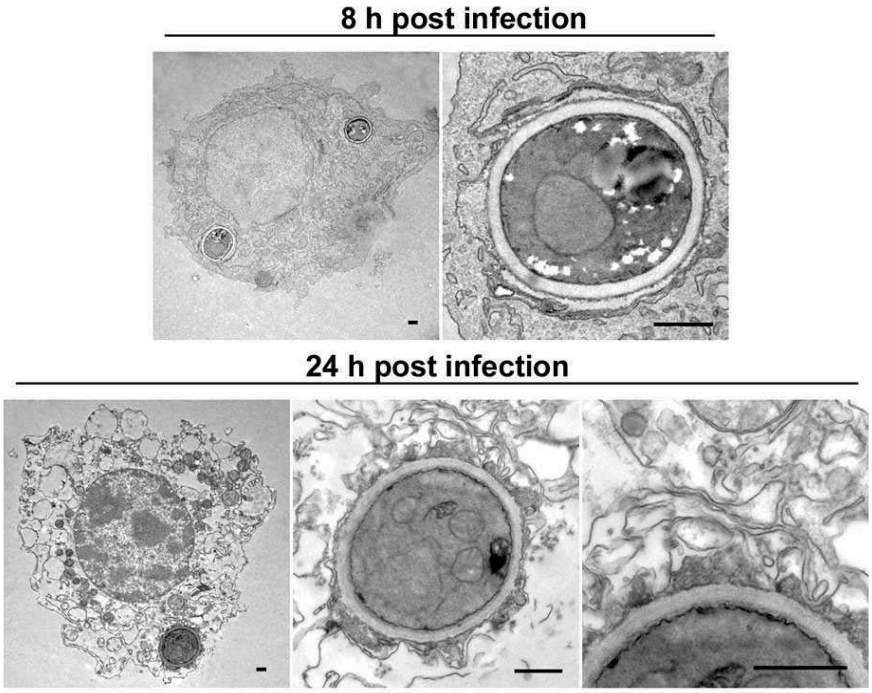

Fig. 34: Transmission electron microscopy of co-incubations of *A. terreus* and MH-S cells 8 h and 24 h post infection

Transmission electron micrograph of phagocytosed *A. terreus* conidia 8 h (upper panel) and 24 h (lower panel) after infection. Scale bars represent 0.5 µm. Phagocytosed conidia are surrounded by a phospholipid bilayer at both time points (images kindly provided by Prof. Martin Schaller, Tübingen).

4.2.7 Investigation on phagolysosomal maintenance and pH resistance of *A. terreus*

The observation that *A. terreus* conidia were not inactivated after phagocytosis led to the hypothesis that resistance to acidic pH may enable *A. terreus* to survive in the phagolysosome. Thus, the *in vitro* survival of conidia of both species in phosphate buffer at different pH values without addition of nutrients, a condition which may closely resemble that in phagolysosomes, was determined. In this nutrient-limited environment, no germination of either *Aspergillus* species was observed. However, *A. terreus* survived incubation at pH 3 and 4 to a higher extent than *A. fumigatus* (Fig. 35). The addition of nutrients showed that both species germinated at pH values > 5, whereas swelling and germination of conidia was suppressed at lower pH (Fig. 36). Thus, it appears that while *A. terreus* conidia survived within the acidified phagolysosome, they were unable to germinate, did not pierce the macrophage membranes and caused less cell damage. In contrast, the ability of

A. fumigatus to inhibit phagolysosome acidification allowed rapid germination of conidia at ambient pH, which caused the high cytotoxicity observed after 24 h (Fig. 29).

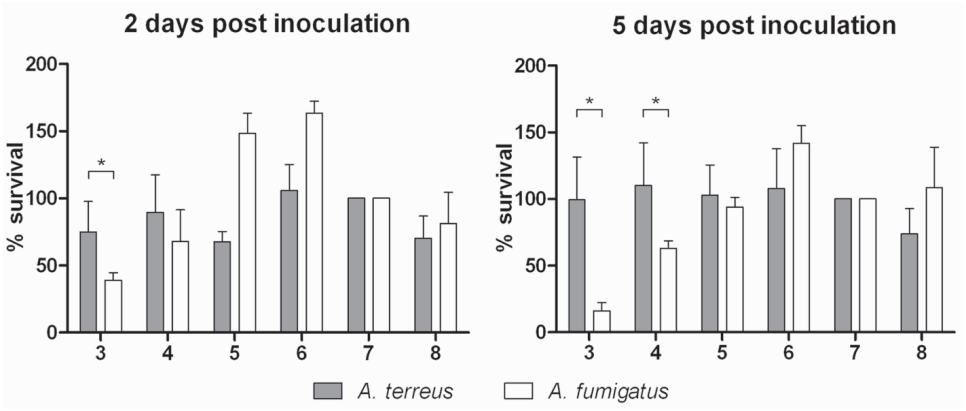

Fig. 35: Influence of environmental pH on *in vitro* survival

Results are shown for *A. terreus* SBUG844 and *A. fumigatus* CBS144.89. Data shown represent mean + SD from three independent experiments. Statistical analysis was performed using paired t-test (* $p < 0.05$); relative survival of *A. terreus* and *A. fumigatus* conidia after incubation in nutrient-free and pH-stabilised buffer. Survival at pH 7 is set to 100%. Left panel: survival after two days of incubation, right panel: survival after five days of incubation.

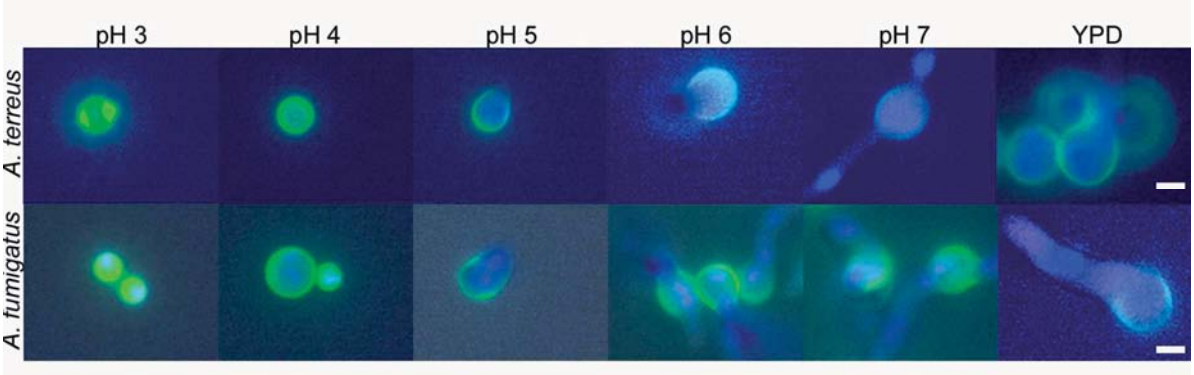

Fig. 36: Influence of environmental pH on conidial germination

Representative images from three independent experiments showing germination of *A. terreus* and *A. fumigatus* conidia in minimal medium with defined pH. All images were acquired after 8 h incubation at 37℃; scale b ars represent 3 µm.

To determine the effect of phagolysosome acidification on conidial germination, macrophage damage in the presence of bafilomycin A was quantified. Bafilomycin A is a potent v-ATPase

blocker which inhibits the acidification of phagolysosomes (Tapper and Sundler 1995). Treatment with bafilomycin A significantly increased cell damage caused by *A. terreus* (Fig. 37A) to the levels observed in macrophages incubated with *A. fumigatus* conidia in the absence of bafilomycin A. In contrast, only a slight increase of cell damage by *A. fumigatus* was observed after bafilomycin A treatment (Fig. 37A). In agreement with increased macrophage damage, *A. terreus* showed faster germination and piercing of macrophages in bafilomycin-treated macrophages (Fig. 37B). These differences were also observed in other *A. fumigatus* and *A. terreus* strains (Fig. 38 and 39). In the absence of macrophages, bafilomycin A had no influence on fungal germination and growth (Fig. 39). These results support the hypothesis that inhibition of germination is due to acidification of phagolysosomes, which reduces escape and the accompanied macrophage damage by *A. terreus*.

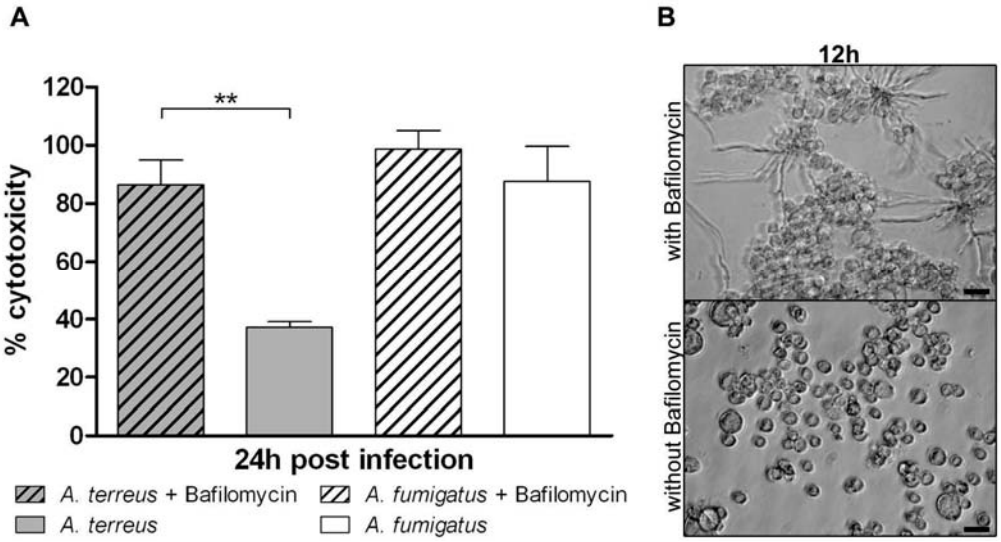

Fig. 37: The effect of bafilomycin A on macrophage damage

(A) Relative cytotoxicity (LDH release) mediated by *A. terreus* and *A. fumigatus* conidia on alveolar macrophages treated with the v-ATPase blocker bafilomycin A or without bafilomycin A treatment. Statistical analysis was performed using paired t-test; ** $p < 0.01$. (B) Brightfield microscopy of *A. terreus* in co-incubation with macrophages (MH-S) without (lower panel) and with bafilomycin A (upper panel) treatment after 12 h. Scale bars represent 10 µm.

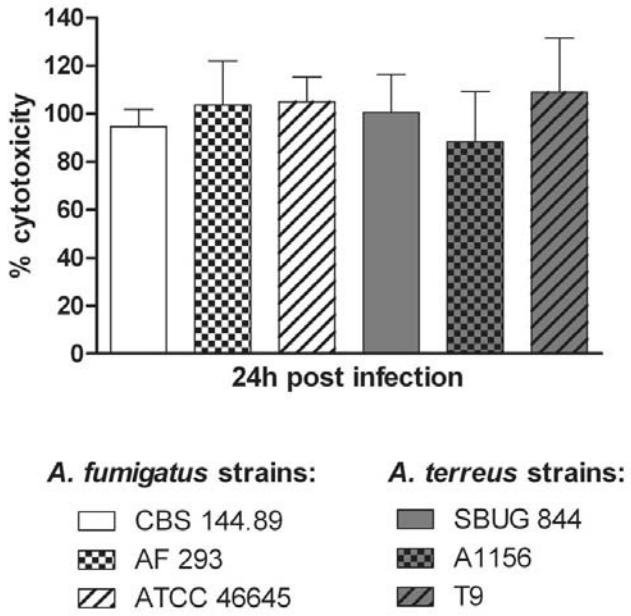

Fig. 38: Cytotoxicity of *A. terreus* and *A. fumigatus* strains on MH-S cells

Relative cytotoxicity (LDH release) mediated by several *A. terreus* and *A. fumigatus* strains on alveolar macrophages treated with the v-ATPase blocker bafilomycin A; mean + SD. Three independent experiments measured in triplicates, statistical analysis was performed using unpaired t-test.

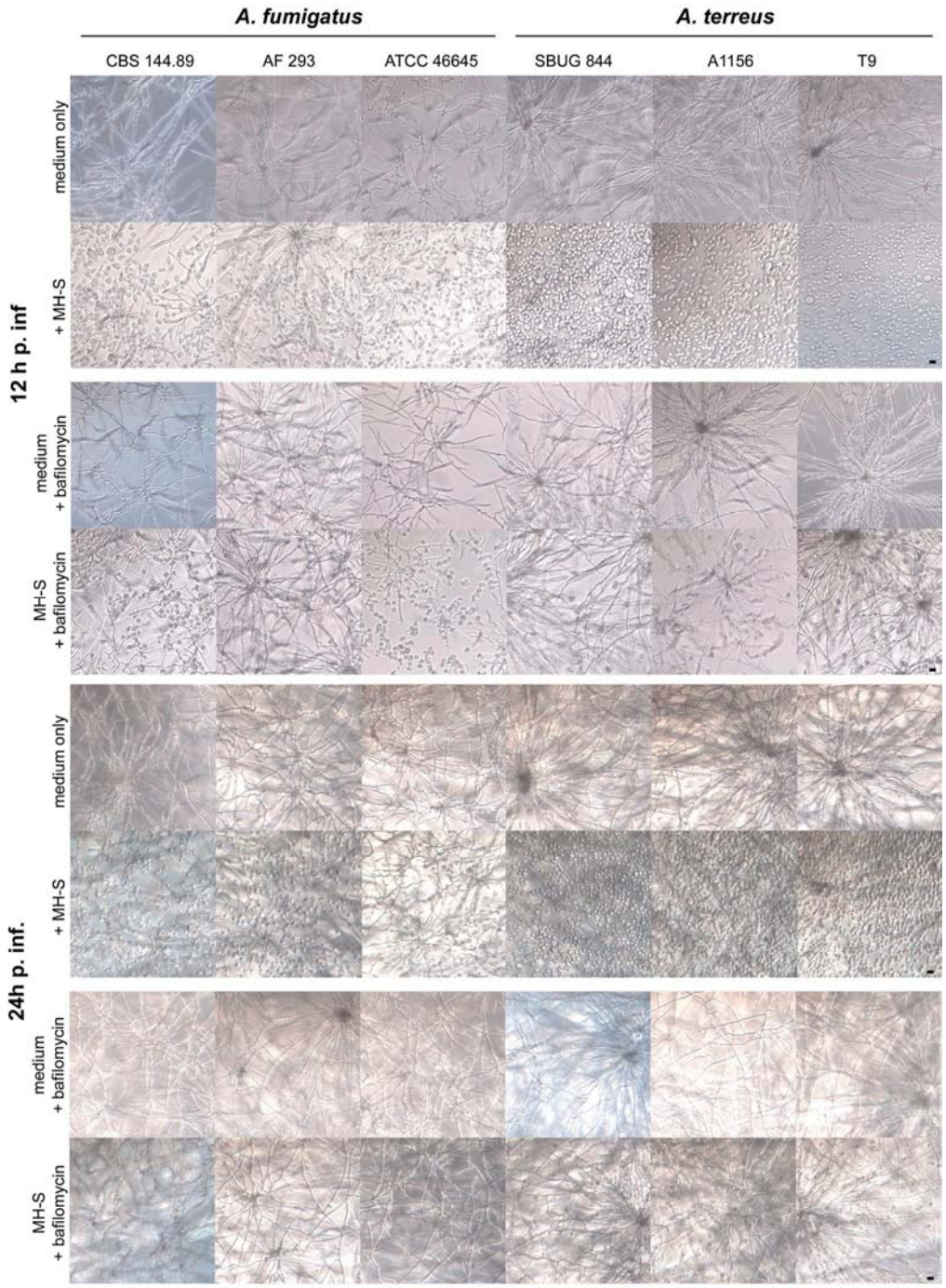

Fig. 39: Influence of bafilomycin A on macrophage lysis by different *A. fumigatus* and *A. terreus* strains

Brightfield microscopy of *A. terreus* in co-incubation with medium (medium only) and macrophages (+MH-S) without and with bafilomycin A (lower lanes of both time points) 12 h and 24 h after infection (p. inf.); no influence of bafilomycin A on germination of the tested strains, but better escape of *A. terreus* strains from macrophages treated with bafilomycin (12 h and 24 h). Scale bars represent 10 µm.

4.3 The role of naphthopyrone in the pathogenesis of *A. terreus*

The ability of *A. fumigatus* to inhibit phagolysosome acidification is linked to the grey-greenish spore colouration derived from dihydroxynaphthalene melanin (DHN-melanin) (Tsai et al. 1998; Jahn et al. 2002). Deletion of the polyketide synthase gene *pksP* in *A. fumigatus* inhibits melanin synthesis and the *pksP* mutant is not longer able to block phagolysosome acidification, resulting in increased susceptibility to killing by macrophages and reduced virulence *in vivo* (Jahn et al. 1997; Jahn et al. 2002). A homologous polyketide synthase responsible for conidia colouration is also present in other aspergilli, like *Aspergillus nidulans* or *Aspergillus niger* (Mayorga and Timberlake 1992; Jorgensen et al. 2011). In *A. nidulans*, the green spore colour derives from the yellow melanin precursor naphthopyrone and is produced by the *wA* gene product (Mayorga and Timberlake 1990; Fujii et al. 2001). Interestingly, although PksP produces DHN-melanin in *A. fumigatus*, the product formed after recombinant expression of *pksP* in *Aspergillus oryza*e is naphthopyrone, which indicates that the initial products formed by *A. nidulans wA* and *A. fumigatus pksP* are identical (Watanabe et al. 2000).

Despite the brownish colouration of *A. terreus* conidia and several polyketide synthase genes present in its genome, *A. terreus* seems to lack a homologue of *pksP* and *wA* (Fig. 40).

	A.fumigatus	*A. clavatus*	*A. flavus*	*A. nidulans*	*A. niger*	*A. oryzae*	*A. terreus*
relative 1	CAA76740 (Alb1, PksP)	XP_001276035	XP_002382817	WA_EMENI (WA)	XP_001393884	XP_001822700	XP_001216121
identity	100%	86%	72%	67%	69%	72%	44%
relative 2	XP_751377	XP_001275038	XP_002384329	XP_681094 (StcA)	XP_001390425	XP_001827098	XP_001210231
identity	38%	35%	47%	39%	44%	47%	41%

Fig. 40: Conservation of polyketide synthases responsible for conidia colouration among different *Aspergillus* species

The nucleotide sequence of the polyketide synthase PksP from *A. fumigatus* was used as a template in BLASTP analyses against genomes from different aspergilli. All identity values (in %) refer to *pksP*. Orange colour indicate high homology to *A. fumigatus*.

With the exception of *A. terreus* all other aspergilli contain a highly homologous polyketide synthase (67 to 86% identity of the nucleotide sequence). The second most closely related polyketide synthase present in genomes of aspergilli (bottom lane) shows between 35 and

47% identity to *pksP*, but seems to be, at least for *A. fumigatus*, *A. nidulans*, and *A. niger*, not involved in conidia colouration. *A. terreus* contains polyketide synthases with high identity to these second polyketide synthases, but not to *pksP*. Deletion of the two polyketide synthases presented for *A. terreus* did not alter the colour of *A. terreus* conidia (data not shown, experiment kindly performed by Markus Gressler).

Consequently, *A. terreus* produces neither DHN-melanin nor naphthopyrone (Fig. 41). While DHN-melanin seems essential for the inhibition of phagolysosome acidification by *A. fumigatus*, it has not yet been investigated whether naphthopyrone is also able to prevent acidification.

4.3.1 Characterisation of a recombinant *A. terreus* strain producing naphthopyrone

To test the hypothesis that the lack of a *pksP*-homologue is responsible for the inability of *A. terreus* to inhibit phagolysosome acidification, a recombinant *A. terreus* strain expressing the polyketide synthase gene *wA* from *A. nidulans* was constructed. Construction of the mutant (kindly performed by Markus Gressler, Jena) denoted as *A. terreus wA* was kindly donated by Markus Gressler. The mutant with a single integration of the *wA* gene showed a yellowish phenotype of conidia comparable to the colour of an *A. nidulans yA* mutant which lacks a *p*-diphenol oxidase polymerising naphthopyrone (Aramayo and Timberlake 1993) (Fig. 41). HPLC-MS analysis confirmed that *A. terreus wA* produced the naphthopyrone derivatives YWA1 and YWA2 (Fujii et al. 2001) in conidia (data not shown, experiments kindly performed by Christoph Zähle, Jena).

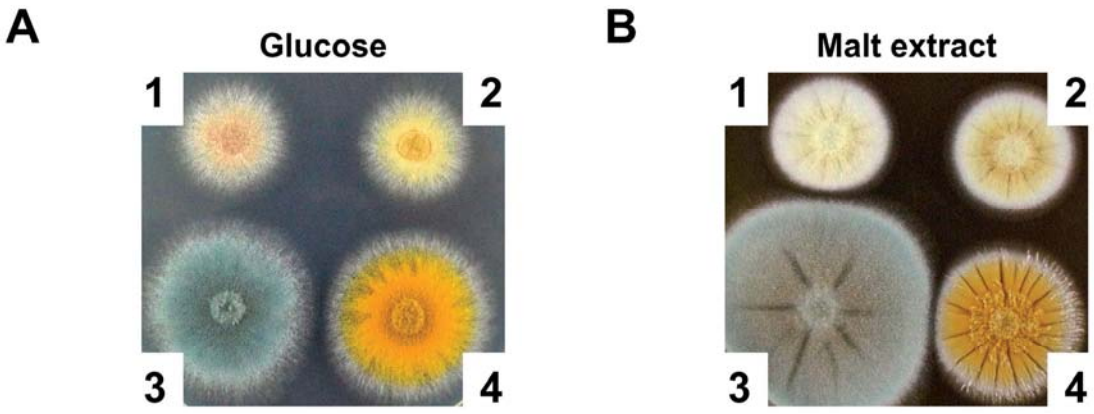

Fig. 41: Determination of naphthopyrone production by *A. terreus wA*

(A) and (B) show the colony appearance of *A. terreus* wild type (1), *A. terreus wA* (2), *A. fumigatus* wild type (3), and *A. nidulans* yA (4) on solid glucose minimal medium (Glucose) and malt extract agar (Malt extract).

4.3.2 Interaction of *A. terreus wA* with macrophages

The proposed function of DHN-melanin is the inhibition of phagolysosome acidification. However, DHN-melanin is associated with the fungal cell wall and might therefore affect PRR exposure and phagocytosis. Although initial phagocytosis of *A. terreus wA* conidia was indeed slightly delayed in comparison to *A. terreus* wild type, phagocytosis rates after 2 h largely resembled the *A. terreus* wild type (Fig. 42A). Thus, expression of *wA* in *A. terreus* did not seem to have a major impact on phagocytosis. In contrast, *A. terreus wA* caused increased damage to MH-S cells compared to the *A. terreus* wild type strain, although damage was still significantly less pronounced than that caused by *A. fumigatus* (Fig. 42B). This increase in cytotoxicity was likewise observed in human monocyte-derived macrophages (Fig. 42C).

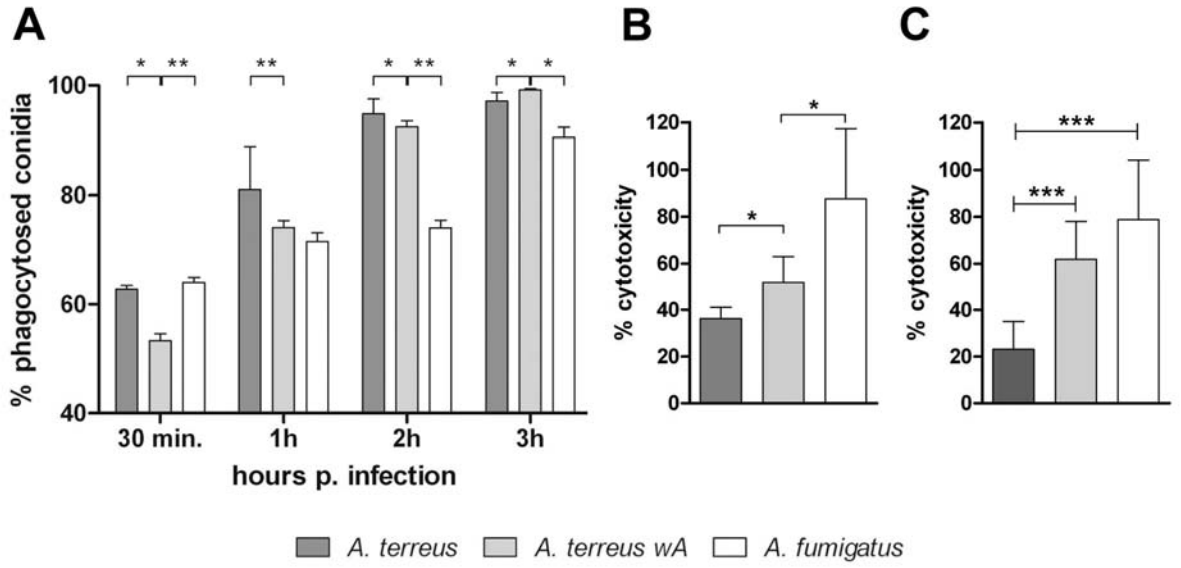

Fig. 42: Phagocytosis and cytotoxicity of *A. terreus wA*

(A) Phagocytosis of *A. terreus wA* by MH-S cells, compared to *A. terreus* wild type and *A. fumigatus* (mean + standard deviation of three independent experiments analysed by 1-way ANOVA and Tukey's multiple comparison test; * $p < 0.05$; ** $p < 0.01$). (B, C) Relative cytotoxicity (LDH release) mediated by *A. terreus wA* compared to *A. terreus* wild type and *A. fumigatus*. (mean + SD of three independent experiments analysed by 1-way ANOVA and Tukey's multiple comparison test; * $p < 0.05$, *** $p < 0.001$). (B) MH-S cells; (C) Human monocyte-derived macrophages.

Consistent with the inhibitory role on phagolysosome acidification proposed for PksP in *A. fumigatus*, phagolysosomes containing viable *A. terreus wA* conidia did not acidify in MH-S cells (data not shown), human monocyte-derived macrophages and primary murine alveolar macrophages (Fig.43).

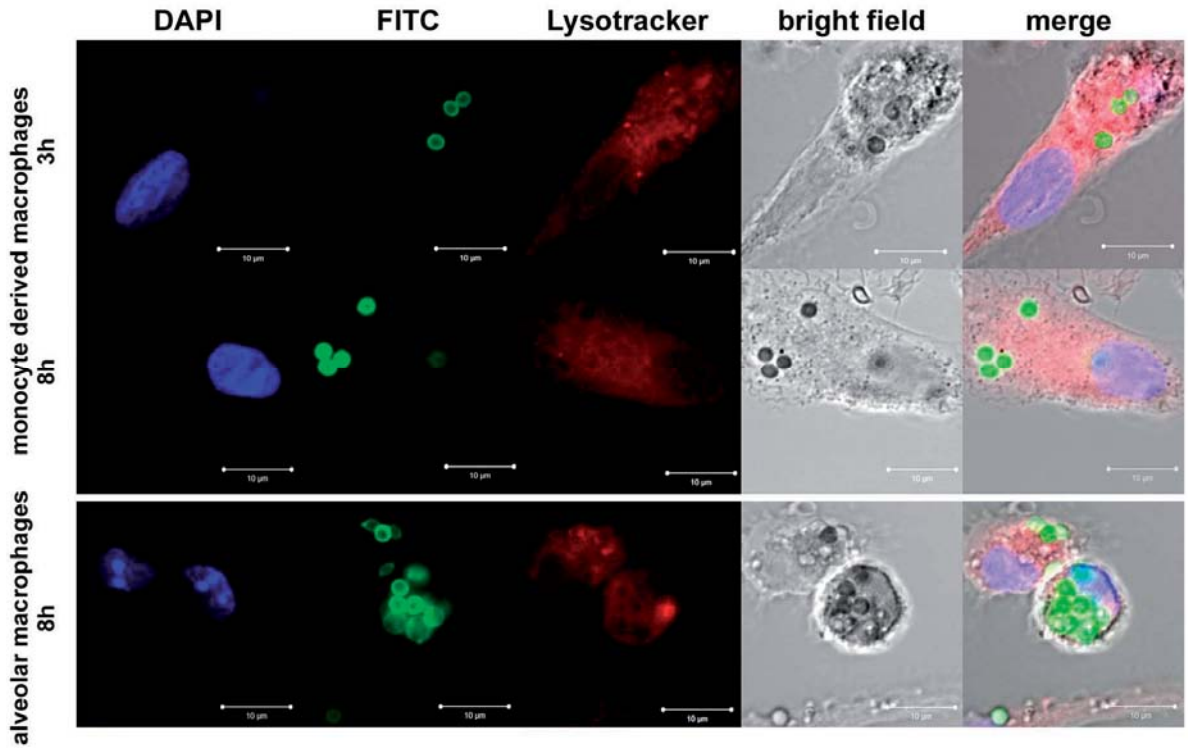

Fig. 43: Acidification of phagolysosomes in primary macrophages containing *A. terreus wA*

FITC-labelled conidia were used. Yellow signals in the merged images indicate co-localization of conidia with the lysotracker stain. All lanes show representative fluorescence microscopy images. Blue: DAPI (nucleus); green: FITC-labelled conidia; red: Lysotracker. Bars represent a size of 10 µm. The cells used for co-incubation are indicated on the left side of the lanes.

Furthermore, in accordance with the observation that blocking of acidification by bafilomycin A allowed faster germination of *A. terreus*, *A. terreus wA* germinated and formed filaments within the first 12 h of incubation within macrophages (Fig. 44A). Since the phagocytosis rate of *A. terreus wA* was comparable to *A. terreus* wild type, the increased cell damage was unlikely to be mediated by non-phagocytosed *A. terreus wA* conidia germinating extracellularly. However, cell damage and germination of *A. terreus wA* was

further enhanced by the addition of bafilomycin A (Fig. 44B and C). Thus, the observed difference in cytotoxicity of *A. terreus wA* compared to *A. fumigatus* could be due to a lower efficiency of naphthopyrone in blocking phagolysosome acidification.

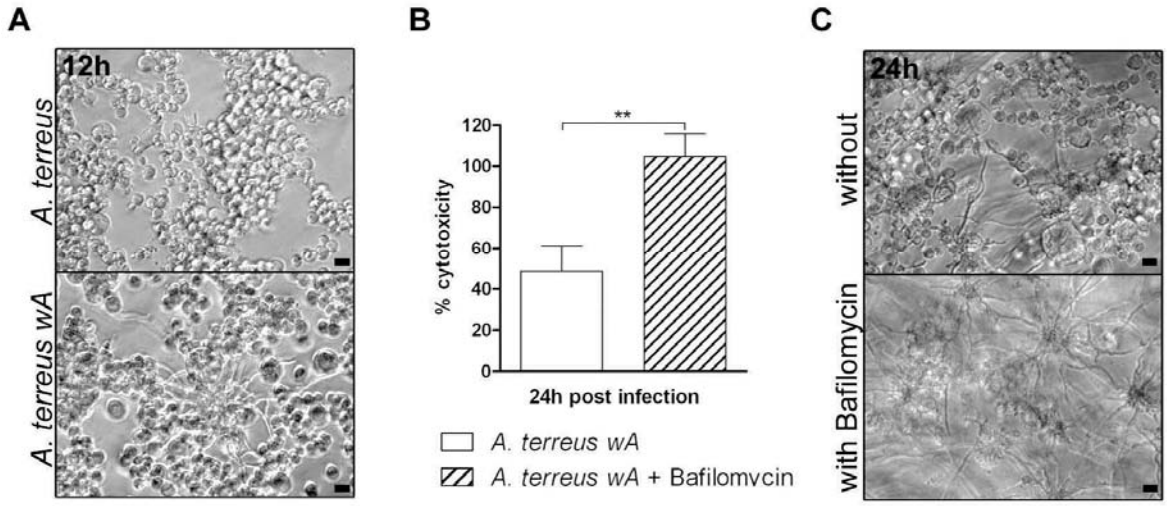

Fig. 44: Effect of bafilomycin A on the cytotoxic potential of *A. terreus wA*

(A) Brightfield microscopy of *A. terreus* and *A. terreus wA* 12 h after infection. *A. terreus wA* but not the wild type started to form mycelium. (B) Effect of bafilomycin A on relative cytotoxicity (LDH release) (mean + standard deviation from three independent experiments, unpaired, two-tailed t-test; ** $p < 0.01$). (C) Brightfield microscopy of *A. terreus wA* 24 h after infection of untreated and bafilomycin-treated macrophages. Scale bars represent 10 µm.

4.3.3 Virulence of *A. terreus wA* in murine infection models

The observation that wild type *A. terreus* conidia persist within alveolar macrophages of immunocompetent mice *in vivo* and are phagocytosed as rapidly as wild type conidia *in vitro*, suggested that the accelerated escape of *A. terreus wA* conidia from macrophages observed *in vitro* could influence virulence *in vivo*. To test this hypothesis, mice rendered either leucopenic by cyclophosphamide or immunosuppressed by cortisone acetate were infected intranasally with wild type *A. terreus* or *A. terreus wA*, respectively.

Survival curves of leucopenic mice infected with *A. terreus wA* were indistinguishable from animals infected with wild type *A. terreus* (Fig. 45A). Histologically, invasive fungal growth and tissue necrosis were observed in the lungs of moribund leucopenic infected mice (Fig. 45B). Further histologic examination revealed that mycelia formation appeared similar in size and mass as well as localisation and severity of the observed lesions. Analysis of MPO

levels and cytokine response failed to reveal any differences between PBS mock infected, *A. terreus* wild type or *A. terreus wA* infected mice as expected in the leucopenic mouse model. No histological alterations could be detected in PBS mock infected animals.

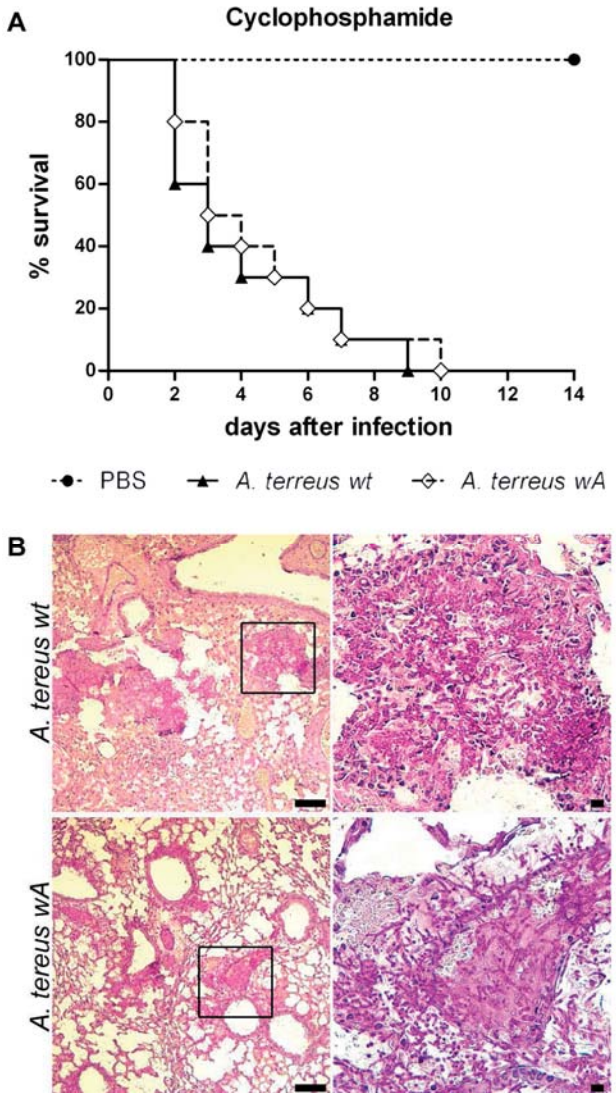

Fig. 45: Survival and histology of leucopenic mice infected with *A. terreus* and *A. terreus wA*

(A) Survival of leucopenic mice and infected with 5×10^6 conidia or mock infected with PBS (PBS: n = 2 × 5, *A. terreus wt / A. terreus wA*: n = 2 × 10); Kaplan-Meyer survival curves analysed by log rank test. (B) Representative lung histology of moribund leucopenic mice either infected with *A. terreus wild type* (wt) (upper panel) or *A. terreus wA* (lower panel). PAS reaction, mycelium is stained in pink. The right panel shows a magnification of the boxed area marked in the respective left panel. Scale bars represent 100 µm in the left panel and 10 µm in the right.

In contrast, cortisone acetate treated mice infected with *A. terreus wA* succumbed faster and at a significantly higher proportion than mice infected with *A. terreus* wild type (Fig. 46A).

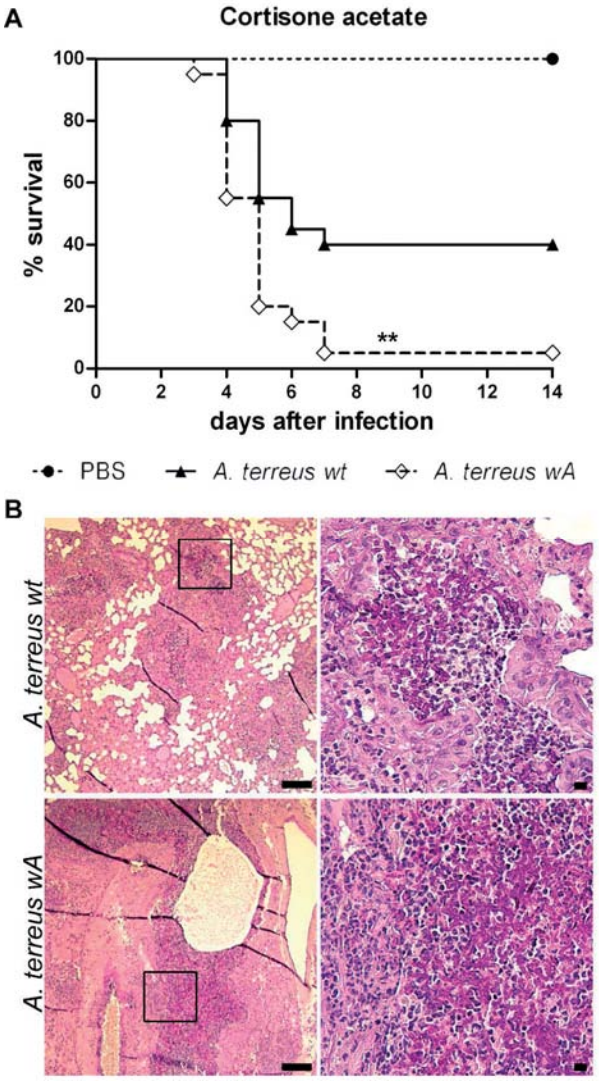

Fig. 46: Survival and histology of corticosteroid-treated mice infected with *A. terreus* and *A. terreus wA*

(A) Survival of mice immunosuppressed with cortisone acetate and infected with 1×10^7 conidia or mock infected with PBS (PBS: n = 2 × 5, *A. terreus wt* / *A. terreus wA*: n = 2 × 10); Kaplan-Meyer survival curves analysed by log rank test (** $p < 0.01$). (B) Representative lung histology of moribund cortisone acetate treated mice either infected with *A. terreus wild type* (wt) (upper panel) or *A. terreus wA* (lower panel). The right panel shows a magnification of the boxed area marked in the respective left panel. PAS reaction, mycelium is stained in pink. Scale bars represent 100 µm in the left panel and 10 µm in the right panel.

Lung histology was characterised by fungal mycelium surrounded by extensive immune cell infiltrates dominated by neutrophils in moribund animals of either group (Fig. 46B), independent of the fungal strain. In moribund animals the severity and localisation of lesions caused by either *A. terreus* strains appeared to be similar. PBS mock infected animals showed no histological alterations.

A time course experiment revealed that 24 h after infection, conidia of both strains were phagocytosed and no obvious immune cell infiltrates were observed. On day 3 after infection, hyphal formation and immune cell infiltrations were more prominent in mice infected with *A. terreus wA* (Fig. 47). Five days after infection, pyogranuloma formation and mycelial growth were observed in mice infected with either fungal strain.

MPO levels in the lungs of infected mice were significantly increased (> 250-fold) in all moribund animals compared to PBS mock infected controls (Fig. 48). Furthermore, *A. terreus wA* infected lungs of moribund animals showed significantly higher MPO levels compared to *A. terreus* wild type infected moribund mice (Fig. 48).

Investigations on the cytokine response to *A. terreus* and *A. terreus wA* revealed moderate differences and only TNF α, IL-1 β and IL-6 showed increased levels in moribund animals compared to the mock infected control group (Fig. 48). INF γ, GM-CSF, IL-10, IL-17 and IL-22 remained unaltered after infection (data not shown). While the faster germination of *A. terreus wA* observed *in vitro* and *in vivo* likely contributes to the increased virulence, it cannot be excluded that further factors may influence the pathogenicity of this mutant.

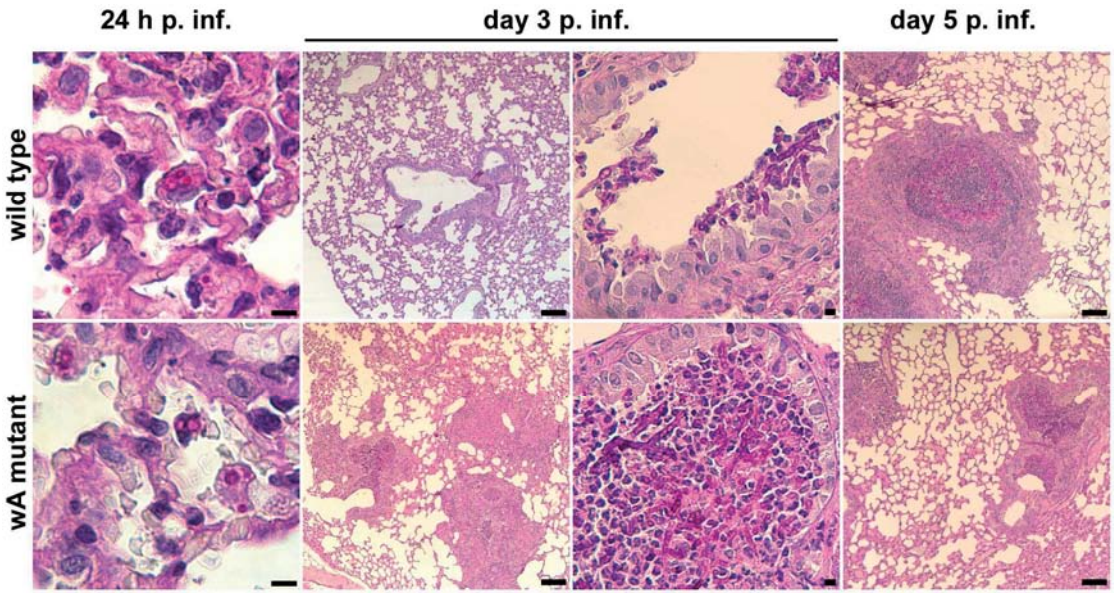

Fig. 47: Histological analysis of *A. terreus* wild type and *A. terreus wA* infected lungs

Histology 24 h, day 3 and day 5 post infection (p. inf.). PAS reaction, fungal elements stained pink. Upper panel: *A. terreus* wild type (wild type). Lower panel: *A. terreus wA* (wA mutant) showing increased fungal growth on day 3 p. inf. (p. inf.= post infection); scale bars represent 100 µm in the overview (second panel and fourth panel) and 10 µm in the detailed pictures (first panel and third panel).

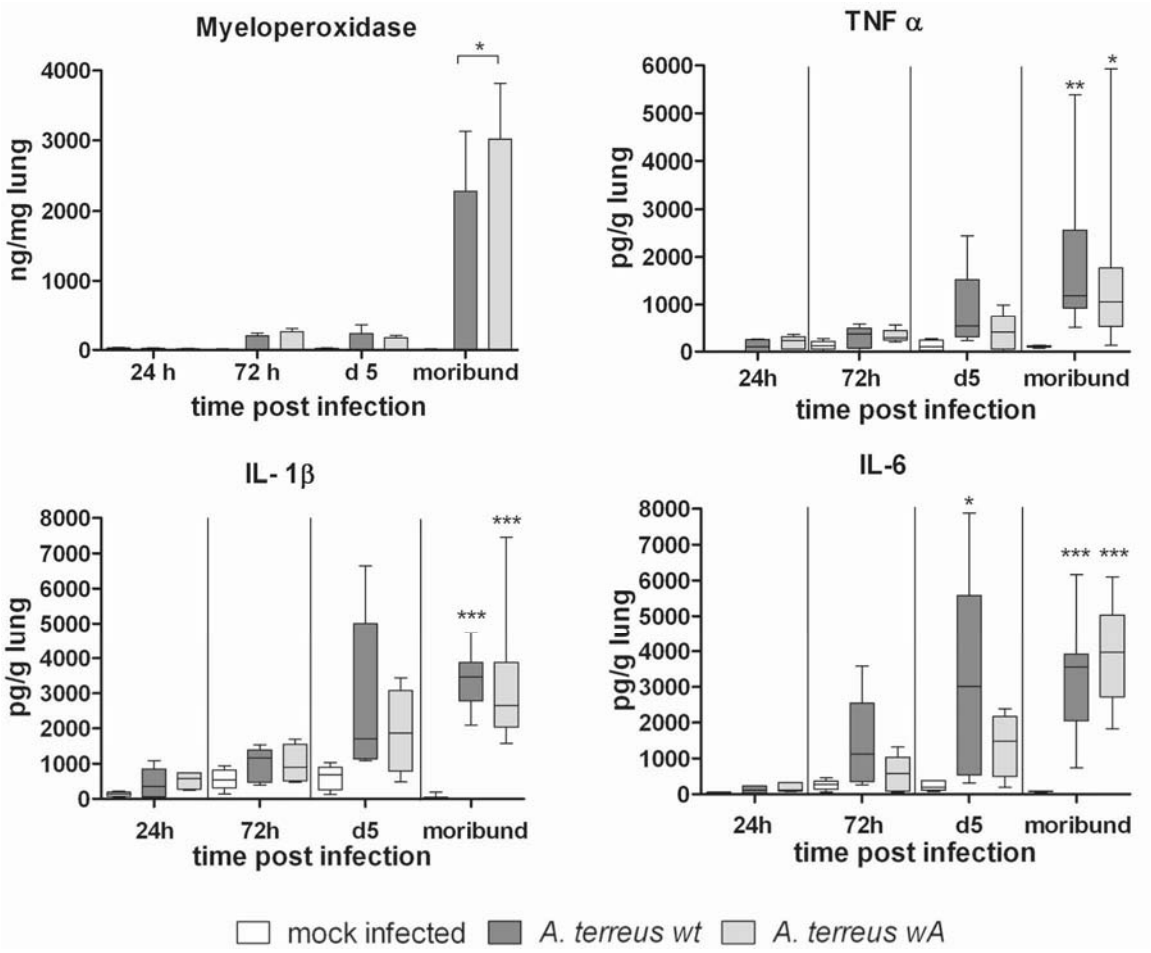

Fig. 48: Myeloperoxidase levels and cytokine response in mice infected with *A. terreus* or *A. terreus wA*

Immune response in the lungs determined by MPO and cytokine levels. White bars: PBS mock infected mice; dark grey bars: *A. terreus* wild type infected mice, light grey bars: *A. terreus wA* infected mice. MPO shown as mean + SD from at least 5 animals per group and time point, cytokine data shown as mean ± SD from at least 5 animals per group and time point. Statistical analysis was performed per time point by 1-way ANOVA (* $p < 0.05$; ** $p < 0.01$; *** $p < 0.001$).

5 Discussion

Aspergillus terreus is an ubiquitous mould with an inherent resistance to the first line drug amphotericin B provoking life-threatening invasive infections in immunocompromised patients. Though the most common cause of invasive bronchopulmonary aspergillosis (IBPA) is *A. fumigatus*, infections with *A. terreus* are emerging (Baddley et al. 2003; Lass-Flörl et al. 2005) and account for up to 12.5% of IBPA (Khoo and Denning 1994; Perfect et al. 2001; Steinbach et al. 2004a; Lass-Flörl et al. 2005). IBPA mediated by *A. terreus* is often associated with mortality rates of up to 98% (Denning et al. 1998; Lin et al. 2001).

Many investigations on the pathogenesis of *A. fumigatus* invasive infections using several *in vitro* and *in vivo* models have been performed and diverse virulence-associated factors have been described (Askew 2008). Similar studies for *A. terreus* have not been undertaken. Therefore, the aim of the first part of this study was to establish suitable infection models to investigate *A. terreus* IBPA in comparison to *A. fumigatus*.

5.1 Development of infection models for the investigation of *A. terreus* mediated IBPA

5.1.1 Chicken embryo model

Murine models are considered the gold standard for the investigation of IBPA, but their use is restricted by ethical, legal and logistical aspects (Clemons and Stevens 2005). Especially large-scale screening experiments are often not feasible in mice but are performed in alternative infection models (Lionakis and Kontoyiannis 2005). In this study, an alternative infection model based on chicken embryos was established to investigate infections due to *A. terreus*.

Chicken embryos have been used in infection research before standardised mice strains became available. Major advantages are that costs are relatively low, the model is comparatively easy to handle and large scale testing is feasible. Furthermore, the developing avian immune system is more complex and therefore likely reflects the mammalian situation (Chute 1975; Lehmann 1985; Martinez-Quesada et al. 1993). In the presented model a mucosal air interface was infected with conidia as described before (Jacobsen et al. 2010), creating an infection site similar to the lung (Latgé 2001). In contrast, in insect models which are also often applied, the immune system is less complex than the avian or mammalian immune system and conidia are usually injected into the hemocoel or are ingested (Lionakis and Kontoyiannis 2005; Lionakis et al. 2005) creating an artificial infection route and site which is not resembling a pulmonary infection.

It could be demonstrated that chicken embryos are a good model to determine virulence differences of *A. fumigatus* strains and that the results closely resemble those obtained in leucopenic or corticosteroid-based murine models (Jacobsen et al. 2010). Therefore the infectious doses applied in the embryonated egg model were used to estimate the infectious doses for murine models.

Survival and histology of an egg infection with *A. terreus* in this study largely resembled an *A. fumigatus* infection. However, *A. terreus* appeared slower in growth which might also contribute to the 1,000 times higher infectious dose required for *A. terreus* lethal infections compared to *A. fumigatus* (Jacobsen et al. 2010).

Furthermore, no differences in virulence regarding the origin of the strains used in this study could be identified. The environmental *A. terreus* strains showed indistinguishable virulence from the clinical isolate. For *A. fumigatus* it has already been shown that differences between clinical or environmental strains cannot be detected in virulence tests (Olias et al. 2011) as well as in tests determining the susceptibility to antimycotic drugs (Araujo et al. 2007).

In conclusion, the embryonated egg model provides a useful tool to screen *A. terreus* strains for virulence and investigate pathogenesis of IBPA before applying murine models.

5.1.2 Murine infections

5.1.2.1 Mortality and lung pathology

Bioluminescence imaging has been proven to be extremely useful in monitoring and characterising invasive infections caused by *A. fumigatus in vivo* (Brock et al. 2008; Ibrahim-Granet et al. 2010). An increase in the bioluminescent signal reflects germination and finally hyphal growth (Brock et al. 2008) and can thus be used to study the kinetics of fungal infections *in vivo*. Furthermore, bioluminescence imaging could detect dissemination from primary target organs to secondary organs (Hyland et al. 2008). Therefore, bioluminescent imaging was chosen for initial experiments in mice. To ensure that results obtained with the bioluminescent *A. terreus* strain were not affected by the necessary genetic manipulation of the fungus, detailed analyses were performed in mice infected with the corresponding wild type *A. terreus* strain.

The leucopenic mouse model for *A. fumigatus* mimics patients with severe immunosuppression, e.g. undergoing bone marrow transplantation, which have a high risk to develop IBPA (Khoo and Denning 1994). In this model, infection with *A. fumigatus* results in rapid fungal growth and tissue necrosis leading to death within few days (Liebmann et al. 2004 and unpublished data). In contrast to *A. fumigatus* (Brock et al. 2008), the onset of bioluminescence increase after infection with *A. terreus* was delayed, suggesting slower

germination and growth of *A. terreus* within leucopenic mice. This was confirmed by histology in experiments using a wild type *A. terreus* strain and is consistent with the slower germination and growth of *A. terreus* in the chicken embryo model and *in vitro*. Consequently, clinical symptoms occurred later after infection with *A. terreus* compared to *A. fumigatus* (Liebmann et al. 2004 and unpublished data). Similarly, increase in bioluminescence and deterioration of health after onset of symptoms was slower than in *A. fumigatus* infected mice. However, the lung lesions in moribund animals closely resembled an infection with *A. fumigatus*, characterised by extensive mycelial growth associated with angio-invasion and necrosis (Brock et al. 2008; Ibrahim-Granet et al. 2010). Thus, it appears that *A. terreus* IBPA in leucopenic hosts qualitatively resembles an *A. fumigatus* infection but requires a higher infectious dose and progresses less rapidly due to the generally slower growth of *A. terreus*.

Long-term corticosteroid treatment is another risk factor for IBPA (Lewis and Kontoyiannis 2009; Salman et al. 2011). Corticosteroids do not affect leucocyte numbers but lead to impaired killing of microorganisms by phagocytes (Lewis and Kontoyiannis 2009). However, immune cells are still recruited to the site of infection (Dixon et al. 1989; Brock et al. 2008). Infection with *A. fumigatus* in a corticosteroid mouse model thus results in broncho-pneumonia with extensive neutrophil infiltrations which significantly contribute to pathogenesis by obstruction of airways (Latgé 2001). Initial fungal growth is rapid, but limited by the immune response at later stages of murine IBPA (Duong et al. 1998).

Similar to infections with *A. fumigatus* (Brock et al. 2008), bioluminescence in *A. terreus* infected mice initially increased but decreased later, coinciding with extensive immune cell infiltration. As in leucopenic mice, lesions in moribund mice infected with *A. terreus* closely resembled findings in *A. fumigatus* infected animals.

Although bioluminescence imaging and clinical symptoms indicated successful initial establishment of infection in all *A. terreus* infected animals, only 50% of the mice succumbed to infection. Modest immune cell infiltration but no hyphae were found in surviving mice 14 days after infection, suggesting that the immune response successfully eliminated *A. terreus* mycelia. Surprisingly, non-germinated, morphologically intact conidia were observed frequently in the lungs of both surviving and moribund mice, irrespective of the immuno-suppressive regimen. Furthermore, since large numbers of colony-forming units were reisolated from surviving animals where no mycelia were observed in the lung, these conidia appeared to be viable. Thus, a lack of germination cannot be fully explained by insufficient viability of these conidia. Interestingly, conidia in surviving mice appeared not to trigger an sustained immune response, since myeloperoxidase and cytokine levels were only mildly

elevated 14 days after infection compared to mock infected controls. This suggests that these particles are either not recognised by the immune system or might actively silence the immune system. Downregulation of the immune response could possibly be facilitated by the secretion or release of factors from the cell wall with immune silencing function as described for *Cryptococcus neoformans* (Lupo et al. 2008). Persistence solely occurred within cellular structures such as macrophages or epithelial cells, in which resting conidia may hide from immune recognition.

Furthermore, the appearance of germlings and hyphae coincided with immune cell recruitment and the increase of pro-inflammatory cytokines, suggesting that germination is necessary to trigger immune cell infiltrations. Thus, if fewer conidia germinate in some animals, less immune cells may be recruited and disease might be less severe, allowing these animals to survive.

Incomplete germination of conidia may also partially explain the requirement of higher infectious doses to induce lethal IBPA by *A. terreus*. Prolonged persistence of conidia in *A. fumigatus* infected immunocompromised animals has not been described (Duong et al. 1998; Brieland et al. 2001 and unpublished data) and it appears plausible that all *A. fumigatus* conidia germinate within the lung. Thus, a relatively higher inoculum might be needed to compensate for incomplete germination of *A. terreus*. Furthermore, it should be noted that the effects of cortisone treatment on the immune system are only temporary and that the immune system regenerated towards the end of the infection experiments. Mirescu et al. demonstrated that immunosuppression has to occur concurrent with or very short after infection with *A. fumigatus* to facilitate clinical disease (Mircescu et al. 2009). Thus, the delayed germination in case of *A. terreus* might allow the immune system to regenerate sufficiently to combat the infection.

IBPA only affects immunocompromised hosts, in immunocompetent mice inhaled conidia are cleared efficiently (Ibrahim-Granet et al. 2003), resulting in steadily decreasing fungal burdens over time (Duong et al. 1998; Brieland et al. 2001). Clearance is associated with recruitment of neutrophils peaking two days after infection, resolving towards day 4 (Duong et al. 1998; Brieland et al. 2001) and only few *A. fumigatus* conidia persist in the lung (Mircescu et al. 2009). In contrast, *A. terreus* conidia were found to persist in high, stable numbers within host cells in the lungs of immunocompetent mice. Although several cytokines and myeloperoxidase significantly increased in immunocompetent mice infected with *A. terreus*, the absolute increase was lower than described for *A. fumigatus* by others (Duong et al. 1998; Brieland et al. 2001). Furthermore, the neutrophil influx occurred later, consistent with the delay in germination observed in immunocompromised mice.

In summary, IBPA caused by *A. terreus* closely resembles an infection with *A. fumigatus*. However, germination of *A. terreus* is delayed in comparison to *A. fumigatus* and growth is slower, leading to longer incubation times in leucopenic mice and likely contributing to the requirement of higher infectious doses in corticosteroid-treated mice. Furthermore, not all conidia germinated and non-germinated conidia are able to persist even in immuno-competent animals. Thus, it appears that the main difference in IBPA between *A. terreus* and *A. fumigatus* occurs in the early stages of infection. Furthermore, due to the prolonged persistence of *A. terreus* conidia it is tempting to speculate that high-risk patients that develop *A. terreus* mediated disease may not need to be infected after the onset of immunosuppression. If persisting *A. terreus* conidia acquired previously may lead to IBPA during severe immunosuppression, identification of carriers and implementation of prophylactic treatment might be necessary to prevent lethal disease.

5.1.2.2 Cytokine response in the lung

The ability of the immune system to recognise a microorganism and to mount an appropriate immune response is critical for the defeat of pathogens. Recognition of aspergilli by immune cells results in cytokine and chemokine production which recruits further immune effector cells helping in combating aspergillosis (Segal 2007). Several strategies have been developed to augment immune responses therapeutically to induce clearance of a fungal pathogen (Segal 2007). Differences in recognition by the immune system and the reaction to *Aspergillus* species therefore may have therapeutical consequences and may lead to a species-specific therapy. Furthermore, the immunosuppressive treatment associated with *A. fumigatus* or *A. terreus* mediated IBPA leads to alterations in the immune response compared to an immunocompetent patient (White 2005; Segal 2007).

As expected, the cytokine response was very limited in the leucopenic mouse model, where the number of immune cells is strongly reduced. Only IL-1β, one of the major pro-inflammatory cytokines in the body (Dinarello and Savage 1989), was mildly increased upon infection. IL-1β is not only produced by professional immune cells but also by the lung epithelium, as it has been shown for *Mycoplasma pneumoniae* infections (Yang et al. 2003). It appears likely that epithelial cells likewise respond to intracellular *A. terreus* by producing IL-1β. However, due to the reduced number of cycling immune cells that could respond to this danger signal, fungal growth is not sufficiently limited, leading to a lethal infection in this model.

In corticosteroid-treated mice, a more complex cytokine response to *A. terreus* infection was detectable. The Th1 cytokines TNFα, IL-1β and IL-6 showed similar increase over time

compared to *A. fumigatus* infections, resulting in fatal or positive outcome of infection depending on the severity and location of immune cell recruitment in the early acute phase of disease establishment (Duong et al. 1998; Schelenz et al. 1999; Balloy et al. 2005). However, some differences to *A. fumigatus* infections were observed: Infections with *A. terreus* led to reduced IL-10 levels compared to mock infected mice, while *A. fumigatus* infection induces an increase in IL-10 (Balloy et al. 2005). Production of IL-10 usually induces a Th2 response and silences the Th1 mediated immune response (Clemons et al. 2000b). Moreover, IL-10 has been shown to have a detrimental effect for the host in *A. fumigatus* infection, likely due to Th2 activation (Clemons et al. 2000b). Furthermore, no induction of IL-17A and IL-22, cytokines indicative of an Th17 response, by infection with *A. terreus* was observed. In contrast, *A. fumigatus* clearly induces a Th17 dominated immune response which has been assumed to be important for the clearance of the fungus (Zelante et al. 2007; Armstrong-James et al. 2009; Werner et al. 2009; Zelante et al. 2009). Thus, the lack of Th17 induction may contribute to the persistence and limited clearance of *A. terreus* resting conidia in the lung.

5.1.2.3 Dissemination and alterations in secondary organs

Dissemination of infection is often observed in human patients infected with *A. terreus* (Lass-Flörl et al. 2005). However, no dissemination was detected in the mouse models, neither by bioluminescence nor histology or reisolation. Possibly, dissemination requires sufficiently large primary foci of infection, without causing immediate lethality, to allow the necessary numbers of fungal elements to enter the blood stream and reach secondary organs. Given the small size of the murine lung, it appears possible that the fungal mass which is compatible with survival of the animal, is too small to facilitate sufficient seeding into the blood stream.

While no fungal growth was observed outside the lung, animals infected with *A. terreus* developed a fatty alteration of liver cells regardless of the immunosuppression regimen applied. This observation has not been described for infections with *A. fumigatus*. Since fungal elements were detected neither by histology nor by bioluminescence imaging, it is likely that the effect derives from *A. terreus* specific secondary metabolites. Given that the alteration was only mildly reflected in marker enzymes in the blood, these metabolites probably affect hepatocyte metabolism rather than directly lysing the cells. Supportive of this hypothesis is the fact that *ascomycetes* are widely known as mycotoxin producers. Several mycotoxins, especially in animal forage, appear as contaminants and lead to severe mycotoxicoses in humans and livestock. For example, ochratoxin induces degeneration in

the liver and kidneys of rats (Aydin et al. 2003). Ochratoxin was also described to induce extended glycogen degeneration of hepatocytes in chicken livers (Dwivedi et al. 1984). The genome of *A. terreus* implies that it contains a large capacity to produce secondary metabolites and several secondary and in part toxic metabolites have already been described, e.g. patulin, terreic acid, terrein or lovastatin. Whether these metabolites play a role in human IBPA and are species-independent (murine vs. human) needs further investigation in future. These metabolites might also serve as useful diagnostic markers to discriminate the fungal species causative for IBPA in patients and could result in faster and more specific therapy.

In conclusion, both murine models were highly reproducible and provided hints to substantial differences in pathogenicity between *A. fumigatus* and *A. terreus*.

5.2 Interaction of *Aspergillus fumigatus* and *Aspergillus terreus* with macrophages

Several studies have focused on the interaction of *A. fumigatus* conidia with alveolar macrophages, elucidating mechanisms involved in the uptake of conidia, the fate of conidia within phagolysosomes and the outbreak of hyphae from macrophages (Ibrahim-Granet et al. 2003; Wasylnka et al. 2005). However, it has not been addressed whether mechanisms used by *A. fumigatus* represent common strategies applied by all *Aspergillus* spp. able to cause invasive aspergillosis. Results obtained in this study from the characterisation of *A. terreus* IBPA suggested that the early stages of disease establishment might differ between the two fungal species. Since alveolar macrophages play a key role in fungal clearance and initiation of lung infection, the interaction of *A. terreus* with macrophages was investigated.

5.2.1 Phagocytosis and effects of pathogen-associated molecular pattern exposure

Previous studies demonstrated that the uptake of *A. fumigatus* conidia by alveolar macrophages is a dynamic process and that the number of phagocytosed conidia increases over time (Akpogheneta et al. 2003; Luther et al. 2006). Likewise a time-dependent kinetic of *A. terreus* phagocytosis was observed. However, uptake of *A. terreus* conidia was significantly faster than phagocytosis of *A. fumigatus* conidia, especially if resting conidia were used. Rapid and complete uptake of *A. terreus* conidia was likewise observed by Green et al. (Green et al. 1980) *in vivo* using scanning electron microscopy in rabbits and rats.

Phagocytosis kinetics are generally influenced by at least two factors: (i) form and size of the particle, e.g. smaller particles are generally phagocytosed more quickly (Kubota et al. 1983) and (ii) interaction with specific cell surface receptors, e.g. PAMPs and PRRs (Hoffmann et

al. 2010). *A. terreus* conidia are comparatively smaller than *A. fumigatus* conidia, which might impact on phagocytosis. However, the difference in size of resting and swollen *A. terreus* conidia did not effect phagocytosis rates for this species suggesting that the size difference is unlikely to fully explain the different phagocytosis rates of *A. fumigatus* and *A. terreus*. Importantly, flow cytometry analysis indicated higher exposure of β-1,3-glucan and galactomannan on the surface of pre-swollen and resting *A. terreus* conidia, in agreement with the microscopical analysis of β-1,3-glucan exposure performed by Deak et al. (Deak et al. 2009). This exposure is likely to contribute to or mediate the faster phagocytosis rates of *A. terreus* conidia, since it has been shown that these ligands facilitate uptake by several PRRs, e.g. dectin-1 as one of the most important receptors (Kerrigan and Brown 2009). However, it should be noted that prolonged pre-incubation of *A. fumigatus* conidia leads to a strong increase of β-1,3-glucan exposure on the surface of early germlings, located primarily at the hyphal tip, which strongly impacts on recognition as well as uptake by macrophages (Hohl et al. 2005; Luther et al. 2007).

Recognition of β-1,3-glucan by macrophages presented on *A. fumigatus* germlings is mediated by dectin-1 (Hohl et al. 2005; Luther et al. 2007), while recognition of mannans, e.g. galactomannan, involves a variety of pathogen recognition receptors, including the mannose receptor, TLR-2 and TLR-4 (Jouault et al. 2009). The blocking experiments performed in this study clearly demonstrate that dectin-1 and the mannose receptor are the main PRRs mediating phagocytosis of *A. terreus* conidia. In contrast, even the combined blocking of dectin-1 and the mannose receptor and simultaneous blocking of the four receptors at least responsible for phagocytosis (dectin-1, the mannose receptor, TLR-2 and TLR-4) only moderately reduced phagocytosis of *A. fumigatus* conidia. Thus, additional PRRs, for example DC-SIGN (dendritic cell-specific ICAM-3-grabbing nonintegrin) (Serrano-Gomez et al. 2004), may be required for phagocytosis of *A. fumigatus*, but not *A. terreus*, conidia. As mentioned above, the pre-swelling time used significantly influences PAMP exposure on *A. fumigatus* conidia and longer pre-swelling exposes β-1,3-glucan facilitating interaction with dectin-1 (Hohl et al. 2005).

5.2.2 Survival of *A. terreus* after phagocytosis

Alveolar macrophages primarily eliminate inhaled pathogens by intracellular killing after phagocytosis (Jonsson et al. 1985). The inactivation of *A. fumigatus* and *A. terreus* conidia was determined by two independent methods: (i) CFU plating and (ii) analysis on the single-conidia level using a metabolic dye (Marr et al. 2001). Results obtained with either method showed significantly higher survival rates of *A. terreus* compared to *A. fumigatus.* This effect

was independent of the fungal strain and type of macrophage used. In contrast, Perkhofer et al. (Perkhofer et al. 2007) did not observe these striking differences. In their study, survival was analysed after a two hour co-incubation, representing a relatively short co-incubation time, and furthermore using resting instead of pre-swollen conidia. Since the initial swelling process is essential for conidial inactivation (Philippe et al. 2003), this experimental setup might have masked differences between both species.

In addition to the role of the NADPH oxidase in killing of *A. fumigatus* conidia (Philippe et al. 2003), inactivation has been shown to be associated with acidification of the phagolysosome (Jahn et al. 2002; Ibrahim-Granet et al. 2003). Mature, acidified phagolysosomes are generally formed in macrophages to efficiently eliminate microorganisms. Not surprisingly, different pathogens have developed mechanisms to interfere with phagolysosome acidification (Haas 1998). Similar to other pathogenic fungi (Seider et al. 2010), *A. fumigatus* is able to inhibit phagolysosome acidification at least to a certain extent (Jahn et al. 2002), while fusion of phagosomes and lysosomes is unaltered. Surprisingly, despite the high survival rates of phagocytosed conidia, phagolysosomes containing *A. terreus* acidified frequently, independent of the macrophage type and *A. terreus* strain used, suggesting that (i) *A. terreus* lacks the ability to inhibit or interfere with acidification and (ii) *A. terreus* is not inactivated within mature acidic phagolysosomes as shown by the killing experiments. Supporting the latter, that low pH did not impact survival of *A. terreus* conidia under nutrient depleted conditions, although acidic pH inhibits germination. In contrast, survival of *A. fumigatus* conidia was significantly impaired at low environmental pH, highlighting the need of *A. fumigatus* to inhibit phagolysosome acidification. However, it should be noted that survival within acidified phagolysosomes does not only depend on pH resistance, but also on the resistance against microbicidal enzymes and compounds, which display optimal activity at low pH (Wiesner and Vilcinskas 2010).

Since conidia are more resistant to damage by adverse environmental conditions than hyphae (Diamond 1988), the delayed germination of *A. terreus* at low pH might enhance persistence in phagolysosomes. In contrast, rapid germination due to inhibition of acidification allows *A. fumigatus* to escape from macrophages, but also renders the fungal cells more vulnerable to antifungal host molecules. This might explain the observed inactivation of a significant proportion of *A. fumigatus* during the time course of co-incubation. It appears that divergent strategies have evolved within pathogenic *Aspergillus* species: while *A. terreus* survives within acidified phagolysosomes of macrophages, *A. fumigatus* interferes with phagolysosome acidification, germinates and eventually escapes from macrophages. Persistence in macrophages may allow *A. terreus* to evade the recognition by

the immune system. Similarly, different strategies for phagolysosomal survival have also been described for other pathogenic fungi (Seider et al. 2010). For example, *Candida albicans* (Nessa et al. 1997) and *Histoplasma capsulatum* (Eissenberg et al. 1993) also inhibit acidification of the phagolysosome, whereas *Crytococcus neoformans* resides and replicates within acidified phagolysosomes (Levitz et al. 1999; Voelz et al. 2009).

Possibly, persistence in macrophages might be involved in the high dissemination rates observed in *A. terreus* infections (Baddley et al. 2001; Lass-Flörl et al. 2005). It has been shown that the pathogens *Cryptococcus neoformans* and *Francisella tularensis* (Buchan et al. 2009; Krishnan et al. 2010; Okagaki et al. 2010) use persistence in macrophages to facilitate dissemination. It appears possible that *A. terreus* might likewise use macrophages as a vehicle to reach secondary organs, as lymph nodes or regional lymphoid centers, also possibly the spleen. In these organs establishment of infection could take place under severe immunosuppression and result in the systemic multi focal infections seen in human patients as well as in dogs (Tracy et al. 1983; Kabay et al. 1985; Hara et al. 1989; Tritz and Woods 1993; Kelly et al. 1995; Watt et al. 1995).

5.3 The role of naphthopyrone in the pathogenesis of *A. terreus*

It has been shown that the ability of *A. fumigatus* to prevent phagolysosome acidification depends on the presence of a functional *pksP* gene. PksP is essential for the synthesis of DHN-melanin from the precursor naphthopyrone and deletion of *pksP* results in white coloured conidia (Langfelder et al. 1998). In agreement with the proposed role of DHN-melanin in preventing acidification (Thywissen et al. 2011), an *A. fumigatus pksP* deletion mutant cannot inhibit acidification of phagolysosomes and shows altered conidial morphology (Jahn et al. 1997; Tsai et al. 1998; Jahn et al. 2002). This altered morphology is characterised by a significantly increased β-1,3-glucan exposure (Luther et al. 2007) which may be due to a weakened affinity of hydrophobins to the conidial surface (Brakhage and Liebmann 2005; Aimanianda et al. 2009). This mutant is inactivated to a higher extent by macrophages and is attenuated in mice, highlighting the role of the inhibition of phagolysosome acidification for *A. fumigatus* virulence (Langfelder et al. 1998; Jahn et al. 2002).

A. terreus lacks this specific *pksP* gene and, although the origin of its pigment is unknown, its conidial colour appears not to be DHN-melanin related. Expression of the *pksP* homologue *wA* from *A. nidulans* in *A. terreus*, which leads to the production of the heptaketide naphthopyrone YWA1 (Watanabe et al. 2000), was sufficient to prevent acidification of

phagolysosomes for the majority of intracellular conidia. This result again emphasises the role of naphthopyrone derivatives in the interaction of *Aspergillus* species with macrophages and defines this pigment as the essential factor leading to phagolysosomal escape in *A. fumigatus* infections. However, the reduced acidification by *A. terreus wA* conidia was not sufficient to increase fungal cytotoxicity to the level of *A. fumigatus* and addition of bafilomycin A still enhanced cytotoxicity of the *A. terreus wA* mutant. This suggests that (i) naphthopyrone might be less efficient than DHN-melanin in interfering with phagolysosome maturation, (ii) that the expression levels of *wA* in *A. terreus wA* do not reach the levels of DHN-melanin in *A. fumigatus* or (iii) that additional, yet unidentified *A. fumigatus* factors absent in *A. terreus* interfere with phagolysosome maturation.

It is tempting to speculate that the lack of a *pksP* homologue in *A. terreus* contributes to the lower incidence of *A. terreus* infections compared to *A. fumigatus*, as the impact of *pksP* on infections *in vivo* has been demonstrated for *A. fumigatus* (Langfelder et al. 1998). However, the distribution of *pksP* homologues within aspergilli does not directly correlate with virulence in mouse models: Both *A. nidulans* and *A. niger* possess *pksP* homologues and show a green or black spore colouration. Nonetheless, only *A. niger* is highly virulent in mice (Ford and Friedman 1967) while *A. nidulans* shows a more attenuated phenotype (Purnell 1974; Bignell et al. 2005). These results from murine models are in accordance with IBPA in human patients, where *A. nidulans* is rarely identified as the causative agent.

However, virulence of aspergilli is multifactorial and depends on several factors in which pigmentation might play diverse roles in different *Aspergillus* species. Since *A. terreus wA* showed significant differences in the interaction with macrophages compared to the wild type, it appeared possible that naphthopyrone production might also alter virulence of *A. terreus in vivo*. It has been shown that the outcome of IBPA in leucopenic animals is mainly determined by fungal growth, due to the absence of a cellular immune response (Balloy et al. 2005). Interaction with macrophages is unlikely to play a major role in this infection model. In agreement, no differences in virulence were observed between *A. terreus* wild type and *A. terreus wA* in this model, suggesting that *A. terreus wA* does not have a general growth advantage within the lung.

In contrast, fungal interaction with immune cells is important during IBPA in corticosteroid-treated mice. An *A. fumigatus* mutant lacking the secondary metabolite gliotoxin was attenuated in this model but not in a leucopenic infection model (Cramer et al. 2006; Kupfahl et al. 2006; Sugui et al. 2007; Kwon-Chung and Sugui 2009). Thus, due to the low frequency of germination of *A. terreus* wild type conidia after phagocytosis and the accelerated escape of *A. terreus wA* conidia from macrophages, differences in the outcome of infection in the

corticosteroid-based model were expected. In agreement, animals infected with *A. terreus wA* succumbed to infection faster and at a significantly higher rate. As persisting, non-germinated conidia were found in all lungs of mice surviving *A. terreus* wild type infection, the difference in virulence could be explained by a comparatively lower induction of inflammation in surviving mice, due to a lower percentage of germinated conidia. The assumption of low germination rates and persistence is also in agreement with the previously discussed data from mouse experiments. Thus, fast escape from macrophages (*A. terreus wA* and *A. fumigatus*) causes increased virulence in corticosteroid-treated animals, whereas a "sit and wait" strategy (*A. terreus*) may allow long-term persistence, especially in immunocompetent hosts.

In summary, *A. fumigatus* and *A. terreus* differ significantly in their interactions with macrophages. *A. fumigatus* prevents phagolysosome acidification due to the presence of DHN-melanin, germinates and escapes from macrophages, leading to local establishment of invasive disease in immunocompromised hosts. In contrast, *A. terreus* is rapidly recognised and phagocytosed by macrophages and persists without germination in acidified phagolysosomes. It appears possible that *A. terreus* conidia inhaled by patients prior to severe immunosuppression persist in a resting, but viable state. Thus, development of disease by *A. terreus* might progress more slowly and might require a stronger immunosuppression regimen than *A. fumigatus*, but due to long-term persistence in macrophages might not necessarily require a *de novo* infection after immunosuppression.

5.4 Outlook

Though this work elucidates for the first time striking differences between two *Aspergillus* species regarding the pathogenicity strategy, several questions still remain unsolved and need further investigation.

First, it would be very interesting to analyse the persistence of *A. terreus* in immuno-competent mice in more detail. Therefore, the kinetics of fungal burden in healthy mice should be determined over a prolonged time of at least two weeks. This approach allows quantification and elucidates whether *A. terreus* burdens reach a plateau or decline over a longer observation period.

Moreover, it remains unclear whether the persisting fungal burden is capable of inducing IBPA under severe immunosuppression. To elucidate this, animals should be infected in the immunocompetent status, followed, after a defined time, by immunosupression. If IBPA

develops in these animals, the hypothesis that patients may acquire *A. terreus* outside the hospital environment before the onset of immunosuppression would be strengthened.

Furthermore, several fungal species were found within single specimens of fungal pneumonia in stork hatchlings (Olias et al. 2011). Similarly, human patients suffering from cystic fibrosis are regularly co-colonised with *A. terreus* and *A. fumigatus* (Simmonds et al. 1994; Vanhee et al. 2008; Millar et al. 2009). Due to the slower growth, *A. terreus* might be missed diagnostically in co-infections with *A. fumigatus* during IBPA. This would be detrimental to the patient if amphotericin B was used to treat the presumed *A. fumigatus* IBPA, since *A. terreus* is resistant to amphotericin B. Therefore, co-infections with both fungi and subsequent therapy studies would help in solving this diagnostic and therapeutic trap.

Finally it should be investigated which factors contribute to the increased pH stability of *A. terreus* in comparison to *A. fumigatus*. Investigations on the cell wall composition of *A. terreus* compared to *A. fumigatus* or factors involved in pH regulation of fungi such as *pacC* (Penalva et al. 2008) would be helpful. *PacC* is a pH regulatory transcription factor in aspergilli. Preliminary investigations using real-time PCR showed that *A. terreus* does not express this transcriptional regulator in ambient pH ranging from 2 to 10 (unpublished data), which is in clear contrast to *A. fumigatus*.

6 Summary

Establishment of Infection Models and Insights into the Pathogenesis of Invasive Aspergillosis mediated by *Aspergillus terreus*

Silvia Slesiona

Invasive bronchopulmonary aspergillosis (IBPA) is a life-threatening disease in severely immunocompromised patients. Although *A. fumigatus* is the most common cause of IBPA, infections with *A. terreus* are emerging and mortality rates are comparable to *A. fumigatus* infections. Although *A. terreus* is distributed ubiquitously, the incidence of *A. terreus* mediated IBPA is comparably low.

To elucidate the pathogenesis of *A. terreus* aspergillosis in comparison to *A. fumigatus* mediated IBPA, an alternative infection model and two distinct pulmonary murine infection models were established and characterised in this study. To induce lethal infections by *A. terreus* an at least 100 times higher infectious dose was required than for *A. fumigatus*, but even with the highest infectious dose only 50% mortality was observed in corticosteroid-treated mice. However, surviving mice transiently displayed clinical symptoms and bioluminescence imaging revealed transient fungal growth, suggesting that the immune system of surviving animals was able to control the infection. In moribund animals, the disease pattern largely resembled *A. fumigatus* IBPA. However, persistent, ungerminated but viable conidia were frequently found in alveolar macrophages and pulmonary epithelial cells of surviving animals. In contrast to *A. fumigatus* infections, all mice infected with *A. terreus* developed a fatty liver degeneration, possibly due to the production of toxic secondary metabolites. Thus, at least in mice, persistence and subclinical liver damage represent unique features of *A. terreus* mediated IBPA. Furthermore, these models provide the necessary tools to investigate the pathogenesis of *A. terreus* mediated aspergillosis in detail.

The persistence and incomplete germination of conidia in macrophages and epithelial cells observed *in vivo* led to the hypothesis that the initial steps of disease establishment might be fundamentally different between *A. terreus* and *A. fumigatus*. Since alveolar macrophages represent the first immune cells facing inhaled conidia in the lung, the interaction of *A. terreus* and *A. fumigatus* conidia with these phagocytes was investigated. Interestingly, *A. terreus* conidia were phagocytosed more rapidly than *A. fumigatus* conidia. This was likely due to the higher exposure of β-1,3-glucan and galactomannan on the surface of *A. terreus* resting and pre-swollen conidia. In agreement with the increased PAMP exposure observed on conidia, blocking of dectin-1 and the mannose receptor, the ligand-specific PRRs, significantly reduced phagocytosis of *A. terreus* to basal levels, but had only a moderate

effect on phagocytosis of *A. fumigatus*. While *A. fumigatus* prevents phagolysosomal acidification which allows germination within this organelle, *A. terreus* conidia persisted in fully matured and acidified phagolysosomes after phagocytosis. The acidic pH of the phagolysosome prevented germination of *A. terreus* conidia, thus resulting in significantly reduced macrophage cytotoxicity. Blocking phagolysosome acidification by the specific v-ATPase inhibitor bafilomycin A increased *A. terreus* germination within phagolysosomes and consequently cytotoxicity. Thus, it appears that the two fungal species have evolved different interaction strategies with macrophages: While *A. fumigatus* interferes with phagosome maturation and escapes from phagocytes by germination, *A. terreus* remains viable but trapped within acidified phagolysosomes. However, possibly because germlings are more sensitive than conidia, *A. fumigatus* is inactivated to a higher extent by macrophages.
To determine factors involved in phagolysosome interaction, this work focused on pigments which are frequently used for morphological species discrimination in *Aspergillus* diagnostics. These pigments are part of the cell wall, provide defence against physiological stresses and can moreover interact with PRRs of immune cells. In *A. fumigatus*, the polyketide synthase PksP produces the pigment DHN-melanin, which prevents phagolysosome acidification, but is absent in *A. terreus*. However, recombinant expression of the *A. nidulans* wA naphthopyrone synthase, a homologue of *A. fumigatus* PksP, in *A. terreus* inhibited phagolysosome acidification and resulted in increased germination, macrophage damage and virulence in corticosteroid-treated mice.

In summary, this study demonstrates for the first time that *A. terreus* and *A. fumigatus* interact fundamentally different with the immune system during disease establishment. Although aspergillosis caused by *A. terreus* resembles *A. fumigatus* IBPA, significant differences in the interaction with macrophages suggest a modified pathogenicity strategy. While *A. fumigatus* hides from phagocytosis and prevents phagolysosome acidification which allows escape from macrophages by germination, *A. terreus* is rapidly phagocytosed, does not interfere with phagolysosomal maturation but persists within macrophages. Consequently, the pathogenicity strategy of *A. fumigatus* cannot be taken as a general model for all aspergilli but requires species-specific investigation.

7 Zusammenfassung

Etablierung von Infektionsmodellen und Einblicke in die Pathogenese der invasiven Aspergillose durch *Aspergillus terreus*

Silvia Slesiona

Die invasive, bronchopulmonale Aspergillose (IBPA) stellt eine lebensbedrohliche Komplikation in immunsupprimierten Patienten dar. Hauptverursacher dieses Krankheitsbildes ist *A. fumigatus*, jedoch nimmt die Häufigkeit von *A. terreus* Erkrankungen mit ähnlichen Letalitätsraten zu. Obwohl *A. terreus* ubiquitär verbreitet ist, ist die Erkrankungsinzidenz jedoch verhältnismäßig gering.

Um die Pathogenese der *A. terreus* Aspergillose vergleichend zu *A. fumigatus* aufzuklären, entwickelte und charakterisierte die vorliegende Studie ein alternatives und zwei murine Infektionsmodelle. Um letale Infektionen in diesen Modellen hervorzurufen, benötigte es einer mindestens 100fach höheren Infektionsdosis im Vergleich zu *A. fumigatus*. Dennoch konnte unter Kortisonbehandlung lediglich eine Mortalität von 50% der infizierten Versuchstiere beobachtet werden. Lumineszenzmessungen zeigten jedoch ein transientes Wachstum des Pilzes in überlebenden Tieren, welches mit klinischer Symptomatik einherging. Dies lässt vermuten, dass eine Kontrolle der Infektion durch das Immunsystem in diesen Tieren möglich war. Der Krankheitsverlauf moribunder Tiere glich weitgehend dem einer IBPA durch *A. fumigatus*. Allerdings waren in überlebenden Tieren häufig lebende, ungekeimte Konidien in Alveolarmakrophagen und Epithelzellen der Lunge auffindbar.

Im Unterschied zu einer *A. fumigatus* IBPA wurde bei allen mit *A. terreus* infizierten Tieren, unabhängig vom Infektionsmodell, eine kleinvakuolige, peripherlobuläre, fettige Degeneration der Leber beobachtet. Diese ist wahrscheinlich auf den Einfluss pilzlicher Sekundärmetabolite zurückzuführen, die während der Infektion gebildet werden. Somit konnten in dieser Studie, die Persistenz von Konidien und eine fettige Leberdegeneration als Besonderheiten der, durch *A. terreus* verursachten, invasiven Aspergillose identifiziert werden. Die hier vorliegenden Modelle liefern zudem die Grundlage für die weitere, detailierte Untersuchung der Pathogenese der *A. terreus*-induzierten IBPA.

Die, während der Etablierung der *in vivo* Infektionsmodelle, beobachtete Persistenz von Sporen in Makrophagen und Epithelzellen führte zu der Hypothese, dass sich die anfänglichen Prozesse des Infektionsverlaufes zwischen beiden Pilzspezies grundlegend unterscheiden. Da Alveolarmakrophagen in der Lunge als professionelle Phagozyten initial mit Pathogenen interagieren, wurde die Interaktion von Makrophagen mit Sporen von *A. terreus* und *A. fumigatus* untersucht. Sporen von *A. terreus* wurden wesentlich schneller

und vollständiger phagozytiert als Sporen von *A. fumigatus*. Dies kann auf eine erhöhte β-1,3-Glukan und Galaktomannan Präsentation auf der Oberfläche der *A. terreus* Sporen zurückgeführt werden. Damit übereinstimmend wurde gezeigt, dass die Blockierung der, zur Erkennung dieser Zellwandbestandteile notwendigen, Rezeptoren Dectin-1 und des Mannose-Rezeptors zu einer deutlichen Verringerung der Phagozytose von *A. terreus* Sporen durch Makrophagen führte. Die Phagozytoserate von *A. fumigatus* wurde durch diese Blockierung nur gering beeinflusst. Sporen von *A. fumigatus* verhindern zudem nach der Phagozytose die Ansäuerung von Phagolysosomen und können durch Auskeimung aus Makrophagen entkommen, was mit einer Schädigung der Makrophagen einhergeht. Im Gegensatz dazu persistierten phagozytierte Konidien von *A. terreus* in angesäuerten Phagolysosomen ohne auszukeimen und ohne die Makrophagen zu schädigen. Die Inhibierung der Ansäuerung des Phagolysosoms durch den spezifischen v-ATPase Inhibitor Bafilomycin A führte zu einer deutlich erhöhten Auskeimungsrate und Zytotoxizität von *A. terreus*. Die beiden *Aspergillus*-Arten scheinen also zwei unterschiedliche Strategien im Umgang mit Makrophagen entwickelt zu haben: Während *A. fumigatus* die Ansäuerung von Phagolysosomen verhindert und durch Auskeimen entkommt, persistiert *A. terreus* als Spore in angesäuerten Phagolysosomen. Dabei wird jedoch ein höherer Anteil von *A. fumigatus* durch Makrophagen inaktiviert. Dies liegt vermutlich an der verstärkten Empfindlichkeit von Keimlingen und Hyphen gegenüber antimikrobiellen Stoffen im Vergleich zu Sporen.

Pigmente als Zellwandbestandteile, haben eine potentielle Rolle in der Interaktion mit dem Phagolysosom und werden in der mikrobiologischen Diagnostik häufig als Spezies-diagnostikum verwandt. *A. fumigatus* produziert das Pigment DHN-Melanin mit Hilfe der Polyketidsynthase PksP, welches die Phagolysosomansäuerung verhindert jedoch in *A. terreus* fehlt. Durch rekombinante Expression der Naphthopyronsynthase wA von *A. nidulans*, einem Homolog der *A. fumigatus* PksP, in *A. terreus* konnte die Ansäuerung des Phagolysosom verhindert werden. Dies führte zu einer erhöhten Auskeimungsrate in Makrophagen, einer verstärkten Zytotoxizität und erhöhte die Virulenz im Kortison-Modell.

Damit zeigt diese Studie erstmalig, dass *A. terreus* und *A. fumigatus* grundlegende Unterschiede in der Interaktion mit Phagozyten aufweisen. Trotz gleicher klinischer Symptomatik, entwickelten *A. terreus* und *A. fumigatus* unterschiedliche Pathogenese-strategien, um der Eliminierung durch das Immunsystem zu entgehen. Während *A. fumigatus* Phagozytose sowie Ansäuerung des Phagolysosom verhindert, wird *A. terreus* schnell phagozytiert und persistiert in Makrophagen. Folglich kann die IBPA durch *A. fumigatus* nicht als Modell für alle Aspergillosen dienen und die Pathogenese sollte abhängig von der *Aspergillus*-Art untersucht werden.

8 Index

8.1 Index of Figures

8.2 Index of Tables

9 References

Aimanianda V, Bayry J, Bozza S, Kniemeyer O, Perruccio K, Elluru SR, Clavaud C, Paris S, Brakhage AA, Kaveri SV, Romani L, Latgé JP (2009) Surface hydrophobin prevents immune recognition of airborne fungal spores. Nature. 460(7259), 1117-21.

Akpogheneta O, Gil-Lamaignere C, Maloukou A, Roilides E (2003) Antifungal activity of human polymorphonuclear and mononuclear phagocytes against non-fumigatus *Aspergillus* species. Mycoses. 46(3-4), 77-83.

Alberts AW, Chen J, Kuron G, Hunt V, Huff J, Hoffman C, Rothrock J, Lopez M, Joshua H, Harris E, Patchett A, Monaghan R, Currie S, Stapley E, Albers-Schonberg G, Hensens O, Hirshfield J, Hoogsteen K, Liesch J, Springer J (1980) Mevinolin: a highly potent competitive inhibitor of hydroxymethylglutaryl-coenzyme A reductase and a cholesterol-lowering agent. Proc Natl Acad Sci U S A. 77(7), 3957-61.

Antunes J, Fernandes A, Borrego LM, Leiria-Pinto P, Cavaco J (2010) Cystic fibrosis, atopy, asthma and ABPA. Allergol Immunopathol (Madr). 38(5), 278-84.

Aramayo R, Timberlake WE (1993) The *Aspergillus nidulans yA* gene is regulated by *abaA*. EMBO J. 12(5), 2039-48.

Araujo R, Pina-Vaz C, Rodrigues AG (2007) Susceptibility of environmental versus clinical strains of pathogenic *Aspergillus*. Int J Antimicrob Agents. 29(1), 108-11.

Armstrong-James DP, Turnbull SA, Teo I, Stark J, Rogers NJ, Rogers TR, Bignell E, Haynes K (2009) Impaired interferon-gamma responses, increased interleukin-17 expression, and a tumor necrosis factor-alpha transcriptional program in invasive aspergillosis. J Infect Dis. 200(8), 1341-51.

Arné P, Thierry S, Wang D, Deville M, Le Loc'h G, Desoutter A, Femenia F, Nieguitsila A, Huang W, Chermette R, Guillot J *Aspergillus fumigatus* in Poultry. Int J Microbiol. 2011, 746356.

Askew DS (2008) *Aspergillus fumigatus*: virulence genes in a street-smart mold. Curr Opin Microbiol. 11(4), 331-7.

Auberger J, Lass-Flörl C, Ulmer H, Nogler-Semenitz E, Clausen J, Gunsilius E, Einsele H, Gastl G, Nachbaur D (2008) Significant alterations in the epidemiology and treatment outcome of invasive fungal infections in patients with hematological malignancies. Int J Hematol. 88(5), 508-15.

Aydin G, Ozcelik N, Cicek E, Soyoz M (2003) Histopathologic changes in liver and renal tissues induced by Ochratoxin A and melatonin in rats. Hum Exp Toxicol. 22(7), 383-91.

Baddley JW, Pappas PG, Smith AC, Moser SA (2003) Epidemiology of *Aspergillus terreus* at a university hospital. J Clin Microbiol. 41(12), 5525-9.

Baddley JW, Stroud TP, Salzman D, Pappas PG (2001) Invasive mold infections in allogeneic bone marrow transplant recipients. Clin Infect Dis. 32(9), 1319-24.

Balajee SA (2009) *Aspergillus terreus* complex. Med Mycol. 47 Suppl 1, S42-6.

Balloy V, Chignard M (2009) The innate immune response to *Aspergillus fumigatus*. Microbes Infect. 11(12), 919-27.

Balloy V, Huerre M, Latgé JP, Chignard M (2005) Differences in patterns of infection and inflammation for corticosteroid treatment and chemotherapy in experimental invasive pulmonary aspergillosis. Infect Immun. 73(1), 494-503.

Beernaert LA, Pasmans F, Van Waeyenberghe L, Haesebrouck F, Martel A (2010) *Aspergillus* infections in birds: a review. Avian Pathol. 39(5), 325-31.

Beffa T, Staib F, Lott Fischer J, Lyon PF, Gumowski P, Marfenina OE, Dunoyer-Geindre S, Georgen F, Roch-Susuki R, Gallaz L, Latge JP (1998) Mycological control and surveillance of biological waste and compost. Med Mycol. 36 Suppl 1, 137-45.

Behnsen J, Hartmann A, Schmaler J, Gehrke A, Brakhage AA, Zipfel PF (2008) The opportunistic human pathogenic fungus *Aspergillus fumigatus* evades the host complement system. Infect Immun. 76(2), 820-7.

Ben-Ami R, Lamaris GA, Lewis RE, Kontoyiannis DP (2010a) Interstrain variability in the virulence of *Aspergillus fumigatus* and *Aspergillus terreus* in a Toll-deficient *Drosophila* fly model of invasive aspergillosis. Med Mycol. 48(2), 310-7.

Ben-Ami R, Lewis RE, Kontoyiannis DP (2010b) Enemy of the (immunosuppressed) state: an update on the pathogenesis of *Aspergillus fumigatus* infection. Br J Haematol. 150(4), 406-17.

Bennett JE, Friedman MM, Dupont B (1987) Receptor-mediated clearance of *Aspergillus* galactomannan. J Infect Dis. 155(5), 1005-10.

Berenguer J, Allende MC, Lee JW, Garrett K, Lyman C, Ali NM, Bacher J, Pizzo PA, Walsh TJ (1995) Pathogenesis of pulmonary aspergillosis. Granulocytopenia versus cyclosporine and methylprednisolone-induced immunosuppression. Am J Respir Crit Care Med. 152(3), 1079-86.

Bhabhra R, Askew DS (2005) Thermotolerance and virulence of *Aspergillus fumigatus*: role of the fungal nucleolus. Med Mycol. 43 Suppl 1, S87-93.

Bhatia S, Fei M, Yarlagadda M, Qi Z, Akira S, Saijo S, Iwakura Y, van Rooijen N, Gibson GA, St Croix CM, Ray A, Ray P (2011) Rapid Host Defense against *Aspergillus fumigatus* Involves Alveolar Macrophages with a Predominance of Alternatively Activated Phenotype. PLoS One. 6(1), e15943.

Bignell E, Negrete-Urtasun S, Calcagno AM, Haynes K, Arst HN, Jr., Rogers T (2005) The *Aspergillus* pH-responsive transcription factor *PacC* regulates virulence. Mol Microbiol. 55(4), 1072-84.

Blum G, Perkhofer S, Haas H, Schrettl M, Wurzner R, Dierich MP, Lass-Flörl C (2008) Potential basis for amphotericin B resistance in *Aspergillus terreus*. Antimicrob Agents Chemother. 52(4), 1553-5.

Braedel S, Radsak M, Einsele H, Latge JP, Michan A, Loeffler J, Haddad Z, Grigoleit U, Schild H, Hebart H (2004) *Aspergillus fumigatus* antigens activate innate immune cells via toll-like receptors 2 and 4. Br J Haematol. 125(3), 392-9.

Brakhage AA, Bruns S, Thywissen A, Zipfel PF, Behnsen J (2010) Interaction of phagocytes with filamentous fungi. Curr Opin Microbiol. 13(4), 409-15.

Brakhage AA, Liebmann B (2005) *Aspergillus fumigatus* conidial pigment and cAMP signal transduction: significance for virulence. Med Mycol. 43 Suppl 1, S75-82.

Brieland JK, Jackson C, Menzel F, Loebenberg D, Cacciapuoti A, Halpern J, Hurst S, Muchamuel T, Debets R, Kastelein R, Churakova T, Abrams J, Hare R, O'Garra A (2001) Cytokine networking in lungs of immunocompetent mice in response to inhaled *Aspergillus fumigatus*. Infect Immun. 69(3), 1554-60.

Brock M, Jouvion G, Droin-Bergere S, Dussurget O, Nicola MA, Ibrahim-Granet O (2008) Bioluminescent *Aspergillus fumigatus*, a new tool for drug efficiency testing and in vivo monitoring of invasive aspergillosis. Appl Environ Microbiol. 74(22), 7023-35.

Brown GD, Gordon S (2001) Immune recognition. A new receptor for beta-glucans. Nature. 413(6851), 36-7.

Brown GD, Herre J, Williams DL, Willment JA, Marshall AS, Gordon S (2003) Dectin-1 mediates the biological effects of beta-glucans. J Exp Med. 197(9), 1119-24.

Brown JE, Greenberger PA, Yarnold PR (1995) Soluble serum interleukin 2 receptors in patients with asthma and allergic bronchopulmonary aspergillosis. Ann Allergy Asthma Immunol. 74(6), 484-8.

Brown JS, Aufauvre-Brown A, Brown J, Jennings JM, Arst H, Jr., Holden DW (2000) Signature-tagged and directed mutagenesis identify PABA synthetase as essential for *Aspergillus fumigatus* pathogenicity. Mol Microbiol. 36(6), 1371-80.

Bruns S, Kniemeyer O, Hasenberg M, Aimanianda V, Nietzsche S, Thywissen A, Jeron A, Latge JP, Brakhage AA, Gunzer M (2010) Production of extracellular traps against *Aspergillus fumigatus* in vitro and in infected lung tissue is dependent on invading neutrophils and influenced by hydrophobin RodA. PLoS Pathog. 6(4), e1000873.

Buchan BW, McCaffrey RL, Lindemann SR, Allen LA, Jones BD (2009) Identification of migR, a regulatory element of the *Francisella tularensis* live vaccine strain iglABCD virulence operon required for normal replication and trafficking in macrophages. Infect Immun. 77(6), 2517-29.

Butterworth SJ, Barr FJ, Pearson GR, Day MJ (1995) Multiple discospondylitis associated with *Aspergillus* species infection in a dog. Vet Rec. 136(2), 38-41.

Chakrabarti A, Denning DW, Ferguson BJ, Ponikau J, Buzina W, Kita H, Marple B, Panda N, Vlaminck S, Kauffmann-Lacroix C, Das A, Singh P, Taj-Aldeen SJ, Kantarcioglu AS, Handa KK, Gupta A, Thungabathra M, Shivaprakash MR, Bal A, Fothergill A, Radotra BD (2009) Fungal rhinosinusitis: a categorization and definitional schema addressing current controversies. Laryngoscope. 119(9), 1809-18.

Chaudhary B, Singh B (1983) Pathogenicity of *aspergillus fumigatus* in chicks, guinea fowl, rabbits and mice. Mykosen. 26(8), 421-9.

Chignard M, Balloy V, Sallenave JM, Si-Tahar M (2007) Role of Toll-like receptors in lung innate defense against invasive aspergillosis. Distinct impact in immunocompetent and immunocompromized hosts. Clin Immunol. 124(3), 238-43.

Chute HL (1975) Characteristics of immunity in fungal infections. Am J Vet Res. 36(4 Pt 2), 601-2.

Claeys S, Lefebvre JB, Schuller S, Hamaide A, Clercx C (2006) Surgical treatment of canine nasal aspergillosis by rhinotomy combined with enilconazole infusion and oral itraconazole. J Small Anim Pract. 47(6), 320-4.

Clemons KV, Calich VL, Burger E, Filler SG, Grazziutti M, Murphy J, Roilides E, Campa A, Dias MR, Edwards JE, Jr., Fu Y, Fernandes-Bordignon G, Ibrahim A, Katsifa H, Lamaignere CG, Meloni-Bruneri LH, Rex J, Savary CA, Xidieh C (2000a) Pathogenesis I: interactions of host cells and fungi. Med Mycol. 38 Suppl 1, 99-111.

Clemons KV, Grunig G, Sobel RA, Mirels LF, Rennick DM, Stevens DA (2000b) Role of IL-10 in invasive aspergillosis: increased resistance of IL-10 gene knockout mice to lethal systemic aspergillosis. Clin Exp Immunol. 122(2), 186-91.

Clemons KV, Stevens DA (2005) The contribution of animal models of aspergillosis to understanding pathogenesis, therapy and virulence. Med Mycol. 43 Suppl 1, S101-10.

Collemare J, Billard A, Bohnert HU, Lebrun MH (2008) Biosynthesis of secondary metabolites in the rice blast fungus *Magnaporthe grisea*: the role of hybrid PKS-NRPS in pathogenicity. Mycol Res. 112(Pt 2), 207-15.

Coulot P, Bouchara JP, Renier G, Annaix V, Planchenault C, Tronchin G, Chabasse D (1994) Specific interaction of *Aspergillus fumigatus* with fibrinogen and its role in cell adhesion. Infect Immun. 62(6), 2169-77.

Cowen LE, Singh SD, Kohler JR, Collins C, Zaas AK, Schell WA, Aziz H, Mylonakis E, Perfect JR, Whitesell L, Lindquist S (2009) Harnessing Hsp90 function as a powerful, broadly effective therapeutic strategy for fungal infectious disease. Proc Natl Acad Sci U S A. 106(8), 2818-23.

Cramer RA, Jr., Gamcsik MP, Brooking RM, Najvar LK, Kirkpatrick WR, Patterson TF, Balibar CJ, Graybill JR, Perfect JR, Abraham SN, Steinbach WJ (2006) Disruption of a nonribosomal peptide synthetase in *Aspergillus fumigatus* eliminates gliotoxin production. Eukaryot Cell. 5(6), 972-80.

D'Enfert C, Diaquin M, Delit A, Wuscher N, Debeaupuis JP, Huerre M, Latgé JP (1996) Attenuated virulence of uridine-uracil auxotrophs of *Aspergillus fumigatus*. Infect Immun. 64(10), 4401-5.

Day MJ (2009) Canine sino-nasal aspergillosis: parallels with human disease. Med Mycol. 47 Suppl 1, S315-23.

Deak E, Nelson M, Hernandez-Rodriguez Y, Gade L, Baddley J, Momany M, Steele C, Balajee SA (2011) *Aspergillus terreus* accessory conidia are multinucleated, hyperpolarizing structures that display differential dectin staining and can induce heightened inflammatory responses in a pulmonary model of aspergillosis. Virulence. 2(3).

Deak E, Wilson SD, White E, Carr JH, Balajee SA (2009) *Aspergillus terreus* accessory conidia are unique in surface architecture, cell wall composition and germination kinetics. PLoS One. 4(10), e7673.

Debono M, Gordee RS (1994) Antibiotics that inhibit fungal cell wall development. Annu Rev Microbiol. 48, 471-97.

Denning DW, Marinus A, Cohen J, Spence D, Herbrecht R, Pagano L, Kibbler C, Kcrmery V, Offner F, Cordonnier C, Jehn U, Ellis M, Collette L, Sylvester R (1998) An EORTC multicentre prospective survey of invasive aspergillosis in haematological patients: diagnosis and therapeutic outcome. EORTC Invasive Fungal Infections Cooperative Group. J Infect. 37(2), 173-80.

Diamond RD (1988) Fungal surfaces: effects of interactions with phagocytic cells. Rev Infect Dis. 10 Suppl 2, S428-31.

Dinarello CA, Savage N (1989) Interleukin-1 and its receptor. Crit Rev Immunol. 9(1), 1-20.

Diniz SN, Nomizo R, Cisalpino PS, Teixeira MM, Brown GD, Mantovani A, Gordon S, Reis LF, Dias AA (2004) PTX3 function as an opsonin for the dectin-1-dependent internalization of zymosan by macrophages. J Leukoc Biol. 75(4), 649-56.

Dixon DM, Polak A, Walsh TJ (1989) Fungus dose-dependent primary pulmonary aspergillosis in immunosuppressed mice. Infect Immun. 57(5), 1452-6.

Duong M, Ouellet N, Simard M, Bergeron Y, Olivier M, Bergeron MG (1998) Kinetic study of host defense and inflammatory response to *Aspergillus fumigatus* in steroid-induced immunosuppressed mice. J Infect Dis. 178(5), 1472-82.

Dwivedi P, Burns RB, Maxwell MH (1984) Ultrastructural study of the liver and kidney in ochratoxicosis A in young broiler chicks. Res Vet Sci. 36(1), 104-16.

Eissenberg LG, Goldman WE, Schlesinger PH (1993) *Histoplasma capsulatum* modulates the acidification of phagolysosomes. J Exp Med. 177(6), 1605-11.

Fontaine T, Simenel C, Dubreucq G, Adam O, Delepierre M, Lemoine J, Vorgias CE, Diaquin M, Latgé JP (2000) Molecular organization of the alkali-insoluble fraction of *aspergillus fumigatus* cell wall. J Biol Chem. 275(52), 41528.

Ford S, Friedman L (1967) Experimental study of the pathogenicity of aspergilli for mice. J Bacteriol. 94(4), 928-33.

Frisvad JC, Larsen TO, Thrane U, Meijer M, Varga J, Samson RA, Nielsen KF (2011) Fumonisin and Ochratoxin Production in Industrial *Aspergillus niger* Strains. PLoS One. 6(8), e23496.

Fujii I, Watanabe A, Sankawa U, Ebizuka Y (2001) Identification of Claisen cyclase domain in fungal polyketide synthase *WA*, a naphthopyrone synthase of *Aspergillus nidulans*. Chem Biol. 8(2), 189-97.

Fujii I, Yasuoka Y, Tsai HF, Chang YC, Kwon-Chung KJ, Ebizuka Y (2004) Hydrolytic polyketide shortening by *ayg1p*, a novel enzyme involved in fungal melanin biosynthesis. J Biol Chem. 279(43), 44613-20.

Gallis HA, Drew RH, Pickard WW (1990) Amphotericin B: 30 years of clinical experience. Rev Infect Dis. 12(2), 308-29.

Georgopapadakou NH (2001) Update on antifungals targeted to the cell wall: focus on beta-1,3-glucan synthase inhibitors. Expert Opin Investig Drugs. 10(2), 269-80.

Gersuk GM, Underhill DM, Zhu L, Marr KA (2006) Dectin-1 and TLRs permit macrophages to distinguish between different *Aspergillus fumigatus* cellular states. J Immunol. 176(6), 3717-24.

Ghori HM, Edgar SA (1973) Comparative susceptibility of chickens, turkeys and Coturnix quail to aspergillosis. Poult Sci. 52(6), 2311-5.

Ghori HM, Edgar SA (1979) Comparative susceptibility and effect of mild *Aspergillus fumigatus* infection on three strains of chickens. Poult Sci. 58(1), 14-7.

Graveline R, Segura M, Radzioch D, Gottschalk M (2007) TLR2-dependent recognition of *Streptococcus suis* is modulated by the presence of capsular polysaccharide which modifies macrophage responsiveness. Int Immunol. 19(4), 375-89.

Green FH, Olenchock SA, Willard PA, Major PC (1980) SEM studies on the *in vivo* uptake of *Aspergillus terreus* spores by alveolar macrophages. Scan Electron Microsc(3), 307-14.

Gressler M, Zaehle C, Scherlach K, Hertweck C, Brock M (2011) Multifactorial induction of an orphan PKS-NRPS gene cluster in *Aspergillus terreus*. Chem Biol. 18(2), 198-209.

Grosse C, Heinekamp T, Kniemeyer O, Gehrke A, Brakhage AA (2008) Protein kinase A regulates growth, sporulation, and pigment formation in *Aspergillus fumigatus*. Appl Environ Microbiol. 74(15), 4923-33.

Gupta J, Pathak B, Sethi N, Vora VC (1981) Histopathology of Mycotoxicosis produced in Swiss albino mice by metabolites of some fungal isolates. Appl Environ Microbiol. 41(3), 752-7.

Haas A (2007) The phagosome: compartment with a license to kill. Traffic. 8(4), 311-30.

Haas A (1998) Reprogramming the phagocytic pathway--intracellular pathogens and their vacuoles (review). Mol Membr Biol. 15(3), 103-21.

Hamilton AJ, Gomez BL (2002) Melanins in fungal pathogens. J Med Microbiol. 51(3), 189-91.

Hara KS, Ryu JH, Lie JT, Roberts GD (1989) Disseminated *Aspergillus terreus* infection in immunocompromised hosts. Mayo Clin Proc. 64(7), 770-5.

Härtl A, Hillesheim HG, Kunkel W, Schrinner EJ (1995) [The *Candida* infected hen's egg. An alternative test system for systemic anticandida activity]. Arzneimittelforschung. 45(8), 926-8.

Herre J, Gordon S, Brown GD (2004) Dectin-1 and its role in the recognition of beta-glucans by macrophages. Mol Immunol. 40(12), 869-76.

Hissen AH, Wan AN, Warwas ML, Pinto LJ, Moore MM (2005) The *Aspergillus fumigatus* siderophore biosynthetic gene *sidA*, encoding L-ornithine N5-oxygenase, is required for virulence. Infect Immun. 73(9), 5493-503.

Hoffmann E, Marion S, Mishra BB, John M, Kratzke R, Ahmad SF, Holzer D, Anand PK, Weiss DG, Griffiths G, Kuznetsov SA (2010) Initial receptor-ligand interactions modulate gene expression and phagosomal properties during both early and late stages of phagocytosis. Eur J Cell Biol. 89(9), 693-704.

Hohl TM, Van Epps HL, Rivera A, Morgan LA, Chen PL, Feldmesser M, Pamer EG (2005) *Aspergillus fumigatus* triggers inflammatory responses by stage-specific beta-glucan display. PLoS Pathog. 1(3), e30.

Hora JF (1965) Primary Aspergillosis of the Paranasal Sinuses and Associated Areas. Laryngoscope. 75, 768-73.

Hyland KV, Asfaw SH, Olson CL, Daniels MD, Engman DM (2008) Bioluminescent imaging of *Trypanosoma cruzi* infection. Int J Parasitol. 38(12), 1391-400.

Ibrahim-Granet O, Jouvion G, Hohl TM, Droin-Bergere S, Philippart F, Kim OY, Adib-Conquy M, Schwendener R, Cavaillon JM, Brock M (2010) In vivo bioluminescence imaging and histopathopathologic analysis reveal distinct roles for resident and recruited immune effector cells in defense against invasive aspergillosis. BMC Microbiol. 10, 105.

Ibrahim-Granet O, Dubourdeau M, Latge JP, Ave P, Huerre M, Brakhage AA, Brock M (2008) Methylcitrate synthase from *Aspergillus fumigatus* is essential for manifestation of invasive aspergillosis. Cell Microbiol. 10(1), 134-48.

Ibrahim-Granet O, Philippe B, Boleti H, Boisvieux-Ulrich E, Grenet D, Stern M, Latge JP (2003) Phagocytosis and intracellular fate of *Aspergillus fumigatus* conidia in alveolar macrophages. Infect Immun. 71(2), 891-903.

Jackson JC, Higgins LA, Lin X (2009) Conidiation color mutants of *Aspergillus fumigatus* are highly pathogenic to the heterologous insect host *Galleria mellonella*. PLoS One. 4(1), e4224.

Jacobsen ID, Grosse K, Slesiona S, Hube B, Berndt A, Brock M (2010) Embryonated eggs as an alternative infection model to investigate *Aspergillus fumigatus* virulence. Infect Immun. 78(7), 2995-3006.

Jacobson ES (2000) Pathogenic roles for fungal melanins. Clin Microbiol Rev. 13(4), 708-17.

Jahn B, Langfelder K, Schneider U, Schindel C, Brakhage AA (2002) *PKSP*-dependent reduction of phagolysosome fusion and intracellular kill of *Aspergillus fumigatus* conidia by human monocyte-derived macrophages. Cell Microbiol. 4(12), 793-803.

Jahn B, Boukhallouk F, Lotz J, Langfelder K, Wanner G, Brakhage AA (2000) Interaction of human phagocytes with pigmentless *Aspergillus* conidia. Infect Immun. 68(6), 3736-9.

Jahn B, Koch A, Schmidt A, Wanner G, Gehringer H, Bhakdi S, Brakhage AA (1997) Isolation and characterization of a pigmentless-conidium mutant of *Aspergillus fumigatus* with altered conidial surface and reduced virulence. Infect Immun. 65(12), 5110-7.

Johnson EM, Oakley KL, Radford SA, Moore CB, Warn P, Warnock DW, Denning DW (2000) Lack of correlation of in vitro amphotericin B susceptibility testing with outcome in a murine model of *Aspergillus* infection. J Antimicrob Chemother. 45(1), 85-93.

Jonsson S, Musher DM, Chapman A, Goree A, Lawrence EC (1985) Phagocytosis and killing of common bacterial pathogens of the lung by human alveolar macrophages. J Infect Dis. 152(1), 4-13.

Jorgensen TR, Park J, Arentshorst M, van Welzen AM, Lamers G, Vankuyk PA, Damveld RA, van den Hondel CA, Nielsen KF, Frisvad JC, Ram AF (2011) The molecular and genetic basis of conidial pigmentation in *Aspergillus niger*. Fungal Genet Biol.

Jouault T, Sarazin A, Martinez-Esparza M, Fradin C, Sendid B, Poulain D (2009) Host responses to a versatile commensal: PAMPs and PRRs interplay leading to tolerance or infection by *Candida albicans*. Cell Microbiol. 11(7), 1007-15.

Kabay MJ, Robinson WF, Huxtable CR, McAleer R (1985) The pathology of disseminated *Aspergillus terreus* infection in dogs. Vet Pathol. 22(6), 540-7.

Kamei K, Watanabe A (2005) *Aspergillus* mycotoxins and their effect on the host. Med Mycol. 43 Suppl 1, S95-9.

Kasperkovitz PV, Cardenas ML, Vyas JM (2010) TLR9 is actively recruited to *Aspergillus fumigatus* phagosomes and requires the N-terminal proteolytic cleavage domain for proper intracellular trafficking. J Immunol. 185(12), 7614-22.

Kelly SE, Shaw SE, Clark WT (1995) Long-term survival of four dogs with disseminated *Aspergillus terreus* infection treated with itraconazole. Aust Vet J. 72(8), 311-3.

Kerrigan AM, Brown GD (2009) C-type lectins and phagocytosis. Immunobiology. 214(7), 562-75.

Khlangwiset P, Wu F (2010) Costs and efficacy of public health interventions to reduce aflatoxin-induced human disease. Food Addit Contam Part A Chem Anal Control Expo Risk Assess. 27(7), 998-1014.

Khoo SH, Denning DW (1994) Invasive aspergillosis in patients with AIDS. Clin Infect Dis. 19 Suppl 1, S41-8.

Kirkpatrick WR, Perea S, Coco BJ, Patterson TF (2002a) Efficacy of caspofungin alone and in combination with voriconazole in a Guinea pig model of invasive aspergillosis. Antimicrob Agents Chemother. 46(8), 2564-8.

Kirkpatrick WR, Perea S, Coco BJ, Patterson TF (2002b) Efficacy of ravuconazole (BMS-207147) in a guinea pig model of disseminated aspergillosis. J Antimicrob Chemother. 49(2), 353-7.

Kirkpatrick WR, McAtee RK, Fothergill AW, Rinaldi MG, Patterson TF (2000) Efficacy of voriconazole in a guinea pig model of disseminated invasive aspergillosis. Antimicrob Agents Chemother. 44(10), 2865-8.

Klenerman P, Hill A (2005) T cells and viral persistence: lessons from diverse infections. Nat Immunol. 6(9), 873-9.

Knutsen AP, Mueller KR, Hutcheson PS, Slavin RG (1990) T- and B-cell dysregulation of IgE synthesis in cystic fibrosis patients with allergic bronchopulmonary aspergillosis. Clin Immunol Immunopathol. 55(1), 129-38.

Kontoyiannis DP, Mantadakis E, Samonis G (2003) Systemic mycoses in the immunocompromised host: an update in antifungal therapy. J Hosp Infect. 53(4), 243-58.

Krishnan N, Robertson BD, Thwaites G (2010) The mechanisms and consequences of the extra-pulmonary dissemination of *Mycobacterium tuberculosis*. Tuberculosis (Edinb). 90(6), 361-6.

Kruskal BA, Sastry K, Warner AB, Mathieu CE, Ezekowitz RA (1992) Phagocytic chimeric receptors require both transmembrane and cytoplasmic domains from the mannose receptor. J Exp Med. 176(6), 1673-80.

Kubota Y, Takahashi S, Matsuoka O (1983) Dependence on particle size in the phagocytosis of latex particles by rabbit alveolar macrophages cultured *in vitro*. J Toxicol Sci. 8(3), 189-95.
Kunkle RA, Rimler RB (1996) Pathology of acute aspergillosis in turkeys. Avian Dis. 40(4), 875-86.

Kupfahl C, Heinekamp T, Geginat G, Ruppert T, Hartl A, Hof H, Brakhage AA (2006) Deletion of the gliP gene of *Aspergillus fumigatus* results in loss of gliotoxin production but has no effect on virulence of the fungus in a low-dose mouse infection model. Mol Microbiol. 62(1), 292-302.

Kwon-Chung KJ, Sugui JA (2009) What do we know about the role of gliotoxin in the pathobiology of *Aspergillus fumigatus*? Med Mycol. 47 Suppl 1, S97-103.

Lambeth JD, Kawahara T, Diebold B (2007) Regulation of Nox and Duox enzymatic activity and expression. Free Radic Biol Med. 43(3), 319-31.

Langfelder K, Streibel M, Jahn B, Haase G, Brakhage AA (2003) Biosynthesis of fungal melanins and their importance for human pathogenic fungi. Fungal Genet Biol. 38(2), 143-58.

Langfelder K, Jahn B, Gehringer H, Schmidt A, Wanner G, Brakhage AA (1998) Identification of a polyketide synthase gene (*pksP*) of *Aspergillus fumigatus* involved in conidial pigment biosynthesis and virulence. Med Microbiol Immunol. 187(2), 79-89.

Larcher G, Bouchara JP, Annaix V, Symoens F, Chabasse D, Tronchin G (1992) Purification and characterization of a fibrinogenolytic serine proteinase from *Aspergillus fumigatus* culture filtrate. FEBS Lett. 308(1), 65-9.

Largent BL, Walton KM, Hoppe CA, Lee YC, Schnaar RL (1984) Carbohydrate-specific adhesion of alveolar macrophages to mannose-derivatized surfaces. J Biol Chem. 259(3), 1764-9.

Lass-Flörl C (2010) *In vitro* susceptibility testing in *Aspergillus* species: an update. Future Microbiol. 5(5), 789-99.

Lass-Flörl C, Griff K, Mayr A, Petzer A, Gastl G, Bonatti H, Freund M, Kropshofer G, Dierich MP, Nachbaur D (2005) Epidemiology and outcome of infections due to *Aspergillus terreus*: 10-year single centre experience. Br J Haematol. 131(2), 201-7.

Lass-Flörl C, Kofler G, Kropshofer G, Hermans J, Kreczy A, Dierich MP, Niederwieser D (1998) *In-vitro* testing of susceptibility to amphotericin B is a reliable predictor of clinical outcome in invasive aspergillosis. J Antimicrob Chemother. 42(4), 497-502.

Latgé JP (2010) Tasting the fungal cell wall. Cell Microbiol. 12(7), 863-72.

Latgé JP (2007) The cell wall: a carbohydrate armour for the fungal cell. Mol Microbiol. 66(2), 279-90.

Latgé JP (2001) The pathobiology of *Aspergillus fumigatus*. Trends Microbiol. 9(8), 382-9.

Latgé JP (1999) *Aspergillus fumigatus* and aspergillosis. Clin Microbiol Rev. 12(2), 310-50.

Lehmann PF (1985) Immunology of fungal infections in animals. Vet Immunol Immunopathol. 10(1), 33-69.

Lepage OM, Perron MF, Cadore JL (2004) The mystery of fungal infection in the guttural pouches. Vet J. 168(1), 60-4.

Levitz SM, Nong SH, Seetoo KF, Harrison TS, Speizer RA, Simons ER (1999) *Cryptococcus neoformans* resides in an acidic phagolysosome of human macrophages. Infect Immun. 67(2), 885-90.

Lewis RE, Kontoyiannis DP (2009) Invasive aspergillosis in glucocorticoid-treated patients. Med Mycol. 47 Suppl 1, S271-81.

Liebmann B, Mühleisen TW, Müller M, Hecht M, Weidner G, Braun A, Brock M, Brakhage AA (2004) Deletion of the *Aspergillus fumigatus* lysine biosynthesis gene *lysF* encoding homoaconitase leads to attenuated virulence in a low-dose mouse infection model of invasive aspergillosis. Arch Microbiol. 181(5), 378-83.

Lin SJ, Schranz J, Teutsch SM (2001) Aspergillosis case-fatality rate: systematic review of the literature. Clin Infect Dis. 32(3), 358-66.

Lionakis MS, Kontoyiannis DP (2005) Fruit flies as a minihost model for studying drug activity and virulence in *Aspergillus*. Med Mycol. 43 Suppl 1, S111-4.

Lionakis MS, Lewis RE, May GS, Wiederhold NP, Albert ND, Halder G, Kontoyiannis DP (2005) Toll-deficient Drosophila flies as a fast, high-throughput model for the study of antifungal drug efficacy against invasive aspergillosis and *Aspergillus* virulence. J Infect Dis. 191(7), 1188-95.

Liu K, Howell DN, Perfect JR, Schell WA (1998) Morphologic criteria for the preliminary identification of *Fusarium*, *Paecilomyces*, and *Acremonium* species by histopathology. Am J Clin Pathol. 109(1), 45-54.

Lozbin LI (1977) [Prevention of mycotoxicoses (review of the literature)]. Vrach Delo(11), 140-7.

Lundborg M, Holma B (1972) *In vitro* phagocytosis of fungal spores by rabbit lung macrophages. Sabouraudia. 10(2), 152-6.

Lupo P, Chang YC, Kelsall BL, Farber JM, Pietrella D, Vecchiarelli A, Leon F, Kwon-Chung KJ (2008) The presence of capsule in *Cryptococcus neoformans* influences the gene expression profile in dendritic cells during interaction with the fungus. Infect Immun. 76(4), 1581-9.

Luther K, Torosantucci A, Brakhage AA, Heesemann J, Ebel F (2007) Phagocytosis of *Aspergillus fumigatus* conidia by murine macrophages involves recognition by the dectin-1 beta-glucan receptor and Toll-like receptor 2. Cell Microbiol. 9(2), 368-81.

Luther K, Rohde M, Heesemann J, Ebel F (2006) Quantification of phagocytosis of *Aspergillus* conidia by macrophages using a novel antibody-independent assay. J Microbiol Methods. 66(1), 170-3.

Maerker C, Rohde M, Brakhage AA, Brock M (2005) Methylcitrate synthase from *Aspergillus fumigatus*. Propionyl-CoA affects polyketide synthesis, growth and morphology of conidia. FEBS J. 272(14), 3615-30.

Malani A, Trimble K, Parekh V, Chenoweth C, Kaufman S, Saint S (2007) Review of clinical trials of skin antiseptic agents used to reduce blood culture contamination. Infect Control Hosp Epidemiol. 28(7), 892-5.

Malani AN, Kauffman CA (2007) Changing epidemiology of rare mould infections: implications for therapy. Drugs. 67(13), 1803-12.

Mantegazza AR, Barrio MM, Moutel S, Bover L, Weck M, Brossart P, Teillaud JL, Mordoh J (2004) CD63 tetraspanin slows down cell migration and translocates to the endosomal-lysosomal-MIICs route after extracellular stimuli in human immature dendritic cells. Blood. 104(4), 1183-90.

Marinkovic D, Aleksic-Kovacevic S, Plamenac P (2007) Cellular basis of chronic obstructive pulmonary disease in horses. Int Rev Cytol. 257, 213-47.

Marr KA, Carter RA, Crippa F, Wald A, Corey L (2002) Epidemiology and outcome of mould infections in hematopoietic stem cell transplant recipients. Clin Infect Dis. 34(7), 909-17.

Marr KA, Koudadoust M, Black M, Balajee SA (2001) Early events in macrophage killing of *Aspergillus fumigatus* conidia: new flow cytometric viability assay. Clin Diagn Lab Immunol. 8(6), 1240-7.

Martinez-Quesada J, Nieto-Cadenazzi A, Torres-Rodriguez JM (1993) Humoral immunoresponse of pigeons to *Aspergillus fumigatus* antigens. Mycopathologia. 124(3), 131-7.

Maschmeyer G, Haas A, Cornely OA (2007) Invasive aspergillosis: epidemiology, diagnosis and management in immunocompromised patients. Drugs. 67(11), 1567-601.

Mayorga ME, Timberlake WE (1992) The developmentally regulated *Aspergillus nidulans wA* gene encodes a polypeptide homologous to polyketide and fatty acid synthases. Mol Gen Genet. 235(2-3), 205-12.

Mayorga ME, Timberlake WE (1990) Isolation and molecular characterization of the *Aspergillus nidulans wA* gene. Genetics. 126(1), 73-9.

Mbawuike IN, Herscowitz HB (1989) MH-S, a murine alveolar macrophage cell line: morphological, cytochemical, and functional characteristics. J Leukoc Biol. 46(2), 119-27.

McCormick A, Loeffler J, Ebel F (2010) *Aspergillus fumigatus*: contours of an opportunistic human pathogen. Cell Microbiol. 12(11), 1535-43.

Millar FA, Simmonds NJ, Hodson ME (2009) Trends in pathogens colonising the respiratory tract of adult patients with cystic fibrosis, 1985-2005. J Cyst Fibros. 8(6), 386-91.

Mircescu MM, Lipuma L, van Rooijen N, Pamer EG, Hohl TM (2009) Essential role for neutrophils but not alveolar macrophages at early time points following *Aspergillus fumigatus* infection. J Infect Dis. 200(4), 647-56.

Moreno MA, Ibrahim-Granet O, Vicentefranqueira R, Amich J, Ave P, Leal F, Latge JP, Calera JA (2007) The regulation of zinc homeostasis by the *ZafA* transcriptional activator is essential for *Aspergillus fumigatus* virulence. Mol Microbiol. 64(5), 1182-97.

Nawada R, Amitani R, Tanaka E, Niimi A, Suzuki K, Murayama T, Kuze F (1996) Murine model of invasive pulmonary aspergillosis following an earlier stage, noninvasive *Aspergillus* infection. J Clin Microbiol. 34(6), 1433-9.

Nessa K, Johansson A, Jarstrand C, Camner P (1997) Alveolar macrophage reaction to *Candida* species. Lett Appl Microbiol. 25(3), 181-5.

Netea MG, Ferwerda G, van der Graaf CA, Van der Meer JW, Kullberg BJ (2006) Recognition of fungal pathogens by toll-like receptors. Curr Pharm Des. 12(32), 4195-201.
Ogawa M, Sasakawa C (2006) Intracellular survival of *Shigella*. Cell Microbiol. 8(2), 177-84.

Okagaki LH, Strain AK, Nielsen JN, Charlier C, Baltes NJ, Chretien F, Heitman J, Dromer F, Nielsen K (2010) Cryptococcal cell morphology affects host cell interactions and pathogenicity. PLoS Pathog. 6(6), e1000953.

Olenchock SA, Green FH, Mentnech MS, Mull JC, Sorenson WG (1983) In vivo pulmonary response to *Aspergillus terreus* spores. Comp Immunol Microbiol Infect Dis. 6(1), 67-80.

Olias P, Gruber AD, Hafez HM, Lierz M, Slesiona S, Brock M, Jacobsen ID (2011) Molecular epidemiology and virulence assessment of *Aspergillus fumigatus* isolates from white stork chicks and their environment. Vet Microbiol. 148(2-4), 348-55.

Olias P, Gruber AD, Winfried B, Hafez HM, Lierz M (2010) Fungal pneumonia as a major cause of mortality in white stork (*Ciconia ciconia*) chicks. Avian Dis. 54(1), 94-8.

Onishi J, Meinz M, Thompson J, Curotto J, Dreikorn S, Rosenbach M, Douglas C, Abruzzo G, Flattery A, Kong L, Cabello A, Vicente F, Pelaez F, Diez MT, Martin I, Bills G, Giacobbe R, Dombrowski A, Schwartz R, Morris S, Harris G, Tsipouras A, Wilson K, Kurtz MB (2000) Discovery of novel antifungal (1,3)-beta-D-glucan synthase inhibitors. Antimicrob Agents Chemother. 44(2), 368-77.

Patterson TF, Kirkpatrick WR, White M, Hiemenz JW, Wingard JR, Dupont B, Rinaldi MG, Stevens DA, Graybill JR (2000) Invasive aspergillosis. Disease spectrum, treatment practices, and outcomes. I3 *Aspergillus* Study Group. Medicine (Baltimore). 79(4), 250-60.

Penalva MA, Tilburn J, Bignell E, Arst HN, Jr. (2008) Ambient pH gene regulation in fungi: making connections. Trends Microbiol. 16(6), 291-300.

Perfect JR, Cox GM, Lee JY, Kauffman CA, de Repentigny L, Chapman SW, Morrison VA, Pappas P, Hiemenz JW, Stevens DA (2001) The impact of culture isolation of *Aspergillus* species: a hospital-based survey of aspergillosis. Clin Infect Dis. 33(11), 1824-33.

Perkhofer S, Trappl K, Striessnig B, Nussbaumer W, Lass-Florl C (2011) Platelets enhance activity of antimycotic substances against non-*Aspergillus fumigatus Aspergillus* species in vitro. Med Mycol. 49(2), 157-66.

Perkhofer S, Speth C, Dierich MP, Lass-Flörl C (2007) In vitro determination of phagocytosis and intracellular killing of *Aspergillus* species by mononuclear phagocytes. Mycopathologia. 163(6), 303-7.

Pfaller MA, Diekema DJ (2010) Epidemiology of invasive mycoses in North America. Crit Rev Microbiol. 36(1), 1-53.

Philippe B, Ibrahim-Granet O, Prevost MC, Gougerot-Pocidalo MA, Sanchez Perez M, Van der Meeren A, Latgé JP (2003) Killing of *Aspergillus fumigatus* by alveolar macrophages is mediated by reactive oxidant intermediates. Infect Immun. 71(6), 3034-42.

Pier AC, Richard JL, Cysewski SJ (1980) Implications of mycotoxins in animal disease. J Am Vet Med Assoc. 176(8), 719-24.

Pitt JI (1994) The current role of *Aspergillus* and *Penicillium* in human and animal health. J Med Vet Mycol. 32 Suppl 1, 17-32.

Prasad NV, Sandhu RS (1975) A modified minimal medium for *aspergillus nidulans*. Indian J Exp Biol. 13(2), 218-20.

Purnell DM (1974) The histopathologic response of mice to *Aspergillus nidulans*: comparison between genetically defined haploid and diploid strains of different virulence. Drugs. 7(1), 95-104.

Ralph P, Prichard J, Cohn M (1975) Reticulum cell sarcoma: an effector cell in antibody-dependent cell-mediated immunity. J Immunol. 114(2 pt 2), 898-905.

Raper B, Fenell I (1965) The Genus *Aspergillus*: Baltimore: Williams and Wilkins Co.

Reeves EP, Messina CG, Doyle S, Kavanagh K (2004) Correlation between gliotoxin production and virulence of *Aspergillus fumigatus* in *Galleria mellonella*. Mycopathologia. 158(1), 73-9.

Richard JL, Peden WM, Sacks JM (1991) Effects of adjuvant-augmented germling vaccines in turkey poults challenged with *Aspergillus fumigatus*. Avian Dis. 35(1), 93-9.

Richard JL, Thurston JR, Peden WM, Pinello C (1984) Recent studies on aspergillosis in turkey poults. Mycopathologia. 87(1-2), 3-11.

Richard JL, Thurston JR (1983) Rapid hematogenous dissemination of *Aspergillus fumigatus* and *A. flavus spores* in turkey poults following aerosol exposure. Avian Dis. 27(4), 1025-33.

Richard JL, Thurston JR, Cutlip RC, Pier AC (1982) Vaccination studies of aspergillosis in turkeys: subcutaneous inoculation with several vaccine preparations followed by aerosol challenge exposure. Am J Vet Res. 43(3), 488-92.

Richard JL, Thurston JR (1975) Effect of aflatoxin on phagocytosis of *Aspergillus fumigatus* spores by rabbit alveolar macrophages. Appl Microbiol. 30(1), 44-7.

Rippon JW, Anderson DN, Hoo MS (1974) Aspergillosis: comparative virulence, metabolic rate, growth rate and ubiquinone content of soil and human isolates of *Aspergillus terreus*. Sabouraudia. 12(2), 157-61.

Riscili BP, Wood KL (2009) Noninvasive pulmonary *Aspergillus* infections. Clin Chest Med. 30(2), 315-35, vii.

Robens JF, Richard JL (1992) Aflatoxins in animal and human health. Rev Environ Contam Toxicol. 127, 69-94.

Robinson NE, Derksen FJ, Olszewski MA, Buechner-Maxwell VA (1996) The pathogenesis of chronic obstructive pulmonary disease of horses. Br Vet J. 152(3), 283-306.

Roilides E, Katsifa H, Walsh TJ (1998) Pulmonary host defences against *Aspergillus fumigatus*. Res Immunol. 149(4-5), 454-65.

Roilides E, Sein T, Holmes A, Chanock S, Blake C, Pizzo PA, Walsh TJ (1995) Effects of macrophage colony-stimulating factor on antifungal activity of mononuclear phagocytes against *Aspergillus fumigatus*. J Infect Dis. 172(4), 1028-34.

Salman N, Torun SH, Budan B, Somer A (2011) Invasive aspergillosis in hematopoietic stem cell and solid organ transplantation. Expert Rev Anti Infect Ther. 9(3), 307-15.

Sanchez JF, Chiang YM, Wang CC (2008) Diversity of polyketide synthases found in the *Aspergillus* and *Streptomyces* genomes. Mol Pharm. 5(2), 226-33.

Sandhu DK, Sandhu RS, Khan ZU, Damodaran VN (1976) Conditional virulence of a p-aminobenzoic acid-requiring mutant of *Aspergillus fumigatus*. Infect Immun. 13(2), 527-32.

Sansonetti P (2001) Phagocytosis of bacterial pathogens: implications in the host response. Semin Immunol. 13(6), 381-90.

Sarfati J, Diaquin M, Debeaupuis JP, Schmidt A, Lecaque D, Beauvais A, Latgé JP (2002) A new experimental murine aspergillosis model to identify strains of *Aspergillus fumigatus* with reduced virulence. Nippon Ishinkin Gakkai Zasshi. 43(4), 203-13.

Schelenz S, Smith DA, Bancroft GJ (1999) Cytokine and chemokine responses following pulmonary challenge with *Aspergillus fumigatus*: obligatory role of TNF-alpha and GM-CSF in neutrophil recruitment. Med Mycol. 37(3), 183-94.

Schmidt A (2002) Animal models of aspergillosis - also useful for vaccination strategies? Mycoses. 45(1-2), 38-40.

Schmidt S, Tramsen L, Hanisch M, Latge JP, Huenecke S, Koehl U, Lehrnbecher T (2011) Human natural killer cells exhibit direct activity against *Aspergillus fumigatus* hyphae, but not against resting conidia. J Infect Dis. 203(3), 430-5.

Schöbel F, Jacobsen ID, Brock M (2010) Evaluation of lysine biosynthesis as an antifungal drug target: biochemical characterization of *Aspergillus fumigatus* homocitrate synthase and virulence studies. Eukaryot Cell. 9(6), 878-93.

Schrettl M, Beckmann N, Varga J, Heinekamp T, Jacobsen ID, Jochl C, Moussa TA, Wang S, Gsaller F, Blatzer M, Werner ER, Niermann WC, Brakhage AA, Haas H (2010) *HapX*-mediated adaption to iron starvation is crucial for virulence of *Aspergillus fumigatus*. PLoS Pathog. 6(9).

Schrettl M, Bignell E, Kragl C, Sabiha Y, Loss O, Eisendle M, Wallner A, Arst HN, Jr., Haynes K, Haas H (2007) Distinct roles for intra- and extracellular siderophores during *Aspergillus fumigatus* infection. PLoS Pathog. 3(9), 1195-207.

Schulert GS, McCaffrey RL, Buchan BW, Lindemann SR, Hollenback C, Jones BD, Allen LA (2009) *Francisella tularensis* genes required for inhibition of the neutrophil respiratory burst and intramacrophage growth identified by random transposon mutagenesis of strain LVS. Infect Immun. 77(4), 1324-36.

Schulert GS, Allen LA (2006) Differential infection of mononuclear phagocytes by *Francisella tularensis*: role of the macrophage mannose receptor. J Leukoc Biol. 80(3), 563-71.

Schultz RM, Johnson EG, Wisner ER, Brown NA, Byrne BA, Sykes JE (2008) Clinicopathologic and diagnostic imaging characteristics of systemic aspergillosis in 30 dogs. J Vet Intern Med. 22(4), 851-9.

Segal BH (2007) Role of macrophages in host defense against aspergillosis and strategies for immune augmentation. Oncologist. 12 Suppl 2, 7-13.

Seider K, Heyken A, Lüttich A, Miramon P, Hube B (2010) Interaction of pathogenic yeasts with phagocytes: survival, persistence and escape. Curr Opin Microbiol. 13(4), 392-400.

Serrano-Gomez D, Dominguez-Soto A, Ancochea J, Jimenez-Heffernan JA, Leal JA, Corbi AL (2004) Dendritic cell-specific intercellular adhesion molecule 3-grabbing nonintegrin mediates binding and internalization of *Aspergillus fumigatus* conidia by dendritic cells and macrophages. J Immunol. 173(9), 5635-43.

Sharma RB, Kumar A, Roy AN (1983) Nature of hepatic damage induced by culture filtrates of seed-borne fungi in the laboratory rat. Toxicol Lett. 19(1-2), 87-92.

Sheppard DC, Rieg G, Chiang LY, Filler SG, Edwards JE, Jr., Ibrahim AS (2004) Novel inhalational murine model of invasive pulmonary aspergillosis. Antimicrob Agents Chemother. 48(5), 1908-11.

Simmonds EJ, Littlewood JM, Hopwood V, Evans EG (1994) *Aspergillus fumigatus* colonisation and population density of place of residence in cystic fibrosis. Arch Dis Child. 70(2), 139-40.

Sokol-Anderson ML, Brajtburg J, Medoff G (1986) Amphotericin B-induced oxidative damage and killing of *Candida albicans*. J Infect Dis. 154(1), 76-83.

Spikes S, Xu R, Nguyen CK, Chamilos G, Kontoyiannis DP, Jacobson RH, Ejzykowicz DE, Chiang LY, Filler SG, May GS (2008) Gliotoxin production in *Aspergillus fumigatus* contributes to host-specific differences in virulence. J Infect Dis. 197(3), 479-86.

Steinbach WJ, Benjamin DK, Jr., Kontoyiannis DP, Perfect JR, Lutsar I, Marr KA, Lionakis MS, Torres HA, Jafri H, Walsh TJ (2004a) Infections due to *Aspergillus terreus*: a multicenter retrospective analysis of 83 cases. Clin Infect Dis. 39(2), 192-8.

Steinbach WJ, Benjamin DK, Jr., Trasi SA, Miller JL, Schell WA, Zaas AK, Foster WM, Perfect JR (2004b) Value of an inhalational model of invasive aspergillosis. Med Mycol. 42(5), 417-25.

Steinberg BE, Huynh KK, Grinstein S (2007) Phagosomal acidification: measurement, manipulation and functional consequences. Biochem Soc Trans. 35(Pt 5), 1083-7.

Stephens-Romero SD, Mednick AJ, Feldmesser M (2005) The pathogenesis of fatal outcome in murine pulmonary aspergillosis depends on the neutrophil depletion strategy. Infect Immun. 73(1), 114-25.

Sturtevant JE, Latgé JP (1992) Interactions between conidia of *Aspergillus fumigatus* and human complement component C3. Infect Immun. 60(5), 1913-8.

Sugui JA, Pardo J, Chang YC, Zarember KA, Nardone G, Galvez EM, Mullbacher A, Gallin JI, Simon MM, Kwon-Chung KJ (2007) Gliotoxin is a virulence factor of *Aspergillus fumigatus*: *gliP* deletion attenuates virulence in mice immunosuppressed with hydrocortisone. Eukaryot Cell. 6(9), 1562-9.

Tapper H, Sundler R (1995) Bafilomycin A1 inhibits lysosomal, phagosomal, and plasma membrane H(+)-ATPase and induces lysosomal enzyme secretion in macrophages. J Cell Physiol. 163(1), 137-44.

Thom CaR, K. B. (1945) A manual of the Aspergilli: The Williams and Wilkins Company, Baltimore.

Thornton CR (2010) Detection of invasive aspergillosis. Adv Appl Microbiol. 70, 187-216.

Thywissen A, Heinekamp T, Dahse HM, Schmaler-Ripcke J, Nietzsche S, F. ZP, Brakhage AA (2011) Conidial dihydroxynaphthalene melanin of the human pathogenic fungus *Aspergillus fumigatus* interferes with the host endocytosis pathway. Front Microbiol 2:96. doi: 10.3389/fmicb.2011.00096

Torosantucci A, Chiani P, Bromuro C, De Bernardis F, Palma AS, Liu Y, Mignogna G, Maras B, Colone M, Stringaro A, Zamboni S, Feizi T, Cassone A (2009) Protection by anti-beta-glucan antibodies is associated with restricted beta-1,3 glucan binding specificity and inhibition of fungal growth and adherence. PLoS One. 4(4), e5392.

Tournu H, Serneels J, Van Dijck P (2005) Fungal pathogens research: novel and improved molecular approaches for the discovery of antifungal drug targets. Curr Drug Targets. 6(8), 909-22.

Tracy SL, McGinnis MR, Peacock JE, Jr., Cohen MS, Walker DH (1983) Disseminated infection by *Aspergillus terreus*. Am J Clin Pathol. 80(5), 728-33.

Tritz DM, Woods GL (1993) Fatal disseminated infection with *Aspergillus terreus* in immunocompromised hosts. Clin Infect Dis. 16(1), 118-22.

Tronchin G, Bouchara JP, Larcher G, Lissitzky JC, Chabasse D (1993) Interaction between *Aspergillus fumigatus* and basement membrane laminin: binding and substrate degradation. Biol Cell. 77(2), 201-8.

Tsai HF, Chang YC, Washburn RG, Wheeler MH, Kwon-Chung KJ (1998) The developmentally regulated *alb1* gene of *Aspergillus fumigatus*: its role in modulation of conidial morphology and virulence. J Bacteriol. 180(12), 3031-8.

Vanden Bossche H, Warnock DW, Dupont B, Kerridge D, Sen Gupta S, Improvisi L, Marichal P, Odds FC, Provost F, Ronin O (1994) Mechanisms and clinical impact of antifungal drug resistance. J Med Vet Mycol. 32 Suppl 1, 189-202.

Vanhee LM, Symoens F, Bouchara JP, Nelis HJ, Coenye T (2008) High-resolution genotyping of *Aspergillus fumigatus* isolates recovered from chronically colonised patients with cystic fibrosis. Eur J Clin Microbiol Infect Dis. 27(10), 1005-7.

Vesper SJ, Haugland RA, Rogers ME, Neely AN (2007) Opportunistic *Aspergillus* pathogens measured in home and hospital tap water by quantitative PCR (QPCR). J Water Health. 5(3), 427-31.

Voelz K, Lammas DA, May RC (2009) Cytokine signaling regulates the outcome of intracellular macrophage parasitism by *Cryptococcus neoformans*. Infect Immun. 77(8), 3450-7.

Wald A, Leisenring W, van Burik JA, Bowden RA (1997) Epidemiology of *Aspergillus* infections in a large cohort of patients undergoing bone marrow transplantation. J Infect Dis. 175(6), 1459-66.

Walsh TJ, Petraitis V, Petraitiene R, Field-Ridley A, Sutton D, Ghannoum M, Sein T, Schaufele R, Peter J, Bacher J, Casler H, Armstrong D, Espinel-Ingroff A, Rinaldi MG, Lyman CA (2003) Experimental pulmonary aspergillosis due to *Aspergillus terreus*: pathogenesis and treatment of an emerging fungal pathogen resistant to amphotericin B. J Infect Dis. 188(2), 305-19.

Wasylnka JA, Hissen AH, Wan AN, Moore MM (2005) Intracellular and extracellular growth of *Aspergillus fumigatus*. Med Mycol. 43 Suppl 1, S27-30.

Wasylnka JA, Moore MM (2003) *Aspergillus fumigatus* conidia survive and germinate in acidic organelles of A549 epithelial cells. J Cell Sci. 116(Pt 8), 1579-87.

Wasylnka JA, Moore MM (2002) Uptake of *Aspergillus fumigatus* Conidia by phagocytic and nonphagocytic cells in vitro: quantitation using strains expressing green fluorescent protein. Infect Immun. 70(6), 3156-63.

Watanabe A, Fujii I, Tsai H, Chang YC, Kwon-Chung KJ, Ebizuka Y (2000) *Aspergillus fumigatus alb1* encodes naphthopyrone synthase when expressed in *Aspergillus oryzae*. FEMS Microbiol Lett. 192(1), 39-44.

Waters D, Higginson L, Gladstone P, Kimball B, Le May M, Boccuzzi SJ, Lesperance J (1994) Effects of monotherapy with an HMG-CoA reductase inhibitor on the progression of coronary atherosclerosis as assessed by serial quantitative arteriography. The Canadian Coronary Atherosclerosis Intervention Trial. Circulation. 89(3), 959-68.

Watt PR, Robins GM, Galloway AM, O'Boyle DA (1995) Disseminated opportunistic fungal disease in dogs: 10 cases (1982-1990). J Am Vet Med Assoc. 207(1), 67-70.

Weidenmaier C, Kristian SA, Peschel A (2003) Bacterial resistance to antimicrobial host defenses--an emerging target for novel antiinfective strategies? Curr Drug Targets. 4(8), 643-9.

Werner JL, Metz AE, Horn D, Schoeb TR, Hewitt MM, Schwiebert LM, Faro-Trindade I, Brown GD, Steele C (2009) Requisite role for the dectin-1 beta-glucan receptor in pulmonary defense against *Aspergillus fumigatus*. J Immunol. 182(8), 4938-46.

White DA (2005) *Aspergillus* pulmonary infections in transplant recipients. Clin Chest Med. 26(4), 661-74, vii.

Wiesner J, Vilcinskas A (2010) Antimicrobial peptides: the ancient arm of the human immune system. Virulence. 1(5), 440-64.

Wood AJ, Douglas RG (2010) Pathogenesis and treatment of chronic rhinosinusitis. Postgrad Med J. 86(1016), 359-64.

Yang J, Hooper WC, Phillips DJ, Talkington DF (2003) Interleukin-1beta responses to *Mycoplasma pneumoniae* infection are cell-type specific. Microb Pathog. 34(1), 17-25.

Zelante T, Bozza S, De Luca A, D'Angelo C, Bonifazi P, Moretti S, Giovannini G, Bistoni F, Romani L (2009) Th17 cells in the setting of *Aspergillus* infection and pathology. Med Mycol. 47 Suppl 1, S162-9.

Zelante T, De Luca A, Bonifazi P, Montagnoli C, Bozza S, Moretti S, Belladonna ML, Vacca C, Conte C, Mosci P, Bistoni F, Puccetti P, Kastelein RA, Kopf M, Romani L (2007) IL-23 and the Th17 pathway promote inflammation and impair antifungal immune resistance. Eur J Immunol. 37(10), 2695-706.

10 Publications out of this dissertation

Manuscripts:

Slesiona S., Ibrahim-Granet O., Olias P., Brock M. and Jacobsen I.D. (2012)
Murine infection models for A*spergillus terreus* pulmonary aspergillosis reveal long-term persistence of conidia and liver degeneration.
Journal of Infectious Disease 205 (8): 1268 - 1277

Slesiona S., Gressler M., Mihlan M., Zaehle C., Schaller M., Barz D., Hube B., Jacobsen I.D. and Brock M. (2012)
Persistence versus Escape: *Aspergillus terreus* and *Aspergillus fumigatus* employ different strategies during interactions with macrophages.
Plos ONE 7 (2): e31223.

Conference Presentations:

Poster:

Slesiona S., Jacobsen I.D. and Brock M.
"Interactions of *A. terreus* with alveolar macrophages: Differences compared to *A. fumigatus*"
Gordon Research Conferences – Immunology of Fungal Infections, Galveston, Texas, USA (16. – 21. January 2011)

Slesiona S., Brock M. and Jacobsen I.D.
"Investigation of murine infection models for *Aspergillus terreus*-mediated invasive aspergillosis reveals unexpected liver damage" (Abstract no.: A-290-0001-00010)
44. Wissenschaftliche Tagung der Deutschsprachigen Mykologischen Gesellschaft e.V., Vienna, Austria (5. – 11. September 2010)

Slesiona S., Brock M. and Jacobsen I.D.
"Characterisation of murine intranasal infection models for *Aspergillus terreus* invasive aspergillosis reveals unexpected liver damage"
Fachgruppentagung der DVG Fachgruppe Bakteriologie und Mykologie, Jena, Germany (22. – 24. June 2010)

11 Acknowledgements

I wish to thank

my supervisors Dr. Ilse D. Jacobsen and Dr. Matthias Brock, first of all for their ideas to this project, for the support and faith they had in me and for the discussions, advice, guidance and the enthusiasm they always gave to me.
Prof. Dr. Achim Gruber for being my first reviewer and giving me the opportunity to receive a doctoral degree.
Prof. Dr. Bernhard Hube for integrating me into his wonderful department of Microbial Pathogenicity Mechanisms helping and advising me in writing papers and for being my second reviewer.

my past and present co-workers at the Junior Research Group Microbial Biochemistry and Physiology and the Department of Microbial Pathogenicity Mechanisms for the support and good working atmosphere. I would further like to thank Dr. Sascha Brunke for discussion around science and help with the cytokine array data; Dr. Betty Wächtler and Katja Seider for introducing me to cell culture work; Dr. Christian Fleck and Dr. Felicitas Schöbel for showing me how to work with fungi; Dr. Michael Mihlan for the help with FACS analysis; Dr. Philipp Olias for the great support in liver histology. Thank you very much Markus for all your passion in *A. terreus* research and the strain you provided. Thanks Christoph for the support with *wA* and discussions about secondary metabolites.
Birgit Fehrenbacher and Prof. Dr. Martin Schaller for processing the transmission electron microscopy images and the rapid answers when questions arose.
Dr. Oumaima Ibrahim-Granet, Dr. Gregory Jouvion and Prof. Dr. Jean-Marc Cavaillon from the Institute Pasteur in Paris for introducing me to bioluminescence *in vivo* imaging and analysis, this taught me a lot besides the “savoir-vivre en Paris”.
Uschi and Birgit for their support and help in all situations of lab life, thank you very much Mädels!

I further like to thank the Netzwerk Grundlagenforschung of the HKI and the Deutsche Forschungsgemeinschaft DFG project BR-2216/4-1 for funding this work.

Frauke, Thomas and Katrin for being my friends and sharing this adventurous time with me.
My family and Mario for reminding me of a life outside the lab.

Thank you very much!

12 Selbständigkeitserklärung

Hiermit bestätige ich, dass ich die vorliegende Arbeit selbständig angefertigt habe. Ich versichere, dass ich ausschließlich die angegebenen Quellen und Hilfen in Anspruch genommen habe.

Berlin, den 27. März 2012

Silvia Slesiona